

# 1 Treatment of non-ideality in the multiphase model

## 2 SPACCIM- Part I: Model development

3  
4 A. J. Rusumdar<sup>1,\*</sup>, R. Wolke<sup>1</sup>, A. Tilgner<sup>1</sup>, and H. Herrmann<sup>1</sup>

5 [1]{Leibniz Institute for Tropospheric Research (TROPOS), Leipzig, Germany}

6 [\*]{Institute for Micro Process Engineering, Karlsruhe Institute of Technology, Germany}

7 Correspondence to: R. Wolke ([wolke@tropos.de](mailto:wolke@tropos.de))

### 9 Abstract

10 Ambient tropospheric deliquesced particles generally comprise a complex mixture of  
11 electrolytes, organic compounds, and water. Dynamic modeling of physical and chemical  
12 processes in this complex matrix is challenging. Thus, up-to-date multiphase chemistry  
13 [models generally do not consider non-ideal solution effects. Therefore, the present study was](#)  
14 [aimed at presenting further development of the SPACCIM \(Spectral Aerosol Cloud](#)  
15 [Chemistry Interaction Model\) model through treatment of solution non-ideality, which has not](#)  
16 [been considered before. The present paper firstly describes the model developments including](#)  
17 [\(i\) the implementation of solution non-ideality in aqueous-phase reaction kinetics in the](#)  
18 [SPACCIM framework, \(ii\) the advancements in the coupling scheme of microphysics and](#)  
19 multiphase chemistry and (iii) the required adjustments of the numerical schemes, especially  
20 in the sparse linear solver and the calculation of the Jacobian. Secondly, results of sensitivity  
21 investigations are outlined aiming at the evaluation of different activity coefficient modules  
22 and the examination of the contributions of different intermolecular forces to the overall  
23 activity coefficients. Finally, first results obtained with the new model framework are  
24 presented.

25 [The parcel model SPACCIM was developed and, so far, applied for the description of](#)  
26 [aerosol-cloud interactions. To advance SPACCIM also for modeling physical and chemical](#)  
27 [processes in deliquesced particles, the solution non-ideality have to be taken into account by](#)  
28 [utilizing activities in reaction terms instead of aqueous concentrations. The main goal of the](#)  
29 [extended approach was to provide appropriate activity coefficients for solved species.](#)  
30 [Therefore, an activity coefficient module was incorporated in the kinetic model framework of](#)

**Gelöscht:** models do generally not consider

**Gelöscht:** never

**Gelöscht:** Therefore, the present study was aimed at the further development of the SPACCIM model to treat both complex multiphase chemistry and phase transfer processes considering newly non-ideality properties of concentrated aerosol solutions. The present paper describes firstly, the performed model development including

**Gelöscht:** the kinetic implementation of the non-ideality in the SPACCIM framework,

**Gelöscht:** performed

1 | [SPACCIM](#). Based on an intercomparison of different activity coefficient models and the  
2 | comparison with experimental data, AIOMFAC [approach was implemented](#), and extended by  
3 | additional interaction parameters from literature for mixed organic-inorganic systems.  
4 | Moreover, the performance and the capability of the applied activity coefficient module were  
5 | evaluated by means of water activity measurements, literature data and results of [other](#)  
6 | [activity coefficient models](#). Comprehensive comparison studies showed that the SpactMod  
7 | (SPACCIM activity coefficient module) is valuable to predict the thermodynamic behavior of  
8 | complex mixtures of multicomponent atmospheric aerosol particles. First simulations with a  
9 | detailed chemical mechanism have demonstrated the applicability of SPACCIM-SpactMod.  
10 | The simulations [indicate that](#), the treatment of [solution](#) non-ideality [might](#) be [needed](#) for  
11 | modeling multiphase chemistry processes in deliquesced particles. The modeled activity  
12 | coefficients implicate that [chemical reaction fluxes](#), of chemical processes in deliquesced  
13 | particles can be both decreased and increased depending on the particular species involved in  
14 | the reactions. For key ions, activity coefficients on the order of 0.1-0.8 and a strong  
15 | dependency on the charge state as well as the r.h. conditions are modeled implicating a  
16 | lowered [chemical processing of ions](#) in concentrated solutions. In contrast, modeled activity  
17 | coefficients of organic compounds are [in some cases larger than 1 under deliquesced particle](#)  
18 | [conditions](#) and suggest the possibility of an increased [chemical processing of organic](#)  
19 | [compounds](#). Moreover, the model runs have shown noticeable differences in the pH values  
20 | calculated with and without consideration of [solution](#) non-ideality. On average, the predicted  
21 | pH values of the simulations considering [solution](#) non-ideality are -0.27 and -0.44 pH units  
22 | lower under 90% r.h. and 70% r.h. conditions, respectively. More comprehensive results of  
23 | detailed SPACCIM-SpactMod studies on the multiphase processing in organic-inorganic  
24 | mixtures of deliquesced particles are described in a companion paper.

**Gelöscht:** The main product of the performed model development is the new kinetic model approach SPACCIM-SpactMod, which utilizes activities in reaction terms instead of aqueous concentrations.

**Gelöscht:** was selected as base model

**Gelöscht:** other thermodynamic equilibrium models

**Gelöscht:** have implied

**Gelöscht:** should

**Gelöscht:** mandatory

**Gelöscht:** turnovers

**Gelöscht:** chemical ion processing

**Gelöscht:** partly >1

**Gelöscht:** organic

## 1 Introduction

The troposphere is a complex multiphase and multicomponent environment with simultaneous occurrence of heterogeneous chemical transformations, which potentially can alter the composition of tropospheric aerosols (Ravishankara, 1997). In order to access the impact of physico-chemical and dynamical processes associated with aerosol particles, a variety of multiphase chemistry mechanisms have been developed and coupled with atmospheric models (Binkowski and Roselle, 2003; Fast et al., 2006; Seinfeld and Pandis, 2006). During the last decade, some progress was made evaluating the role of chemical aqueous phase processes in deliquesced particles and cloud droplets (see e.g., Hallquist et al. (2009); Tilgner and Herrmann (2010); Ervens et al. (2011); Tilgner et al. (2013); Guo et al. (2014)). Beside the multiphase chemistry developments and findings, the inclusion of reliable thermodynamic modules in multiphase models is required in order to adequately calculate the particle deliquescence, associated water content, chemical reactions and phase transfer processes in multicomponent aerosols at given conditions. Furthermore, these modules are in demand to compute the reactive mass transfer driving forces for dynamic gas-particle partitioning of various semi-volatile species considering complex chemical transformations in aqueous phase.

The calculation of gas to particle partitioning of water, semi-volatile inorganic and organic compounds requires the corresponding vapor pressures, which depend on the saturation vapor pressures of pure compounds and the activity coefficients in the liquid mixture. The Köhler theory (Köhler, 1936) gives a relation between the equilibrium saturation ratio  $S_w$  of water vapor above an aqueous solution droplet and the droplet equilibrium size:

$$S_w = \frac{p_w}{p_w^o} = \frac{RH}{100} = a_w \exp\left(\frac{2v_w \sigma_{w,s}}{RT r_{drop}}\right) \quad (1)$$

where  $p_w$  is the equilibrium partial pressure of water over the solution droplet,  $p_w^o$  is the equilibrium water vapor pressure over a flat surface of pure water,  $RH$  (-) is the ambient relative humidity;  $\sigma_{w,s}$  ( $N m^{-1}$ ) is the droplet solution surface tension;  $R$  ( $J mol^{-1} K^{-1}$ ) is the universal gas constant;  $T$  ( $K$ ) is the temperature;  $r_{drop}$  ( $m$ ) is mean wet radius of droplet; and  $v_w$  ( $m^3 mol^{-1}$ ) is the partial molar volume of water. The water activity  $a_w$  is given as the product of the mole fraction of water  $x_w$  in a solution and the [molality based](#) water activity

1 coefficient  $\gamma_w$ , which accounts for the effects of all intermolecular interactions that takes  
2 place in the solution. Activity coefficients give an indication of the degree of thermodynamic  
3 non-ideality. Such non-ideal conditions can be expected in deliquesced particles, where, e.g.,  
4 ionic strengths of about 1-45 mol L<sup>-1</sup> (Herrmann, 2003; Herrmann et al., 2015) are present. In  
5 a highly concentrated solution, ions and non-water molecules are more close to each other;  
6 therefore they influence each other through electrostatic forces or other physical interactions.  
7 These intermolecular forces modify the affinity of a substance to transfer from one phase into  
8 another phase or to enter into a chemical reaction. Hence [a recent review by Herrmann et al.](#)  
9 [\(2015\) suggested that for modeling of multiphase chemical processes in a concentrated](#)  
10 [solution, it is reasonable to consider the non-ideal behavior instead of assuming ideal](#)  
11 [solutions.](#) Thus, activities have to be used instead of concentrations and the appropriate  
12 calculation methods have to be [employed](#) in multiphase chemistry models. [Consequently, a](#)  
13 [range of sensitivity studies with models accounting for composition dependent processes need](#)  
14 [to be carried out to clarify the role of the non-ideal behavior, e.g., for the tropospheric](#)  
15 [multiphase chemistry in deliquesced particles and, overall, its inclusion or neglect in aerosol](#)  
16 [chemistry models.](#)

17 [In order to simulate gas/particle mass transfer in aerosol models, three main approaches \(i.e.,](#)  
18 [equilibrium, kinetic \(or dynamic\), and hybrid\) have been used in literature \(Zhang et al.,](#)  
19 [2004\). The equilibrium approach assumes equilibrium between multiple aerosol phases and](#)  
20 [the ambient gas concentrations reach equilibrium concentrations at the particle surface](#)  
21 [instantaneously. The kinetic approach does not rely on the instantaneous equilibrium](#)  
22 [assumption. In this approach, the gas/particle mass transfer due to the difference between the](#)  
23 [ambient gas concentration and equilibrium gas concentration is explicitly simulated for each](#)  
24 [particle class. Usually, hybrid models employ the kinetic approach for coarse particles and the](#)  
25 [equilibrium approach for fine particles. Thus, an aerosol thermodynamic model is an essential](#)  
26 [part of all three gas/particle mass transfer approaches.](#)

27 [Considerable effort has been devoted to develop a number of thermodynamic models with](#)  
28 [reliable accuracy and efficiency to simulate aerosol thermodynamic equilibrium. These](#)  
29 [models treat particle compositions of varying levels of complexity, often associated by the](#)  
30 [numerical technique chosen and the activity coefficient model applied. They can be divided](#)  
31 [into two types, i.e., equation-based approach and Gibbs free energy minimization approach.](#)  
32 [In the equation-based approach \(e.g. ISORROPIA II, Fountoukis and Nenes \(2007\), Nenes et](#)

Gelöscht: 19

Gelöscht: the

Gelöscht: the assumption of ideal solution in aerosol models has to be abandoned and non-ideal behavior has to be considered.

Gelöscht: applied

1 al. (1998); [EQSAM3](#), Metzger and Lelieveld (2007), Metzger et al. (2006); [EQUISOLV II](#),  
2 Jacobson (1997), Jacobson et al. (1996); [MARS-A](#), Binkowski and Roselle (2003), Saxena et  
3 al. (1986); [MESA](#), Zaveri et al. (2005a)) a set of reactions is assumed to occur in the  
4 atmospheric chemical system (including both gas phase and aerosol phase). The equilibrium  
5 state is predicted through the solution of the nonlinear equations system. In the Gibbs free  
6 energy minimization approach (e.g. [AIM](#), Clegg et al. (1998b, 1998a); [GFEMIN](#), Ansari and  
7 Pandis (1999a); [ADDEM](#), Topping et al. (2005a, 2005b); [UHAERO](#), Amundson et al. (2006);  
8 Amundson et al. (2007)), the equilibrium state of the aerosol system is predicted through the  
9 solution of minimization of the Gibbs free energy of the system. Some of the thermodynamic  
10 models mentioned above have been compared and evaluated in several studies (Ansari and  
11 Pandis, 1999b; Zhang et al., 2000; Yu et al., 2005; Metzger et al., 2006). The equilibrium  
12 approach assumes that particles are in thermodynamic equilibrium with the corresponding gas  
13 phase, i.e., the mass transfer between the phases is instantaneous. However, this assumption  
14 must not be necessarily valid for every compound and condition, for example in case of  
15 coarse particles (e.g., Wexler and Seinfeld (1990)). Therefore, the mass transfer has to be  
16 described dynamically by using kinetic or hybrid approaches (e.g., [MADM](#) by Pilinis et al.  
17 (2000)). Such aerosol modules, that treat dynamically gas-particle partitioning of inorganic  
18 and organic gases coupled to thermodynamics modules, are developed for the more general  
19 use in 3D models (e.g., [MOSAIC](#) by Zaveri et al. (2008), [MADRID](#) by Zhang et al. (2004)) or  
20 for detailed process descriptions in laboratory (e.g., [ADCHAM](#) by Roldin et al. (2014)).  
21 As mentioned above, determining appropriate activity coefficients is required in the  
22 thermodynamic models. This was achieved by using both mixing rules and potentially more  
23 accurate techniques for calculating the activity coefficients. Attempts at realistic estimation of  
24 activity coefficients can be traced back to extensive literature for inorganic electrolyte  
25 solutions (e.g., Prusnitz et al. (1986); Pitzer (1991); Clegg et al. (1998b, 1998a); Nenes et al.  
26 (1998); Metzger et al. (2002); Topping et al. (2005a); Zaveri et al. (2005a); Fountoukis and  
27 Nenes (2007)). While the interactions between inorganic compounds are relatively well-  
28 known, interactions between organic components as well as organic-electrolyte mixtures  
29 comprised in complex multiphase systems have remained elusive for some-time, due to the  
30 large number of organic species with highly variable properties available in the gas phase and  
31 in ambient particles. Starting with the more conceptual paper of Clegg et al. (2001), several  
32 approaches for the treatment of organic-inorganic mixtures in ambient particles were  
33 developed and incorporated in thermodynamic models (e.g., Ming and Russell (2002);

1 Topping et al. (2005b); Erdakos et al. (2006); Metzger et al. (2006); Clegg et al. (2008);  
 2 Zaveri et al. (2008); Zuend et al. (2008); Zuend et al. (2011); Ganbavale et al. (2015)).  
 3 Raatikainen and Laaksonen (2005) have compared different activity coefficient models, and  
 4 four models were extended by fitting new parameters for aqueous organic-electrolyte  
 5 solutions. Most of these revised activity coefficient models are based on an extension of the  
 6 UNIFAC concept. Erdakos et al. (2006) further developed these extended UNIFAC models.  
 7 Zuend et al. (2008) fitted the interaction parameters for the organic compounds (alcohols and  
 8 polyols) and inorganic ions. AIOMFAC is based on the group-contribution model LIFAC  
 9 (Yan et al., 1999) and yet modified in many respects to better represent relevant species,  
 10 reference states, and the relative humidity range of the atmosphere. Recently, Zuend et al.  
 11 (2011), Mohs and Gmehling (2013) and Ganbavale et al. (2015) proposed revised and  
 12 extended parameterizations for mixtures containing various organic functional groups, water  
 13 and inorganic ions.  
 14 Complex multiphase chemistry model dealing with deliquesced particles usually do neglect or  
 15 roughly estimate the effect of solution non-ideality on the chemical processing (see, e.g.,  
 16 Tilgner and Herrmann (2010); Bräuer et al. (2013); Mao et al. (2013); Tilgner et al. (2013);  
 17 Guo et al. (2014)). However, model studies (e.g., Bräuer et al. (2013); Tilgner et al. (2013))  
 18 implicated that deliquesced particles might be a potentially important medium for multiphase  
 19 chemistry. Thus, the present study was aimed at the implementation of solution non-ideality  
 20 in aqueous-phase reaction kinetics into the Spectral Aerosol Cloud Chemistry Interaction  
 21 Model (SPACCIM, Wolke et al. (2005)). Accordingly, an activity module has to be  
 22 implemented in SPACCIM to provide appropriate activity coefficients for dissolved species.  
 23 The parcel model SPACCIM was originally developed for the dynamical description of  
 24 chemical and microphysical cloud processes. SPACCIM was successfully applied in several  
 25 process studies using the complex multiphase mechanism CAPRAM (Herrmann et al., 2005;  
 26 Tilgner and Herrmann, 2010; Bräuer et al., 2013; Tilgner et al., 2013).  
 27 In this paper, we present an extended model approach for the kinetic description of phase  
 28 transfer and complex multiphase chemistry considering the non-ideality of solutions by means  
 29 of activity coefficient models. This paper split into 4 sections. In section 2, we described the  
 30 implementation of solution non-ideality into the SPACCIM model. In subsequent subsections,  
 31 the coupling between microphysics and multiphase chemistry models as well as the necessary  
 32 adjustments of numerical schemes is discussed. In Sect. 2.3, the activity coefficient module is

**Gelöscht:** (Bräuer et al., 2013; Tilgner et al., 2013)

**Gelöscht:** Ganbavale et al. (2015)

**Gelöscht:** proposed a revised and extended parameterization for mixtures containing various organic functional groups, plus water and inorganic ions. As this work incorporated the first set of parameterization from Zuend et al., 2008, and since the inorganic ions and organic functional groups are limited, we extended the interaction parameter dataset from mod. LIFAC (Kiepe et al., 2006). Since the large set of experimental data is required in order to fit the parameters, which is not focus of this study, we have taken the additional interaction parameters from mod. LIFAC and created a parameter matrix in order to estimate the activity coefficients in multicomponent mixture. ... [3]

**[1] verschoben (Einfügung)**

**Gelöscht:** Attempts at realistic estimation of activity coefficients can be traced back to extensive literature for inorganic, organic and mixed inorganic-organic solutions (e.g., Prausnitz et al. (1986); Pitzer (1991); Li et al. (1994); Yan et al. (1999); Ming and Russell (2002); Raatikainen and Laaksonen (2005); Topping et al. (2005a, 2005b); (Zaveri et al., 2005a); Erdakos et al. (2006); Clegg et al. (2008); Zuend et al. (2008); Zuend et al. (2011)). Considerable effort has been devoted formerly to develop a number of thermodynamic models with reliable accuracy and efficiency to simulate aerosol thermodynamic equilibrium (e.g. AIM (Clegg et al., 1998b, a), GFEMIN (Ansari and Pandis, 1999a), ISORROPIA and ISORROPIA II (Nenes et al., 1998; Fountoukis and Nenes, 2007), EQSAM3 (Metzger et al., 2006; Metzger and Lelieveld, 2007), EQUISOLV II (Jacobson et al., 1996; Jacobson, 1997); MARS-A (Saxena et al., 1986; Binkowski and Roselle, 2003), MESA (Zaveri et al., 2005b); UHAERO (Amundson et al., 2006; Amundson et al., 2007)). Various numerical techniques were developed based on direct minimization of Gibbs free energy, which is highly accurate, yet computationally expensive (Ansari and Pandis, 1999a; Wexler et al., 2002). Most of these models assume that particles are in thermody... [1]

**Gelöscht:** Pilinis et al. (2000)

**Gelöscht:** Zuend et al. (2011)

**Gelöscht:** ). Only very few model approaches exist so far, that treat dynamically gas-particle partitioning of inorganic and organic gases co... [2]

**Gelöscht:** Zaveri et al. (2008)

**Gelöscht:** . ADCHAM by

**[1] nach oben verschoben:** Hence, the development of kinetic model frameworks for modeling of processes in multicomponent atmospheric particles, which include both a d... [5]

**Gelöscht:** Roldin et al. (2014)

**Gelöscht:** Ervens et al. (2011)

**Gelöscht:** ). However, such a kinetic model framework is needed to more precisely examine the role of concentrated aerosol solutions for the chemical processing of aerosol constitutes an... [4]

**Gelöscht:** Wolke et al. (2005)

**Gelöscht:** ). The parcel model SPACCIM was originally developed for the dynamical description of chemical and microphysical cloud processes. SPACCIM was successfully applied in sever... [6]

1 [introduced, that is specifically designed to treat multicomponent mixed organic–inorganic](#)  
2 [aerosol particles. Section 3 presents an evaluation of the currently implemented activity](#)  
3 [coefficient module in SPACCIM. In order to validate the model performance and the](#)  
4 [capability, the model results were compared with available measurements and other activity](#)  
5 [coefficient models such as mod. LIFAC \(Kiepe et al., 2006\), E-AIM \(Clegg et al., 1998b, a\),](#)  
6 [and AIOMFAC \(Zuend et al., 2008\). Furthermore, Sect. 3 presents sensitivity studies on the](#)  
7 [importance of the different interactions and first model results obtained with the new model](#)  
8 [framework.](#)

Gelöscht: .

... (7)

## 10 **2 Methodology and model development**

### 11 **2.1 Multiphase model SPACCIM (original code)**

12 In this section, a brief summary is provided for the methods used in SPACCIM original  
13 code and the current limitations are outlined. The air parcel model SPACCIM was  
14 developed for the description of simultaneously occurring chemical and physical processes in  
15 cloud droplets and deliquesced particles. Thus, SPACCIM combines a complex multiphase  
16 chemistry model with a detailed cloud microphysics for a size-resolved particle/droplet  
17 spectrum in a box model framework (Wolke et al., 2005). Depending on the used  
18 microphysical model, external and internal mixing of aerosol can be taken into account. The  
19 activation of droplets is explicitly described. Either the movement of the air parcel can follow  
20 a predefined trajectory (e.g., simulated by a 3D atmospheric model) or the vertical velocity is  
21 calculated based on the parcel updraft compared to prescribed environmental conditions.  
22 Entrainment and detrainment processes are considered in a parameterized form. The model  
23 allows a detailed description of the processing of gases and particles shortly before cloud  
24 formation, during the cloud life time and shortly after cloud evaporation (Sehili et al., 2005).  
25 [The droplet activation depending on the particle size and composition is explicitly described](#)  
26 [\(see Sehili et al. \(2005\) and Wolke et al. \(2005\)\).](#)

27 All microphysical parameters needed by the multiphase chemistry are taken over from the  
28 microphysical model. For this purpose, [a robust and efficient](#) coupling scheme between  
29 microphysical and multiphase chemical models is implemented. The coupling scheme [is](#)  
30 [adjusted to the applied time integration method and](#) provides time-interpolated values of the  
31 microphysical parameters (temperature, water vapor, liquid water content) and time-averaged

Gelöscht: an advanced

1 mass fluxes between different droplet classes caused by microphysical processes (e.g., by  
2 aggregation, break up, condensation). Changes of the chemical aerosol composition by gas  
3 scavenging and chemical reactions feed back on the microphysical processes (e.g., water  
4 condensation growth rates via changes in the Raoult term). [Consequently, related processes](#)  
5 [such as co-condensation \(see Topping et al. \(2013\) for details\) are considered in the model.](#)

6 The multiphase chemistry is performed for ideal solutions assuming well-mixed droplets.  
7 Activity coefficients and the diffusion inside of the droplets are not considered. Dissociations  
8 are described dynamically as forward and backward reactions. The [applied multiphase](#)  
9 [chemical mechanism \(including phase transfer data and kinetic reaction constants\) is provided](#)  
10 as an input file. Therefore, a high flexibility concerning changes in the chemical mechanism  
11 or the replacement of the entire reaction system is guaranteed. For further details, the reader  
12 is referred to the original publication by (Wolke et al., 2005). The performance of the model  
13 was shown for both simple chemical mechanisms considering inorganic chemistry only and  
14 for very complex mechanisms of the CAPRAM family, which contain a detailed description  
15 of the inorganic and organic chemistry (Herrmann et al., 2005; Tilgner and Herrmann, 2010;  
16 Bräuer et al., 2013; Tilgner et al., 2013).

17 In the published version of SPACCIM (Wolke et al., 2005), the influence of [solution](#) non-  
18 ideality on multiphase processing was not considered. In fact, the assumption of an ideal  
19 solution is not valid particularly for deliquescent particles, where highly concentrated  
20 solutions are typical present. Accordingly, the chemical reaction terms in the aqueous phase  
21 chemistry have to be modified by using the activities and therefore an activity coefficient  
22 module has to be added. Furthermore, the feedback approach is enhanced by using the  
23 calculated water activity for the Raoult term and by the consideration of surface tension  
24 effects. The changes in the model code are given in the following subsection.

## 25 **2.2 Further development of SPACCIM**

### 26 **2.2.1 Mass balance equations**

27 For the consideration of [solution](#) non-ideality effects in SPACCIM, it is required that rate  
28 expressions have to be written in terms of species activities, rather than mole fractions or  
29 concentrations. The activity  $a_i$  of species  $i$  can be expressed by  $a_i = \gamma_i \cdot m_i = \gamma_i \cdot c_i / L$  where  
30  $\gamma_i$  denotes the molality based activity coefficient,  $m_i$  the molality and  $c_i$  the mass

Gelöscht: used

Gelöscht: given

1 concentration of an aqueous phase species  $i$ . The liquid water content  $L$  is given as the water  
 2 [mass](#) in the corresponding box volume. In the proposed approach, the non-ideal behavior is  
 3 taken into account by means of activity coefficients. It should be emphasized that the activity  
 4 coefficient  $\gamma_i$  depends usually on the concentrations of all species dissolved in the solution.

Gelöscht: volume

Gelöscht: fraction

5 In Eqs. (1) and (2), the mass balance equations of the modified version of SPACCIM  
 6 extended by the treatment of [solution](#) non-ideality are presented. [In particular](#), the aqueous  
 7 concentrations in the original mass balance equations of the SPACCIM (see Eqs. (1) and (2)  
 8 in Wolke et al. (2005)) are replaced by corresponding activities.

Gelöscht: Mainly

9 The description of both microphysical and multiphase chemical processes is performed for a  
 10 size-resolved particle/cloud droplet spectrum, which is subdivided into several classes  
 11  $k = 1, \dots, M$ . In each particle/droplet class,  $N_A$  aqueous phase species are treated, which are  
 12 not necessarily identical to the number of gas phase species  $N_G$ . In the parcel model  
 13 SPACCIM, the prognostic equations for the mass concentrations of a gas phase chemical  
 14 species  $c_i^G$  and an aqueous phase chemical species  $c_i^k$  in the  $k^{\text{th}}$  class have to take into  
 15 account the chemical productions and degradations, phase transfers, mass transport between  
 16 different classes caused by microphysical processes, and ent-/detrainment. These processes  
 17 can be described by the following mass balance equations:

$$18 \quad \frac{d(c_i^G)}{dt} = \underbrace{R_i^G(t, c_1^G, \dots, c_{N_G}^G)}_{\text{gas phase chemistry}} - \underbrace{\kappa_i \sum_k L_k k_i^{ki} \left[ c_i^G - \frac{a_i^k}{H_i} \right]}_{\text{phase transfer}} + \underbrace{\mu [c_i^G - c_i^{G_{ent}}]}_{\text{entrainment/ outflow}}, \quad (2)$$

$$19 \quad \frac{d(c_i^k)}{dt} = \underbrace{L_k R_i^A(t, a_1^k, \dots, a_{N_A}^k)}_{\text{aqueous phase chemistry}} + \underbrace{\kappa_i L_k k_i^{ki} \left[ c_i^G - \frac{a_i^k}{H_i} \right]}_{\text{phase transfer}} + \underbrace{F(c_1^1, \dots, c_i^M)}_{\text{mass transfer by microphysics}} + \underbrace{\mu [c_i^k - c_i^{k_{ent}}]}_{\text{entrainment/ outflow}}, \quad (3)$$

20 with  $i^s = 1, \dots, N_G$ ;  $i = 1, \dots, N_A$ ;  $k = 1, \dots, M$ .

21 In the above formulation,  $L_k$  denotes [the liquid water content](#) of the  $k^{\text{th}}$  droplet class inside  
 22 the box volume. The values  $a_i^k, k = 1, \dots, M$ , represent the activities of species  $i$  in the  $k^{\text{th}}$   
 23 liquid water fraction. The vector  $c^G$  stands for the concentrations of the gas phase species  
 24 and  $k_i^{ki}$  is the mass transfer coefficient. The chemical reaction terms of the corresponding  
 25 species are denoted by  $R_i^G$  and  $R_i^A$ . The second term on the right-hand side of the

Gelöscht: the

Gelöscht: volume fraction  $[V_k/V_{\text{box}}]$

Gelöscht: /

1 aforementioned equations describe the change of mass concentration of the soluble species  
 2 due to phase transfer between the gas phase and particle/cloud droplet classes. Hence, this  
 3 term will be referred to as the Henry term in the following. The value  $H_i$  denotes here the  
 4 dimensionless Henry's law coefficient for species  $i$ . The prefactor  $\kappa_i$  of the Henry term is a  
 5 solubility index and defined to be equal to 1 as well as 0 for soluble and insoluble species,  
 6 respectively (see Wolke et al. (2005)). The term  $F(c_i^1, \dots, c_i^M)$  in Eq. (3) stands for the mass  
 7 transfer between different droplet classes by microphysical exchange processes (e.g. by  
 8 aggregation, break up, condensation). The time-dependent natural and anthropogenic  
 9 emissions as well as dry and wet deposition are parameterized in the last terms of the right  
 10 hand sides using a time dependent entrainment/detrainment rate  $\mu$ . One should note that,  
 11 above-mentioned mass balance equations are not only limited to "non-ideal" approach.  
 12 Whenever, the activity coefficients are defined as unity then this numerical model formulation  
 13 will reduce to the original version of SPACCIM.

### 14 2.2.2 Reaction kinetics

15 The first terms  $R_i^G$  and  $R_i^A$  in the right hand sides of the mass balance Eqs. (2) and (3)  
 16 comprise the chemical transformations (production and degradation fluxes). However, the  
 17 reaction term included in Eq. (2) is only a function of concentrations of gas phase species.  
 18 Since, the gas phase mixture is assumed to be behaving as an ideal gas phase mixture, the  
 19 non-ideality is not considered in this term.

20 Suppose, for an irreversible reaction  $A + B \rightarrow C + D$  in the aqueous phase, the reaction rate  
 21  $r_A$  can be written while considering the [solution](#) non-ideality as follows:

$$22 \quad r_A = -k_A \cdot [a_A] \cdot [a_B] = -k_A \cdot \gamma_A [A] \cdot \gamma_B [B], \quad (4)$$

23 Here, the activities of A, B, C, and D are used instead of the concentrations. The activity of A  
 24 ( $a_A$ ) is proportional to its molar concentration (either molality based or mole fraction based)  
 25  $[A]$ , where the proportional constant is the activity coefficient  $\gamma_A$  of that particular species.

26 The treatment of [solution](#) non-ideality was also considered for equilibrium reaction types,  
 27 which should be explained with the generic example shown as:



29 The relative quantities (i.e. thermodynamic activities) of reactants and products in an

1 equilibrium reaction are determined from the equilibrium relation,

$$2 \quad \sum_i \{a_i\}^{\lambda_i} = \frac{\{A\}^{v_A} \cdot \{B\}^{v_B}}{\{C\}^{v_C} \cdot \{D\}^{v_D}} = \frac{(\gamma_A^{v_A} \cdot [A]^{v_A}) \cdot (\gamma_B^{v_B} \cdot [B]^{v_B})}{(\gamma_C^{v_C} \cdot [C]^{v_C}) \cdot (\gamma_D^{v_D} \cdot [D]^{v_D})} = K_{eq}, \quad (6)$$

3 where  $K_{eq}$  called as equilibrium coefficient,  $\{a_i\}$  is the thermodynamic activity of species  $i$ ,  
4  $\{A\}$ , etc., are individual thermodynamic activities,  $\lambda_i = +1$  for products, and  $\lambda_i = -1$  for  
5 reactants. As mentioned earlier, activity of a species A is its molality  $m_A$  multiplied by its  
6 activity coefficient  $\gamma_A$ . A solute activity coefficient represents the deviation from ideal  
7 behavior of the solute in solution. Hence, the concentration dependent activity coefficients are  
8 estimated for all soluble species. Note, that the activity coefficients for neutral inorganic  
9 species (such as  $O_{2(aq)}$ ) are defined as unity. At the same time, the activity coefficients of  
10 radicals are also defined as unity, since their reactivity is quite fast and lifetime is rather  
11 small. The consideration of activities in the SPACCIM framework for different types of  
12 species is summarized in Table 1.

### 13 2.2.3 Phase transfer processes

14 The dynamical description of phase transfer processes between the gas and liquid phases in  
15 SPACCIM is specified according to the Schwartz approach (Schwartz, 1986). During  
16 dissolution, the saturation vapor pressure of gas A can be determined from the equilibrium  
17 relationship  $A_{(g)} \rightleftharpoons A_{(aq)}$ . Thus, in terms of an arbitrary gas  $i$  the Henry's law is defined as:

$$18 \quad p_{i,k}^s = \frac{m_i^k}{K_i^H}, \quad (7)$$

19 where  $p_{i,k}^s$  is the saturation vapor pressure (atm) of gas phase species  $i$  over a particle in size  
20 bin  $k$ ,  $m_i^k$  (mol kg<sup>-1</sup>) is the molality of dissolved gas phase species  $i$  in particle class  $k$ , and  
21  $K_i^H$  (mol kg<sup>-1</sup> atm<sup>-1</sup>) is the corresponding Henry constant. [It has to be noted here that the](#)  
22 [Henry's law constants of an aqueous solution depend on the composition of the aqueous](#)  
23 [solution, e.g., on the electrolyte identity of the solution \(ionic strength, etc.\). Non-ideal](#)  
24 [electrolyte solutions are able to both suppress the uptake \("salting-out"\) and enhance the](#)  
25 [uptake \("salting-in"\) of soluble gases compared to value for pure water uptake \(Herrmann et](#)  
26 [al., 2015\). These salting effects can be quantitatively described by the Setschenow equation](#)

(Sander, 2015). However, as reported in the review of Sander (2015), there are unfortunately only limited data available. Therefore, salt effects are only considered in the SPACCIM model due to the consideration of the activity coefficients in the uptake calculation. The model results should be therefore treated with caution particularly at higher ionic strengths of the solution due to the lower range of functionality of Henry's law coefficients compared to the applicability range of present activity coefficient models.

The above-mentioned saturation vapor pressure is related to the saturation vapor mole concentration  $c_{i,k}^s$  ( $\text{mol m}^{-3}$ ) by

$$p_{i,k}^s = c_{i,k}^s RT, \quad (8)$$

where  $R$  denotes the universal gas constant in ( $\text{atm m}^3 \text{mol}^{-1} \text{K}^{-1}$ ) and  $T$  (K) the temperature.

Then, Eq. (7) can be expressed in terms of concentrations rather than molalities and partial pressures as:

$$c_{i,k}^s = \frac{p_{i,k}^s}{RT} = \frac{m_i^k}{K_i^H RT} = \frac{m_i^k}{H_i}. \quad (9)$$

Here  $H_i = K_i^H RT$  stands for the dimensionless Henry constant. Considering the solution non-ideality in the aqueous phase, the molalities  $m_i^k$  are replaced by the activities  $a_i^k = \gamma_i^k m_i^k$ . Considering  $M$  classes of particles associated, we state the appropriate expression for gas-phase loss while neglecting the Kelvin effect (following Jacobson (1997)):

$$\frac{dc_i^G}{dt} = -\sum_k k_i^{ki} L_k \left( c_i^G - \frac{a_i^k}{H_i} \right). \quad (10)$$

Eq. (10) pertains to the case of a single gas phase species equilibrating between the gas and aqueous aerosol phases, with the mass transfer coefficient  $k_i^{ki}$  defined by

$$k_i^{ki} = \left( \frac{r_k^2}{3D_i^G} + \frac{4r_k}{3v_i\alpha_i} \right), \quad (11)$$

which depends on the droplet size  $r_k$ , the gas diffusion coefficient  $D_i^G$ , the molecular speed  $v_i$  and the mass accommodation coefficient  $\alpha_i$  of the  $i^{\text{th}}$  species. These quantities play a decisive role in determining the rate of uptake of gaseous species by, and evaporation from

Gelöscht: On the other hand, the

1 aerosol particles, respectively, governing the timescale for a droplet to attain an equilibrium  
2 (Schwartz, 1986).

### 3 2.2.4 Coupling scheme

4 The coupling between microphysics and multiphase chemistry models in SPACCIM follows  
5 the so-called “operator splitting” technique. As described in Sehili et al. (2005), the coupling  
6 scheme provides time-interpolated values of the meteorological variables (temperature, water  
7 vapor, liquid water content) and generates the time-averaged mass fluxes  $F$  over the coupling  
8 time interval. The changes in the chemical aerosol composition by gas scavenging and the  
9 chemical reactions have a continuous feedback on the microphysical processes (e.g. water  
10 condensation growth rates via changes in surface tension and the Raoult term/water activity).

11 For the “non-ideal” approach in SPACCIM, the coupling scheme is modified, since activity  
12 coefficients have to be considered in both models. At the same time, the activity coefficients  
13 are repeatedly required to compute the chemical transformations and the phase transfer terms  
14 (see Sect. 2.2.2 and 2.2.3). Furthermore, the modified activity coefficients as well as the  
15 parameterized surface tension are delivered back to the microphysical model. Fig. 1 illustrates  
16 this coupling strategy between microphysical and multiphase chemistry model as well as their  
17 interexchange while considering non-ideal solutions and surface tension effects (see Sect.  
18 2.2.6). The coupling strategy enables a continuous feedback of the multiphase chemistry on  
19 the microphysical processes such as water condensational growth. The two models run  
20 separately and exchange information at every coupling time step (see Fig. 2). Moreover, both  
21 widely separated operating models use its individual time-step control. This is necessary in  
22 order to ensure a high flexibility regarding the usage of models with different complexities  
23 and numerical efficiency. The coupling between both models and the activity coefficient  
24 module utilize well-defined interfaces for the intercommunication of codes while considering  
25 the aqueous phase chemistry in non-ideal solutions. Furthermore, the interpolation and  
26 averaging of the required meteorological variables and parameters are arranged and  
27 implemented in the same way as described in Wolke et al. (2005).

### 28 2.2.5 Feedback of non-ideal aqueous phase chemistry on microphysics

29 Microphysical processes described in SPACCIM include equilibrium growth of aerosol  
30 particles and condensational growth of the droplets (Simmel and Wurzler, 2006). The Köhler  
31 equation (see e.g., Köhler (1936); Pruppacher and Klett (1997)) gives the saturation ratio of

1 water vapor at particle/air interface, which depends on the chemical composition, the droplet  
 2 diameter and the surface tension of the particle. In SPACCIM, the non-linear relationship  
 3 Eq. (1) is used to determine the equilibration of water between the liquid and surrounding  
 4 vapor phase [for non-activated particles](#). The water saturation pressure in Eq. (1) is affected by  
 5 the curvature of the particle (also known as Kelvin effect) and the water activity, which is  
 6 determined by the solutes (Raoult effect). Previously, Wolke et al. (2005) calculated the  
 7 Raoult term in the condensation rate using osmotic coefficient, according to Pruppacher and  
 8 Klett (1997). While, the intention was to allow the feedback of chemical particle composition  
 9 onto microphysics, the Raoult term was replaced by the sum of molar ratios of all soluble  
 10 species included in the multiphase system:

$$11 \quad Raoult_{chem}^k = \frac{\sum_i^{N_A} mol_{sol_i}^k}{mol_w^k}. \quad (12)$$

12 Here, the quantities  $mol_{sol_i}^k$  of soluble material are obtained from the multiphase chemistry.  
 13 The molar water fraction  $mol_w^k$  varies and is taken directly from the microphysics. The Raoult  
 14 term in Eq. (12) depends on all soluble species. In the non-ideal approach of SPACCIM, the  
 15 water activity  $a_w^k$  estimated from activity coefficient module (see Sect. (2.3)), is used directly  
 16 for the Raoult term in microphysics. On the other hand, the description of change in droplet  
 17 curvature (Kelvin effect) is [treated with surface tension approaches](#) (see Subsect. 2.2.6).

18 Both effects are [influenced](#) by the particle composition, which is continuously changed by  
 19 phase transfer and multiphase processes. However, the mass concentrations of all species are  
 20 kept fixed for the microphysics over a coupling time step (see Fig. 1). But the molalities and,  
 21 therefore, the Kelvin and Raoult terms are changed caused by the adjustment of the [liquid](#)  
 22 [water content](#), Eq. (1) has to be fulfilled simultaneously for all non-activated particle classes.

23 The droplet activation is described explicitly and takes place for all particles, which grow  
 24 over the critical radius. The condensation and evaporation of the activated droplet classes are  
 25 described dynamically. The predicted saturation vapor pressure is used as input into the  
 26 droplet growth equation. The coupled system for all classes has to be solved simultaneously,  
 27 whereas the total amount of water (liquid or gaseous) is prescribed. This leads to a nonlinear  
 28 system, which has to be solved iteratively at each microphysical time step. A more detailed  
 29 description of the iterative procedure is given in Simmel and Wurzler (2006). A new solution  
 30 of the system is obtained, and defines the equilibrium saturation ratio and the corresponding

**Gelöscht:** precisely

**Gelöscht:** primarily appointed

**Gelöscht:** LWCs

1 | particle/droplet diameters. This implies changes in the corresponding [liquid water contents](#)  
2 | and, hence, in the molalities. Consequently, the water activity and the surface tension have to  
3 | be recalculated at each microphysical time step. A description of the equilibration algorithm is  
4 | presented schematically in Fig. 2. Based on this, SPACCIM allows an ongoing feedback of  
5 | the chemical particle composition onto microphysics. Conversely, the microphysical model  
6 | provides all microphysical variables for integrating the multiphase chemical system, such as  
7 | [liquid water content](#),  $T$  and the mass fluxes  $F$  at the coupling time step (see Fig. 1).

Gelöscht: LWC

Gelöscht: LWC

## 8 | [2.2.6 Surface tension](#)

9 | [Surface-active substances present at the interface and organic compounds dissolved in the](#)  
10 | [solution can significantly influence the surface tension and thus can affect cloud droplet](#)  
11 | [activation and hygroscopic growth \(Shulman et al., 1996; Facchini et al., 2000; Tuckermann](#)  
12 | [and Cammenga, 2004; Topping et al., 2007; Prisle et al., 2012\). A reduction of surface](#)  
13 | tension in atmospheric cloud and fog water samples was highlighted in several studies (e.g.,  
14 | Facchini et al. (1999); Facchini et al. (2000); Mircea et al. (2002); Nenes et al. (2002)).  
15 | Furthermore, Henning et al. (2005) and Svenningsson et al. (2006) measured a surface tension  
16 | [lowering for organic mixtures in laboratory studies. On the other hand, Sorjamaa et al. \(2004\)](#)  
17 | [and Sorjamaa and Laaksonen \(2006\) pointed out that surface-active substances can enrich at](#)  
18 | [the particle/droplet surface.](#)

19 | [A first specific relationship between water-soluble organic aerosol concentration and surface](#)  
20 | [tension has been derived by fitting the equation of Szyszkowski-Langmuir to Po Valley fog](#)  
21 | [data \(Facchini et al., 1999\). Model approaches that can estimate the surface tension of](#)  
22 | [inorganic, organic systems and mixed inorganic/organic systems were proposed by Topping](#)  
23 | [et al. \(2007\). Recently, sophisticated parameterizations were developed for modeling the](#)  
24 | [combined effects of both bulk-surface partitioning and surface tension on cloud droplet](#)  
25 | [activation of organic aerosols \(Topping \(2010\); Prisle et al. \(2011\); Raatikainen and](#)  
26 | [Laaksonen \(2011\)\). However, Prisle et al. \(2012\) suggested neglecting the surfactant effects](#)  
27 | [instead of employing the numerical parameterizations calculating the reduction of surface](#)  
28 | [tension.](#)

29 | [Since the present paper is aimed at the treatment of solution non-ideality in a multiphase](#)  
30 | [chemistry model framework, the model development considered the influence of surface](#)  
31 | [tension on droplet activation, as a first step, with more simplified parameterizations of](#)

1 [Facchini et al. \(1999\)](#) and [Ervens et al. \(2004\)](#) only. The implementation of more advanced  
2 approaches in SPACCIM will be subject of future development efforts.

3 [In the present work](#), the following relationship proposed by [Facchini et al. \(1999\)](#) was  
4 implemented in the SPACCIM framework:

$$5 \sigma_{w,s}^k = \sigma_w^k - 0.01877 \cdot T \cdot \ln(1 + 628.14 \cdot [C^k]), \quad (13)$$

6 where  $T$  is the temperature in K and  $[C^k]$  represents the concentration of WSOC (Water  
7 Soluble Organic Carbon,  $\text{mol C L}^{-1}$ ) in particle class  $k$ . In addition, a combined approach for  
8 accounting for a simultaneous change in  $\sigma_{w,s}^k$  and the mean molar mass of solute  $M_{sol}$  derived  
9 by [Ervens et al. \(2004\)](#) was also implemented in the present work:

$$10 \sigma_{w,s}^k = \sigma_w^k - 0.01877 \cdot T \cdot \ln(1 + 628.14 n_c c_{sol}^k), \quad (14)$$

11 where  $c_{sol}^k$  is the solute concentration in ( $\text{mol L}^{-1}$ ) and  $n_{cb}$  represents the number of carbon  
12 atoms defined by

$$13 n_{cb} = \frac{M_{sol}}{2.2 M_c}, \quad (15)$$

14 with  $M_c = 12 \text{ g mol}^{-1}$ .

## 15 2.2.7 Adjustment of numerical schemes

16 In order to treat aqueous phase chemistry considering newly [solution](#) non-ideality effects, the  
17 numerical schemes used in [Wolke et al. \(2005\)](#) are required to adjust, mainly, (i) the time  
18 integration scheme, (ii) the computation of Jacobian matrix and (iii) the sparse linear solver.  
19 The system of mass balance equations (Eqs. (2) and (3)) is integrated in an implicit and  
20 coupled manner by higher order backward differential formula (BDF) schemes (e.g., [Hairer et](#)  
21 [al. \(1993\)](#)). In any implicit multistep method, the main computational task is the solution of a  
22 non-linear equation of the form:

$$23 \mathbf{F}(\mathbf{c}^{n+1}) = \mathbf{c}^{n+1} - \mathbf{X}^n - \beta \Delta t_n \mathbf{f}(t_{n+1}, \mathbf{c}^{n+1}) = 0, \quad (16)$$

24 where  $\mathbf{f}(t_{n+1}, \mathbf{c}^{n+1})$  stands for the right hand side of Eqs. (2) and (3).  $\beta > 0$  is a parameter of

**Gelöscht:** The calculation of droplet solution surface tension  $\sigma_{w,s}$  with simultaneous changes in solute concentration  $C_{sol}$  is almost a linear approximation: ... [8]

**Gelöscht:** [Facchini et al. \(1999\)](#)

**Gelöscht:** , was implemented in SPACCIM ... [9]

**Gelöscht:** [Ervens et al. \(2004\)](#)

**Gelöscht:** was also implemented in the present work: ... [10]

**Gelöscht:** 7

1 the integration method and  $\mathbf{X}^n$  is a linear combination of previous values. If equation (16) is  
2 solved by a Newton-like method, the main burden is the approximate solution of linear  
3 systems of the form:

$$4 \quad (\mathbf{I} - \beta \Delta t \mathbf{J}) \Delta \mathbf{c} = \mathbf{b} \quad (17)$$

5 where  $I$  denotes the identity matrix and  $\Delta t$  represents the time step size. The matrix  $\mathbf{J}$  stands  
6 for an approximation of the Jacobian  $\partial \mathbf{f}(t, \mathbf{c}) / \partial \mathbf{c}$  of the right hand side of the ordinary  
7 differential equation (ODE) system. The vector  $\mathbf{b}$  is given as:

$$8 \quad \mathbf{b} = \mathbf{c}^n - \mathbf{X}^n - \beta \Delta t_n \mathbf{f}(t_n, \mathbf{c}^n) \quad (18).$$

9 Usually, the dimension of the linear system Eq. (17) is rather high. Large systems can be  
10 solved with reasonable effort by iterative or direct sparse solvers, which utilize the special  
11 structure of the system (sparsity, block structure, different types of coupling). Such efficient  
12 solvers are already developed and applied in the former version of SPACCIM for the “ideal”  
13 approach (see Wolke and Knoth (2002); Wolke et al. (2005) for further details).

14 In this case, the Jacobian structure of the right-hand side of the multiphase system (Eq. (2)  
15 and Eq. (3)) for two droplet classes is shown in Fig. 3. As can be seen, the dots are usually  
16 non-zero entries means that the species in the row depends on the species in the column. The  
17 diagonal elements of the Jacobian describe the dependence from the species itself. These  
18 entries can be caused by chemical reactions and phase transfer, but also by the terms from  
19 microphysical fluxes and entrainment.

20 The block structure shown in Fig. 3 can be explained as follows: the blocks in the diagonal  
21 correspond to the Jacobian of the gas phase and aqueous phase reaction terms, respectively.  
22 The upper left block (light blue) represents the gas phase. The other two diagonal blocks  
23 (blue) are related to the aqueous phase chemistry attained to have the same sparse structure.  
24 The left and upper boundary blocks (green) represent the phase interchange between gas  
25 phase species and corresponding aqueous phase species in each class, according to (Schwartz,  
26 1986). The orange diagonal matrices include the coupling terms resulting from the mass  
27 transfer between liquid species and the corresponding species in the other classes. These  
28 sparse block matrices are generated explicitly and stored in sparse form. The linear system  
29 (see Eq. (18)) is solved by a sparse LU decomposition with diagonal pivoting. An optimal  
30 order of the pivot elements to avoid fill-in is determined by an adjusted Meis–Markowitz

Gelöscht: 7

Gelöscht: 8

Gelöscht: J

Gelöscht: b

Gelöscht: 9

Gelöscht: 8

Gelöscht: 9

1 strategy (Wolke and Knoth, 2002). In fact, only an appropriate approximation of the Jacobian  
 2 is required to ensure the convergence of the Newton-like method for the corrector iteration  
 3 (Eq. (17)). Therefore, the sparse factorization is stored and has to be performed only when the  
 4 Jacobian  $J$  is recomputed.

Gelöscht: 8

5 The adjusted numerical scheme works robust and very efficient for the “ideal” case. But these  
 6 effective approaches can only be used in the “non-ideal” case, if the special sparse and block  
 7 structure can be largely preserved. The calculation of the Jacobian has to be performed by  
 8 applying the “chain rule” for the aqueous phase reaction and mass transfer terms in the model  
 9 equations Eq. (2) and Eq. (3). These terms depend on the activities instead of the molalities in  
 10 difference to the ideal case. While the “outer” derivatives are unchanged, the “inner”  
 11 derivatives have to be modified. In case that  $\mathbf{c}^k$  is the vector of all concentrations and  $L^k$  the  
 12 liquid water content in the  $k^{\text{th}}$  droplet class, the gradient with respect to vector  $\mathbf{c}^k$  is denoted  
 13 as

$$14 \quad \nabla_{\mathbf{c}^k} = \left( \frac{\partial}{\partial \mathbf{c}_1^k}, \dots, \frac{\partial}{\partial \mathbf{c}_{N_A}^k} \right). \quad (19)$$

Gelöscht: 20

15 In the ideal approach the molalities depend only on the corresponding species itself. Then the  
 16 gradient of the molalities is given as follows:

$$17 \quad \nabla_{\mathbf{c}^k} m_j^k(c_j^k) = \frac{1}{L^k} (0, \dots, 0, 1, 0, \dots, 0). \quad (20)$$

Gelöscht: 1

18 In the above formulation, the gradient has only one entry in the  $j^{\text{th}}$  position, which conserves  
 19 the structure of the “outer” Jacobian. Contrary, while applying the chain rule, the gradient for  
 20 non-ideal solutions would be:

$$21 \quad \nabla_{\mathbf{c}^k} a_j^k(\mathbf{c}^k) = \frac{c_j^k}{L^k} \cdot \left( \nabla_{\mathbf{c}^k} \gamma_j^k(\mathbf{c}^k) \right) + \frac{1}{L^k} \cdot (0, \dots, 0, \gamma_j^k, 0, \dots, 0) \quad (21)$$

Gelöscht: 2

22 where the gradient  $\nabla_{\mathbf{c}^k} (\gamma_j^k(\mathbf{c}^k))$  of activity coefficients depends usually on all concentrations  
 23 of the vector  $\mathbf{c}^k$  considered in the activity calculations.

24 The first term in Eq. (21) is a vector with entries in several positions depending on the activity  
 25 coefficient module. This leads to “fill-in” in the corresponding lines of the Jacobian from  
 26 aqueous phase chemistry (blue blocks) and the phase transfer terms (green blocks).

Gelöscht: 2

1 Consequently, the efficient direct sparse solvers are used in SPACCIM for the linear system  
2 cannot be utilized. However, since only a “good” approximation for the Jacobian is needed,  
3 the first term shown in Eq. (21) is omitted assuming that the dependency of the activity  
4 coefficients from the concentrations can be neglected over the time step. The second term  
5 involves the activity coefficient  $\gamma_j^k$  that yields from the derivative of the activity with respect  
6 to molality of that particular species  $m_j$ . Although, the derivative of activity coefficients is  
7 omitted, the same data structures are obtained as in ideal case. The second term on the right  
8 hand side of Eq. (21) has the same structure as on the right hand side of Eq. (20). Only the  
9 non-zero entry in the  $j^{\text{th}}$  position changes from 1 to  $\gamma_j^k$ . This leads to modifications of the  
10 non-zero entries in the Jacobians of the chemistry (blue blocks) and the phase transfer (green  
11 blocks) terms. However, the sparse structure of the systems is conserved effectively.

Gelöscht: 2

Gelöscht: 2

Gelöscht: 1

## 12 2.3 SPACCIM's activity coefficient module

13 [A main task in the extended approach \(Fig. 2\) is to provide appropriate activity coefficients](#)  
14 [for the solved species. Therefore, several suitable activity models have been tested and](#)  
15 [compared regarding their suitable applicability in order to achieve the above-mentioned](#)  
16 [objective. \(see Subsect. 3.1\). Overall, AIOMFAC seems to be most qualified for the aimed](#)  
17 [applications. Therefore, the implementation of the related module SpactMod was performed](#)  
18 [by using the theoretical framework and the available parameters of Zuend et al. \(2008\).](#) The  
19 AIOMFAC was originally developed for systems composed of organic compounds with  $-\text{CH}_n$   
20 ( $n = 0,1,2,3$ ) and  $-\text{OH}$  as functional groups. On the other hand, several authors (e.g., Gilardoni  
21 et al. (2009); Liu et al. (2009); Russell et al. (2009); Takahama et al. (2011)) reported that  
22 other individual organic compounds and compound classes have also a strong impact on  
23 multiphase chemical processing on ambient aerosols for instance, aldehydes, ketones,  
24 carboxylic acids, and multifunctional organic compounds. Moreover, the aforementioned  
25 organic compound classes are almost omnipresent in tropospheric aerosol particles and,  
26 therefore, explicitly treated in complex multiphase chemistry mechanism such as CAPRAM  
27 (see e.g., Herrmann et al. (2005); Tilgner et al. (2013)). Hence, the prediction of the activity  
28 coefficients for complex multi-component aerosols, composed of various organic functional  
29 groups and electrolytes dissolved in water is the primary purpose of SpactMod. In order to  
30 treat various aerosol constituents, [additional parameters were included from the mod. LIFAC](#)  
31 [approach of Kiepe et al. \(2006\), which can be rewritten in the AIOMFAC formalism \(see](#)

Gelöscht: Ultimately

**Gelöscht:** In this section, we present the mixed-solvent electrolyte model that is designed to predict the activity coefficients, based mainly on AIOMFAC (Zuend et al., 2008), which is valid for systems over a wide concentration range.

1 [Appendix A1](#)) and incorporated without new parameter fitting. A compilation of the  
2 [SpactMod](#) parameters is given in Tables A1-A6. The differences to AIOMFAC are  
3 [highlighted](#).

### 4 2.3.1 Model treatment of solution non-ideality

5 The development of thermodynamic models for mixed-solvent electrolyte systems was an  
6 active area of research during the last three decades. In general, these models contain several  
7 contributions to describe the system non-ideality, that define the excess Gibbs energy

8  $G^{ex}(p, T, n_j)$ :

$$9 \quad G^{ex}(p, T, n_j) = G_{LR}^{ex} + G_{MR}^{ex} + G_{SR}^{ex}, \quad (22)$$

10 where  $G_{LR}^{ex}$  represents the long-range (LR) electrostatic interactions,  $G_{SR}^{ex}$  is the short-range  
11 (SR) contribution resulting from dipole ↔ dipole and dipole ↔ induced dipole interactions,  
12 and an additional term (middle-range, MR)  $G_{MR}^{ex}$ , which accounts for ionic interactions (e.g.,  
13 ion ↔ ion, ion ↔ dipole, ion ↔ induced dipole interactions),  $p$  is the total pressure,  $T$  the  
14 absolute temperature, and  $n_j (j=1, \dots, N)$  the number of moles of component  $j$  in a system.

15 Accordingly, the corresponding activity coefficient  $\gamma_j^k$  of a species  $j$  with amount of moles  $n_j$   
16 in the mixture are derived from expressions for the different parts of  $G^{ex}$  using the relation:

$$17 \quad \ln \gamma_j = \left( \frac{\partial G^{ex} / RT}{\partial n_j} \right)_{p, T, n_{j \neq j}}, \quad (23)$$

18 where  $R$  is the universal gas constant. Correspondingly, the activity coefficients are calculated  
19 from the aforementioned three different contributions:

$$20 \quad \ln \gamma_j = \ln \gamma_j^{LR} + \ln \gamma_j^{MR} + \ln \gamma_j^{SR}. \quad (24)$$

### 21 2.3.2 The [long-range](#) contribution

22 The LR interactions [described as they are in original AIOMFAC](#), based on the Debye-Hückel  
23 theory (Debye and Hückel, 1923). In contrast to other works Li et al. (1994); Yan et al.  
24 (1999); Chang and Pankow (2006), AIOMFAC uses the water properties for all solvent  
25 components for density and dielectric constant of the solvent mixture, instead of using mixing  
26 rules. With this assumption, the corresponding LR activity coefficient expressions for the

**Gelöscht:** the model interaction parameters were extended based on the activity coefficient model of mod. LIFAC (Kiepe et al., 2006), while using the mathematical model expressions according to

**Gelöscht:** Zuend et al. (2008)

**Gelöscht:** . Thus, SpactMod allows a reliable prediction of activity coefficients of the considered organic-electrolyte mixture, flexibly, from these two approaches AIOMFAC (Zuend et al., 2008) and modified LIFAC (Kiepe et al., 2006), within a single model framework. The two different frameworks including the estimated interaction parameters are described in detail in

**Gelöscht:** Zuend et al. (2008)

**Gelöscht:** and

**Gelöscht:** Kiepe et al. (2006)

**Gelöscht:** , therefore, only main features are discussed here.

**Gelöscht:** 3

**Gelöscht:** 4

**Gelöscht:** 5

**Gelöscht:** Long

**Gelöscht:** are described same as original AIOMFAC

1 solvents and ions are defined according to Zuend et al. (2008) as

$$2 \quad \ln \gamma_s^{LR,(x)} = \frac{2AM_s}{b^3} \left( 1 + b\sqrt{I} - \frac{1}{1+b\sqrt{I}} - 2\ln(1+b\sqrt{I}) \right), \quad (25)$$

$$3 \quad \ln \gamma_i^{LR,(x),\infty} = \frac{-z_i^2 A \sqrt{I}}{1+b\sqrt{I}}. \quad (26)$$

4 Eq. (26) gives the activity coefficient of ion  $i$  in the mole fraction basis ( $x$ ) with the reference  
5 state of infinite dilution in water, indicated by super script  $\infty$ .  $M_s$  represents the molar mass  
6 of solvent  $s$  and  $z_i$  is the number of elementary charges of ion  $i$ . The ionic strength  
7  $I$  ( $\text{mol kg}^{-1}$ ) is given as

$$8 \quad I = \frac{1}{2} \sum_i m_i z_i^2 \quad (27)$$

9 with the Debye-Hückel parameters:

$$10 \quad A = 1.327757 \cdot 10^5 \cdot \frac{\sqrt{\rho_w}}{(\epsilon_w T)^{3/2}}, \quad (28)$$

$$11 \quad b = 6.359696 \cdot \sqrt{\frac{\rho_w}{(\epsilon_w T)}}. \quad (29)$$

12 The Debye-Hückel parameters  $A$  ( $\text{kg}^{1/2} \text{mol}^{-1/2}$ ) and  $b$  ( $\text{kg}^{1/2} \text{mol}^{-1/2}$ ) depend on temperature  $T$   
13 (K), density  $\rho_w$  ( $\text{kg/m}^3$ ) and static permittivity  $\epsilon_w$  ( $\text{C}^2 \text{J}^{-1} \text{m}^{-1}$ ) of water, calculated based on  
14 a distance of closest approach between ions (see Demaret and Gueron (1993); Antypov and  
15 Holm (2007)).

16 Moreover, this simplification to a water-property based expression for LR activity coefficients  
17 are favorable, due to the uncertainties to estimate unknown dielectric constants of certain  
18 organic compounds and maintaining the thermodynamic consistency regarding the selection  
19 of reference states (see Raatikainen and Laaksonen (2005); Zuend et al. (2008)). In a real  
20 mixture, solvents have densities and dielectric properties different from those of pure water.  
21 For this reason, these simplifications of the LR part were made in other mixed solvent models  
22 in chemical engineering and technical chemistry applications (see Iliuta et al. (2000)). [The](#)  
23 [uncertainties occurred due to the adopted assumptions to derive the LR and SR activity](#)  
24 [coefficients with respect to approximations of parameters, were described in the semi-](#)

Gelöscht: 6

Gelöscht: 7

Gelöscht: 7

Gelöscht: 8

Gelöscht: 9

Gelöscht: 30

Gelöscht: of

1 | [empirical SR part as in the original AIOMFAC](#) (Zuend et al., 2008).

### 2 | 2.3.3 The Middle-range contribution

3 | The  $G_{MR}^{ex}$  term is the contribution of the indirect effects of the ionic interactions such as ion  
4 |  $\leftrightarrow$  dipole interactions and ion  $\leftrightarrow$  induced dipole interactions to the excess Gibbs energy. For  
5 | any mixture containing  $n_k$  ( $k=1, \dots, s$ ) moles of solvent  $k$  (main groups of organics and  
6 | water) and  $n_i$  moles of ion  $i$ ,  $G_{MR}^{ex}$  can be expressed as described by Zuend et al. (2008):

$$\begin{aligned} \frac{G_{MR}^{ex}}{RT} = & \frac{1}{\sum_k n_k M_k} \sum_k \sum_i B_{k,i}(I) n_k n_i \\ & + \frac{1}{\sum_k n_k M_k} \sum_c \sum_a B_{c,a}(I) n_c n_a \\ 7 \quad & + \frac{1}{\sum_k n_k M_k} \sum_c \sum_a C_{c,a}(I) n_c n_a \sum_i \frac{n_i |z_i|}{\sum_k n_k M_k} \\ & + \frac{1}{\sum_k n_k M_k} \sum_c \sum_{c' \geq c} R_{c,c'}(I) n_c n_{c'} \\ & + \frac{1}{\left(\sum_k n_k M_k\right)^2} \sum_c \sum_{c' \geq c} \sum_a Q_{c,c',a} n_c n_{c'} n_a \end{aligned} \quad (30)$$

8 | where  $n_c$  and  $n_{c'}$  are the moles of cations,  $n_a$  are the moles of anions, and  $I$  is the ionic  
9 | strength as defined in Eq. (27).  $B_{k,i}(I)$  ( $\text{kg mol}^{-1}$ ) and  $B_{c,a}(I)$  ( $\text{kg mol}^{-1}$ ) are ionic strength  
10 | dependent binary interaction coefficients between solvent main groups and ions, and between  
11 | cations and anions, respectively.  $C_{c,a}(I)$  ( $\text{kg}^2 \text{mol}^{-2}$ ) are interaction coefficients between  
12 | cation  $\leftrightarrow$  anion pairs with respect to the total charge concentration. The coefficients  
13 |  $R_{c,c'}(I)$  ( $\text{kg mol}^{-1}$ ) and  $Q_{c,c',a}(I)$  ( $\text{kg}^2 \text{mol}^{-2}$ ) are defined as binary and ternary interactions  
14 | involving two different cations. These binary and ternary interaction coefficients have been  
15 | introduced in AIOMFAC to improve the description of various ion combinations, specifically  
16 | at high ionic strength. Hence, these two terms in Eq. (30) can be vanished or neglected in  
17 | other cases, i.e. for low to moderate ionic strengths.

18 | In the current approach, the MR terms of activity coefficients for the species and organic  
19 | functional groups described in AIOMFAC are estimated using Eq. (30). As mentioned earlier,

**Gelöscht:** Compensation of these inaccuracies is controlled by this simplification, in the semi-empirical MR part as performed in original AIOMFAC (Zuend et al., 2008)

**Gelöscht:** 1

**Gelöscht:** 8

**Gelöscht:** 1

**Gelöscht:** 1

1 the first three interaction coefficients in Eq. (30) are parameterized as functions of ionic  
2 strength  $I$ , which are similar to the ones used for the Pitzer model of Knopf et al. (2003):

$$3 \quad B_{k,i}(I) = b_{k,i}^{(1)} + b_{k,i}^{(2)} \exp(-b_{k,i}^{(3)} \sqrt{I}), \quad (31)$$

$$4 \quad B_{c,a}(I) = b_{c,a}^{(1)} + b_{c,a}^{(2)} \exp(-b_{c,a}^{(3)} \sqrt{I}), \quad (32)$$

$$5 \quad C_{c,a}(I) = c_{c,a}^{(1)} \exp(-c_{c,a}^{(2)} \sqrt{I}), \quad (33)$$

6 where  $b_{k,i}^{(1)}$ ,  $b_{k,i}^{(2)}$ ,  $b_{c,a}^{(1)}$ ,  $b_{c,a}^{(2)}$ ,  $c_{c,a}^{(1)}$  and  $c_{c,a}^{(2)}$  are adjustable parameters, which are determined by  
7 fitting AIOMFAC activity coefficients to experimental data sets (see Zuend et al. (2008) for  
8 further details). The parameter  $b_{c,a}^{(3)}$  was used mostly to describe aqueous salt solutions  
9 assuming a fixed value of  $0.8 \text{ kg}^{1/2} \text{ mol}^{1/2}$ . Similarly, we have considered the same value for  
10 the ions when the activity coefficients are estimated from AIOMFAC. Furthermore, Zuend et  
11 al. (2008) argued that for such cases, where this value did not result in a satisfactory data fit,  
12  $b_{c,a}^{(3)}$  allow to vary. On the other hand, the parameter  $b_{k,i}^{(3)}$  was fixed for all mixed organic-  
13 inorganic solutions assuming a value of  $1.2 \text{ kg}^{1/2} \text{ mol}^{1/2}$ . All interaction coefficients in the MR  
14 part are symmetric  $B_{c,a}(I) = B_{a,c}(I)$ . Subsequently, water is defined as the reference solvent  
15 for inorganic ions, no explicit ion  $\leftrightarrow$  water interactions are determined, i.e.,  $B_{k=\text{H}_2\text{O},i}(I)$  is  
16 prescribed as zero for all inorganic ions. However, the effects of [solution](#) non-ideality from  
17 cations and anions interacting with water molecules are indirectly accounted for via the cation  
18  $\leftrightarrow$  anion interaction coefficients,  $B_{c,a}(I)$ ,  $C_{c,a}(I)$ ,  $R_{c,c'}$  and  $Q_{c,c',a}$  as the corresponding  
19 interaction parameters, that were determined on the basis of (organic-free) aqueous electrolyte  
20 solutions.

21 As depicted earlier, the MR interaction parameters in AIOMFAC were fitted for limited  
22 organic compounds (i.e. alkyl and hydroxyl) and ions. Contrary, interaction parameters were  
23 not evenly available for over all systems of current interest, i.e. to treat the organic  
24 compounds and ions involved in multiphase mechanism such as CAPRAM. Hence, in this  
25 study, the ion  $\leftrightarrow$  ion and organic main group  $\leftrightarrow$  ion interaction parameter database is  
26 extended by incorporating parameters of the modified LIFAC approach of Kiepe et al. (2006).  
27 The complete procedure of the extension of model interaction parameters is explained in  
28 Appendix A.1.

Gelöscht: 1

Gelöscht: 2

Gelöscht: 3

Gelöscht: 4

### 1 2.3.4 The short-range contribution

2 The SR contribution  $\ln \gamma_{SR}^{ex}$  to the total Gibbs excess energy in SpactMod is represented by the  
3 modified group-contribution method UNIFAC (Fredenslund et al., 1975), as performed by  
4 Zuend et al. (2008). AIOMFAC incorporates the revised parameter set of Hansen et al. (1991)  
5 (standard UNIFAC) for most of the functional group interactions. Besides, these  
6 modifications include the insertion of further inorganic ions to account for their effects on the  
7 thermodynamic properties such as entropy and enthalpy of mixing apart from their charge-  
8 related interactions (Li et al., 1994; Yan et al., 1999; Zuend et al., 2008). AIOMFAC utilizes  
9 the specific UNIFAC parameterizations of Marcolli and Peter (2005) for hydroxyl and alkyl  
10 functional groups.

11 Similar to the addition of interaction parameters derived for MR part, the same functional  
12 groups are also included in the SR part, while maintaining the compatibility with the  
13 mathematical model expressions proposed in AIOMFAC. As Zuend et al. (2008), we used the  
14 UNIFAC parameterizations of Marcolli and Peter (2005), which are adopted from Hansen et  
15 al. (1991). Additionally, the revised parameterizations for the functional group COOH are  
16 taken from Peng et al. (2001), which differs from the parameter matrix proposed in standard  
17 UNIFAC by Hansen et al. (1991). Since the same mathematical formulations are used in these  
18 models and differs only in main group interaction parameters, the parameter matrix is  
19 compatible to use. The influence of estimated activity coefficients when merging specific  
20 parameters from the distinctive UNIFAC parameterizations within SpactMod has been tested.  
21 Sensitivity studies have shown, that SpactMod predict relatively better results when  
22 combining the main functional group interaction parameters instead of using the standard  
23 UNIFAC parameter set only (see Sect. 3.2). The interaction parameters for these organic  
24 functional groups are shown in Appendix B.

25 In UNIFAC, the activity coefficient  $\gamma_j$  of a molecular component  $j$  ( $j$  can be used for solute  
26 or solvent) in a multicomponent mixture is in general expressed as the summation of  
27 contributions of (i) a combinatorial part ( $C$ ) accounting for the geometrical properties of the  
28 molecule and (ii) a residual part ( $R$ ), which results from inter-molecular interactions:

$$29 \ln \gamma_j^{SR} = \ln \gamma_j^C + \ln \gamma_j^R. \quad (34)$$

30 Since ions are treated such as solvent components in the SR terms, resulting activity  
31 coefficients in Eq. (34) are with respect to the symmetrical convention on mole fraction basis.

Gelöscht: comprised

Gelöscht: Similar to

Gelöscht: However, the standard UNIFAC parameter set, when the same mathematical model expressions are used.

Gelöscht: SPACCIM

Gelöscht: produce

Gelöscht: . It was found that the model produce relatively better results in most of the cases in comparison with the parameters from standard UNIFAC only.

Gelöscht: A1

Gelöscht: 5

Gelöscht: 5

1 For ions, the unsymmetrical normalized activity coefficient is determined from:

$$2 \quad \ln \gamma_i^{SR,(x),\infty} = \ln \gamma_i^{SR,(x)} + \ln \gamma_i^{SR,(x),ref} \quad (35)$$

3 The symmetrically normalized value at the reference state is computed from the combinatorial  
4 and residual parts, by introducing the reference state conditions of the ions (setting

5  $x_w = 1, \sum_s x_s = 0$  for  $s \neq w$  and  $\sum_i x_i = 0$ ):

$$6 \quad \ln \gamma_i^{SR,(x),ref} = \ln \frac{r_i}{r_w} + 1 - \frac{r_i}{r_w} \\ + \frac{z}{2} q_i \left[ \ln \left( \frac{r_w q_i}{r_i q_w} \right) - 1 + \frac{r_w q_i}{r_i q_w} \right] \\ + q_i (1 - \ln \psi_{w,i} - \psi_{i,w}), \quad (36)$$

7 where subscript  $w$  stands for the reference solvent (water). The parameters  $q_i$  and  $r_i$  represent  
8 the surface area and the volume, respectively, of component  $i$ . The last term on the right-hand  
9 side of Eq. (36) reflects the residual part reference contribution and becomes zero as we  
10 defined the SR ion  $\leftrightarrow$  solvent interactions to be zero. Fig. 4 shows the binary species  
11 combinations, for which the specific parameters have been used in this study. Mean  
12 interactions between ions and water are indirectly represented by the parameters of the cation  
13  $\leftrightarrow$  anion interaction pairs according to (Zuend et al., 2008), since the aqueous solution is  
14 defined as the reference system similar to the assumption used in conventional Pitzer models  
15 (Pitzer, 1991). The relative van der Waals subgroup volume and surface area parameters,  $R_i$   
16 and  $Q_i$ , account for pure component properties. At the same time,  $R_i$  and  $Q_i$  values for the  
17 ions can be estimated from the ionic radii. In order to maintain the compatibility with the  
18 model equations of AIOMFAC, the hydrated group volume and surface area parameters  $R_i^H$   
19 and  $Q_i^H$  are calculated using an empirical parameterization given by Achard et al. (1994). For  
20 those ions, the activity coefficients are estimated using the mod. LIFAC approach. Likewise,  
21 the database is extended for other ions in order to estimate the activity coefficients from the  
22 SR part. The measured apparent dynamic hydration numbers ( $N_i^{ADH}$ ) data are adopted from  
23 Kiriukhin and Collins (2002) to estimate the final values  $R_i^H$  and  $Q_i^H$  instead of  $R_i$  and  $Q_i$ .  
24  $R_i^H$  and  $Q_i^H$  are computed consistently in the model equations (see Table A2 in the Appendix)  
25 by:

$$26 \quad R_i^H = R_i + N_i^{ADH} \cdot R_w, \quad (37)$$

Gelöscht: 6

Gelöscht: 7

Gelöscht: 7

Gelöscht: 8

$$Q_t^H = Q_t + N_t^{ADH} \cdot Q_w, \quad (38)$$

where  $R_w$  and  $Q_w$  refer to the values of the water molecule and  $N_t^{ADH}$  are measured apparent dynamic hydration numbers at 303.15 K (Kiriukhin and Collins, 2002). As shown in Fig. 4, the interactions of the ions  $Mg^{2+}$ ,  $Ca^{2+}$ ,  $F^-$ ,  $I^-$ ,  $OH^-$ ,  $NO_2^-$ ,  $CO_3^-$  and  $CH_3COO^-$  are implemented from Kiepe et al. (2006). Due to the increasing interest on remaining ions included in the multiphase mechanism CAPRAM (e.g.  $Fe^{2+}$ , succinate, and malonate) the activity coefficients are computed while prescribing the corresponding interaction parameters as zero.

### 2.3.5 Total activity coefficients

Finally, SPACCIM's activity coefficient module (SpactMod) estimates the total activity coefficients for each species according to the Gibbs energy (cp. Eqs. (22) and (24)). Then, the activity coefficient of a solvent species  $s$  is determined by Li et al. (1994); Yan et al. (1999); Kiepe et al. (2006); Zuend et al. (2008)

$$\ln \gamma_s^{(x)} = \ln \gamma_s^{LR,(x)} + \ln \gamma_s^{MR,(x)} + \ln \gamma_s^{SR,(x)} \quad (39)$$

Accordingly, the complete expression for the ions, with regard to the unsymmetrical convention on molality basis at which the standard state is the hypothetical ideal solution of unit molality at system pressure and temperature, can be written as follows:

$$\ln \gamma_i^{(m)} = \left[ \ln \gamma_i^{LR,(x),\infty} + \ln \gamma_i^{MR,(x),\infty} + \ln \gamma_i^{SR,(x),\infty} \right] - \ln \left[ \frac{M_w}{\sum_s x_s^* M_s} \right] + M_w \sum_{i'} m_{i'} \quad (40)$$

where  $M_s$  is the molar mass of solvent component  $s$ ,  $x_s^*$  its salt-free mole fraction, and  $m_{i'}$  is the molality of ion  $i'$ . The last term on the right-hand side of Eq. (40) converts the activity coefficient  $\ln \gamma_s^{(x)}$  (infinitely diluted reference state on the mole fraction basis) to the activity coefficient on molality basis and infinitely diluted (in water) reference state. One can derive this term based on convention-independence of the chemical potentials  $\left( \mu_i^{(m)}(p,T,n_j) = \mu_i^{(x)}(p,T,n_j) \right)$  and the definitions of the chosen reference states (Zuend et al., 2008).

The extension of database by the combination of AIOMFAC and modified LIFAC makes

Gelöscht: 9

Gelöscht: 3

Gelöscht: 5

Gelöscht: 40

Gelöscht: 1

Gelöscht: 1

1 | SPACCIM a versatile tool to study the influence of the treatment of [solution](#) non-ideality on  
2 multiphase aerosol chemistry. SpactMod is highly flexible to extension and further inclusion  
3 of organic functional groups and ions, whenever the required data become available. During  
4 the implementation of the code, the activity coefficients responsible for LR and SR  
5 contribution terms are computed for all the ions (either cation or anion) included in the  
6 considered chemical system. For those species, where the interaction parameters are not  
7 available to compute MR contribution terms; they are prescribed as unity (i.e.,  $\gamma_i^{MR,(x),\infty} = 1$ )  
8 due to the lack of extensive database.

### 9 **3 Model evaluation and applications**

10 In this section we will examine the model extensions described above. Especially, the activity  
11 coefficient module SpactMod is evaluated and compared with literature data. The reliability  
12 of the extended SPACCIM code is shown in the last subsection. Furthermore, the deviation of  
13 the activity coefficients from ideality and, consequently, the impact on the chemical behavior  
14 are demonstrated for a test scenario. A more detailed analysis of the impact of the non-ideality  
15 approach on the multiphase will be published in a separate paper.

#### 16 **3.1 Evaluation of the activity coefficient module**

17 Considerable effort has been devoted by several authors (see e.g., Raatikainen and Laaksonen  
18 (2005); Tong et al. (2008); Zuend et al. (2008)) to compare different established activity  
19 coefficient models that could be potentially suitable for modeling of hygroscopic properties of  
20 organic-electrolyte particles as well as the prediction of activity coefficients of aqueous  
21 species. The investigations summarized here were aimed to evaluate the robustness of the  
22 implemented module SpactMod and to check the reproducibility towards original model  
23 results. However, the interaction parameters in the applied models were fitted against  
24 measurements. Hence, this comparison can be considered as indirect comparison with  
25 measurements. Furthermore, results are also compared with direct also water activity  
26 measurements and the AIM model (Aerosol Inorganic Model) of Clegg et al. (1998b, 1998a).  
27 The model comparisons cover a scale, ranging from very simple to complex simulations.  
28 Initially, the comparison is performed for selected binary aqueous electrolyte solutions, then  
29 aqueous organic solutions, followed by mixtures of aqueous organic-electrolyte solutions.  
30 However, here we present the results of selected examples only.

### 3.1.1 Comparison between activity coefficient models for inorganic systems

Naturally, the reproducibility of the original AIOMFAC results in Zuend et al. (2008) was verified in a first step. Note that the graphs of the newly implemented module SpactMod depicted in Figs. 5 and 6 correspond to the original results given in Zuend et al. (2008). Fig. 5 shows the comparison between calculated water activities predicted by the selected four models and experimental data. The differences for the electrolyte mixture of NaCl + NH<sub>4</sub>NO<sub>3</sub> are in good agreement up to moderate salt concentrations ( $x_w \geq 0.5$ ). The values for high concentrations ( $x_w \leq 0.4$ ) indicate the formation of a solid salt (or hydrate), when the solution becomes supersaturated as well as the deliquescent point of the particular salt. The models do not reproduce this, since the formation of solids was not incorporated in the present model calculations. As can be seen from Figs. 5 and 6, the modeled water activities agree well with each other at low concentrations. Contrary at high salt concentrations, mod. LIFAC strongly deviates from SpactMod as shown in Fig. 5, by a steep increase in  $a_w$  and in Fig. 6 by an increase followed by a sharp decrease, as shown by Zuend et al. (2008). Note that the Ca(NO<sub>3</sub>)<sub>2</sub> parameterization of mod. LIFAC (see Fig. 6) results only from water activity data of bulk measurements as the approach of Ming and Russell (2002) model, behaves similar to SpactMod at medium concentrations and proceed to formation of solids. The interaction coefficients of AIOMFAC applied in SpactMod were fitted from vapor-liquid as well as liquid-liquid equilibrium data, salt solubilities and electromotive force measurements covering also high solution concentrations and ternary mixtures (Zuend et al., 2008). Hence, the slope of the curve enables much better descriptions and predictions up to high concentrations, even very low water concentration available and at high ionic strength. It is noted that Ca(NO<sub>3</sub>)<sub>2</sub> is not available in the AIM, thus Fig. 6 includes only results of the other activity coefficient approaches.

Apart from the predicted water activities, the calculated mean activity coefficients also have differences with each other. Therefore, a comparison of mean activity coefficients is presented additionally in Fig. 6. The mean activity coefficient ( $\gamma_{\pm}$ ) is related to single ion-activity coefficients by

$$\gamma_{\pm} = (\gamma_{+}^{V_{+}} \cdot \gamma_{-}^{V_{-}})^{1/(V_{+}+V_{-})} \quad (41)$$

where  $\gamma_{+}$  and  $\gamma_{-}$  are the activity coefficients of a cation and anion, respectively.  $V_{+}$  and  $V_{-}$  are the corresponding stoichiometric coefficients. The mean activity coefficients predicted by

Gelöscht: but is described here.

Gelöscht: 2

1 AIOMFAC and the approach of Ming and Russell (2002) show a similar curve shape with  
2 5 % of difference. In contrast, mod. LIFAC shows a different behavior especially for water  
3 fractions later than 0.8.

### 4 3.1.2 Verification of SpactMod for organic-electrolyte mixtures

5 In this section, the performance of different activity coefficient models is evaluated by  
6 comparing calculated and measured water activities of mixtures of electrolyte and organic  
7 system. For all water activity calculations, the organic acids are treated as non-dissociating  
8 solutes, and a single liquid phase is assumed with no solid phases present. All calculations are  
9 performed at atmospheric pressure (1 atm) and at 298 K.

10 Fig. 7 shows the comparison of experimental data with predicted water activities using  
11 different UNIFAC parameterizations. Here, the parameters for the original UNIFAC are  
12 adopted from Hansen et al. (1991). Furthermore, a revised set of fitted UNIFAC parameters  
13 given by Peng et al. (2001) for the [interactions of](#) functional groups OH, H<sub>2</sub>O and COOH is  
14 used for the comparison. As depicted in Fig. 7, the original UNIFAC and Ming and Russell  
15 (2002) exhibit similar behavior for all water fractions. Moreover, SpactMod and the version  
16 of Peng et al. (2001) have deviations that are usually less than 50% of the deviations with the  
17 original UNIFAC. Furthermore, the original UNIFAC exhibits much bigger deviations than  
18 the UNIFAC version of Peng et al. (2001) and SpactMod. The last two models show a similar  
19 behavior and a good agreement with the measurements. In difference to the Peng approach,  
20 SpactMod take into account dynamic hydration numbers (see Eq. (37) and (39)), which is in  
21 consistency with the computation of the combinatorial term in AIOMFAC.

Gelöscht: Hanson and Ravishankara (1993)

Gelöscht: 8

22 [Fig. 8 shows the comparison of mean ionic activity coefficients of binary electrolyte mixtures.](#)  
23 [As can be seen from the plot, good results were obtained by SpactMod based on mod. LIFAC](#)  
24 [parameterization. Mod.LIFAC shows better results compared to LIFAC due to the improved](#)  
25 [reference state calculation of ions in the SR part. Due to the normalization of ions, SpactMod](#)  
26 [gives better agreement compared to original LIFAC for these binary electrolytes.](#)

27 [Fig. 9 shows the comparison between predicted water activities from different activity](#)  
28 [coefficient models for the mixture of \(NH<sub>4</sub>\)<sub>2</sub>SO<sub>4</sub> + Glycerol + H<sub>2</sub>O \[\(2:1:1\) mole ratio\]. As](#)  
29 [expected, SpactMod accurately reproduces the results from the original AIOMFAC. All the](#)  
30 [models behave similarly up to moderate concentrations \( \$x\_w = 0.6\$ \). As in Fig. 6, at lower water](#)  
31 [activity, mod. LIFAC and LIFAC strongly deviate from SpactMod. As argued earlier, LIFAC](#)

Gelöscht: at the deliquescent phase

1 and mod. LIFAC are able to predict vapor liquid equilibria and liquid liquid equilibria but  
2 cannot describe the deviations from ideality at high concentrations. A steep increase of  $a_w$   
3 shown in Fig. 9 have to be rated as artefacts of the LIFAC and mod. LIFAC parameterization.

4 Fig. 10 shows the comparison between experimental and predicted water activities for the  
5 mixture of  $(\text{NH}_4)_2\text{SO}_4$  + Ethanol + Acetic acid [(2:1:1) mole ratio]. All the models strongly  
6 agree with the measurements at high relative humidities or at low and moderate salt  
7 concentrations ( $x_w \approx 0.8$ ). However at the deliquescent phase ( $x_w \approx 0.6$ ), the mod. LIFAC  
8 and Ming and Russell (2002) model strongly deviate from SpactMod. These differences for  
9 lower water fractions are mainly caused by the different treatment of ion  $\leftrightarrow$  organic  
10 interactions included in the models. It can be seen from Fig. 10 that the strange behavior does  
11 not appear for the pure organic and pure electrolyte mixture predictions. The MR interaction  
12 term in the model is responsible for this atypical shape in the predictions. Moreover,  
13 Raatikainen and Laaksonen (2005) argued that, in the MR part, the logarithms of activity  
14 coefficients are calculated as sums of terms, which are proportional to the fitting parameters,  
15 ion molalities and ionic strength. Because these terms have quite large numerical values, and  
16 a small change in the interaction parameters or molality can cause a very big change to  
17 activity coefficients. The MR part and modification of SR part given in SpactMod could be  
18 the main reason, since this model can predict the water activities at high salt concentrations as  
19 well. Consequently, as can be seen from Fig. 10, mod. LIFAC have an increase followed by a  
20 sharp decrease, features that have to be rated as artifacts of the mod. LIFAC parameterization,  
21 whereas the Ming and Russell (2002) model has also a strong increase after the water fraction  
22 is about ( $x_w \approx 0.3$ ). As mentioned earlier, these artifacts indicate the formation of a solid salt  
23 (or hydrate), when the solution becomes supersaturated, since the formation of solids was not  
24 enabled in the model calculations.

25  
26 However, the consideration here is only a limited set of mixtures of organic-electrolyte  
27 compounds. Hence, the presented results should be viewed as a first assessment. The scarcity  
28 of experimental data for mixtures of atmospheric relevance remains a limitation for testing  
29 activity coefficient models. When experimental data become available in the future, the  
30 models can be validated against measurements, while comparing the water activity and  
31 species activity coefficients against water fraction  $x_w$ . All in all, despite the difficulties in  
32 determining the ion  $\leftrightarrow$  organic mixture parameters, it should be noted that the ion  $\leftrightarrow$  organic

Gelöscht: 8

Gelöscht: (Ming and Russell, 2002)

Gelöscht: 8

Gelöscht: 8

**Gelöscht:** Fig. 9 shows the comparison of mean ionic activity coefficients of binary electrolyte mixtures. As can be seen good results were obtained by SpactMod based on mod. LIFAC parameterization. The reliable prediction of activity coefficients with improved reference state calculation, the mod. LIFAC produced better results compare to LIFAC. Due to the normalization of ions SpactMod gives better accuracy compare with original LIFAC for these binary electrolytes ... [11]

1 interaction parameters have improved the model performance, a fact which was already noted  
2 in previous studies (Clegg and Seinfeld, 2006b, a; Clegg et al., 2001; Tong et al., 2008)

### 3 **3.2 Sensitivity studies on the importance of the different interactions**

4 Tong et al. (2008) studied the importance of inclusion of a treatment of ion ↔ organic  
5 interactions and states that these interactions would substantially improve the performance of  
6 the coupled models over that of the decoupled models. It has been concluded that, decoupled  
7 approaches, such as those in CSB (Clegg et al., 2001), ADDEM (Topping et al., 2005a, b),  
8 performs well, and in some cases better than the coupled models (Ming and Russell, 2002;  
9 Erdakos et al., 2006a, b). Additionally in such cases, the ion ↔ organic terms do not  
10 necessarily lead to improved model predictions. At the same time, models are prerequisite,  
11 composed of an aqueous electrolyte term, an (aqueous) organic term, and an organic ↔ ion  
12 mixing term in order to treat the organic-inorganic mixtures. In contrast to the study of Tong  
13 et al. (2008), the present study aims at the evaluation of the importance of different interaction  
14 terms in the model approach Eq. (24) for the computation of water activities and the activity  
15 coefficients.

Gelöscht: 5

16 Intermolecular forces or interactions are essential in the deliquesced particle phase, where  
17 high solute concentrations and low water fractions are available. They are important because  
18 they are responsible for many of the physical properties of solids, liquids, and gases.  
19 Moreover, these interaction forces become significant at the molecular range of about  
20 1 nanometer or less, but are much weaker than the forces associated with chemical bonding.  
21 The characteristic contribution of different interaction forces from the model development  
22 point of view in the solution can be computed using Eq. (24). Utilizing this conceptual idea in  
23 the computation of activity coefficients, here we address the question, which intermolecular  
24 forces of attraction are important and need be considered for the treatment of [solution](#) non-  
25 ideality for organic-electrolyte mixtures. In order to answer this question, the SpactMod is  
26 used for sensitivity studies. Overall, the studies have revealed that middle-range (MR)  
27 interactions are important to compute the total activity coefficients.

Gelöscht: 5

28 Fig. 11 shows the contribution of different interaction forces in the solution for the mixture of  
29 NaCl + (NH<sub>4</sub>)<sub>2</sub> SO<sub>4</sub> + Ethanol + Malonic acid [1:1:1:1 (mole ratio)] as an example. However,  
30 the deviations regarding the different interactions depend on the considered mixture. As can  
31 be seen in Fig. 9, the water activity strongly deviates in absence of MR interaction forces,

Gelöscht: 9

1 mainly caused from ion ↔ ion, ion ↔ dipole and ion ↔ induced dipole forces. Thus, the MR  
2 interactions were found important. Similar to the findings of Tong et al. (2008), it is expected  
3 that ion ↔ organic interactions be of most importance in solutions with high solute  
4 concentrations, for which inclusion of ion ↔ organic parameters would be beneficial.  
5 However, the absence of each interaction terms can be seen in Fig. 11. The short-range  
6 interactions also influence in the total contribution of computation of water activity, where the  
7 deviations are about 10%. In the case of considered the MR and SR interactions, the  
8 deviations are about 25%. It should be noted that the ion ↔ organic interactions are the  
9 dominant interaction forces in the solution, however the further interaction forces need to be  
10 considered. The deviations from the total contribution of interaction forces is significant in all  
11 ranges of relative humidity as well as in the full range of concentration. Nevertheless, the  
12 deviations are increasing from lower salt/acid concentration to higher. During the low  
13 salt/acid concentration ( $x_w \approx 0.9$ ) the contribution of the considered interactions were found  
14 similar.

### 15 3.3 First application of the advanced SPACCIM model

16 To demonstrate the functioning of the whole advanced SPACCIM model framework  
17 including the newly considered activity coefficient module SpactMod and a complex  
18 multiphase aerosol chemistry mechanism, first air parcel simulations have been performed  
19 with a simple model scenario. In the two following subsections, the applied model scenario  
20 and chemical mechanism is briefly outlined, and subsequently selected model results are  
21 presented. However, it is noted that the presented simulations are not aimed at the detailed  
22 examination of non-ideal solution effects on multiphase chemical processes. The detailed  
23 investigation of this complex issue will be given in a companion paper (Rusumdar et al.,  
24 2015).

#### 25 3.3.1 Model scenario and chemical mechanism

26 In the applied meteorological scenario, an air parcel moves along a predefined 3-hour model  
27 trajectory that involves three cloud passages and non-cloud periods in which the aerosol  
28 particles are deliquesced. Simulations were performed with and without consideration of non-  
29 ideal solutions. Furthermore, the simulations have been performed with two different relative  
30 humidity levels (90 % r.h. and 70% r.h.) during the non-cloud periods. In total, simulations  
31 have been performed for four cases: with and without consideration of non-ideal solutions and

1 both with a 90% and 70% relative humidity level during the non-cloud periods, respectively.  
2 For the modeling, mono-disperse aerosol particles with a radius of 200 nm and a number  
3 concentration of  $1.0 \cdot 10^{+8} \text{ cm}^{-3}$  were used.

**Gelöscht:** For the two cases without treatment of non-ideal effects, the aqueous phase chemistry is treated as ideal.

4 For the test simulations, a complex multiphase chemistry mechanism has been applied. The  
5 applied mechanism consists of the gas phase mechanism RACM-MIM2ext (Tilgner and  
6 Herrmann, 2010) and an extended version of the aqueous phase mechanism CAPRAM2.4  
7 (CAPRAM2.4 + organicExt). The employed aqueous phase mechanism consists of the  
8 CAPRAM2.4 mechanism (Ervens et al., 2003) combined with the reduced organic extension  
9 of CAPRAM3.0i-red (Deguillaume et al., 2010) along with the condensed oxidation scheme  
10 of malonic acid and succinic acid based on the CAPRAM3.0i-red (see Deguillaume et al.  
11 (2010) for further details). Thus, the aqueous phase mechanism contains a detailed oxidation  
12 scheme of inorganic as well as organic compounds with 204 species and 477 reactions. In the  
13 considered organic reaction scheme describes the chemistry of organic compounds with up to  
14 4 carbon atoms and different functional groups. All model simulations have been performed  
15 for continental remote environmental conditions (see Ervens et al. (2003) for further details).

### 16 3.3.2 Model results

#### 17 *Modeled activity coefficients of key inorganic ions*

18 Fig. 12 depicts the time evolution of the activity coefficients of main inorganic ions and key  
19 transition metal ions (TMIs) modeled for the two different relative humidity cases. The plots  
20 show, expectedly, a strong dependency on the microphysical conditions. During cloud  
21 conditions, the modeled activity coefficients are almost equal to unity for the depicted ions.  
22 The in-cloud activity coefficients of ions with charge state 3+ deviate a bit more from the one  
23 than less charged ions. Under concentrated deliquesced particle conditions, the activity  
24 coefficients of ions are much lower and show a strong dependence on the relative humidity  
25 level. In the 90% r.h. case, the activity coefficients of singly charged ions are in the range of  
26 0.6-0.7, whereas the modeled coefficients for the doubly and triply charged ions are 0.3-0.35  
27 and 0.1, respectively. Additionally, Fig. 12 reveals that the deviations from ideal behavior  
28 strongly depend on the species regarded but mainly on the charge state. The comparison with  
29 the 70% r.h. case shows clearly that the activity coefficients do not change linearly with  
30 relative humidity. This fact is caused by a non-linear change of activity coefficients in terms  
31 of the molality due to the different types of interactions in the solution. From Fig. 10 it can be

**Gelöscht:** 0

**Gelöscht:** 0

1 seen that the activity coefficients of singly or doubly charged ions are significantly lowered in  
2 the 70% r.h. case compared to the 90% r.h. case. However, no substantial decrease is  
3 simulated for triply charged ions such as  $\text{Fe}^{3+}$ , which are still in the range of 0.1. Interestingly,  
4 the activity coefficient of  $\text{H}^+$  show only a drop of 0.1 between the two cases, while the activity  
5 coefficients of other singly charged ions are lowered by approximately 0.2.

6 In total, the simulated activity coefficients of inorganic ions with values below 1 implicate  
7 that the mass fluxes of chemical processes in deliquesced particles involving those ions are  
8 most likely decreased leading thus to a different chemical regime than present under ideal  
9 cloud conditions. For example, the huge differences in the activity coefficients of the TMIs  
10 can lead to substantial differences in the redox cycling.

Gelöscht: turnover

Gelöscht: partly quite

11

### 12 *Modeled activity coefficients of important organic compounds*

13 Fig. 13 illustrates the modeled time evolution of the activity coefficients of important organic  
14 carbonyl compounds and organic acids (both free acid and anions) for the two different  
15 relative humidity cases. For organic carbonyl compounds, the depiction reveals quite uneven  
16 pattern. For hydrated glyoxal and glycolaldehyde, the predicted activity coefficient are larger  
17 than 1 in both model cases. In contrast, activity coefficients below 1 are predicted for the  
18 other unhydrated organic carbonyls and the hydrated formaldehyde. As shown for the organic  
19 ions, there is a strong dependence of the non-ideal behavior on the species and their specific  
20 forms (i.e., functional groups included) as well as additionally the relative humidity  
21 conditions. For the hydrated glyoxal and glycolaldehyde with more than 3 OH functionalities  
22 included, activity coefficient values of about 1.2 and 1.6, respectively, are modeled in the  
23 90% r.h. case. Many times higher activity coefficients are calculated for the 70% r.h. case.

Gelöscht: 1

24 The predicted activity coefficients of the organic acid anions behave similarly to the inorganic  
25 ions. Differences can be observed for the 2 free acids plotted in Fig. 13. While the activity  
26 coefficient of formic and acetic acid corresponds mainly to the present supersaturation of 0.9  
27 in the 90% r.h. case, the activity coefficient of acetic acid are higher during the more  
28 concentrated case at 70% r.h. This behavior is caused by the additional methyl group. In  
29 summary, the predicted activity coefficients of organic compounds imply that the chemical  
30 processing of organics can be either increased or decreased under deliquesced particle  
31 conditions depending on the particular compound.

Gelöscht: 1

Gelöscht: organic

1

## 2 *Modeled acidity*

3 The modeled pH-values for the four different simulations are plotted in Fig. 14. The pH  
4 values simulated with and without consideration of non-ideal solution effects reveal no  
5 difference during the cloud periods but substantial deviations during the non-cloud periods.  
6 During the cloud periods under almost ideal conditions, an decrease of the pH value is  
7 modeled due to occurring acidifying reactions such as the S(IV) to S(VI) conversion. The  
8 acidification is strongest during the first cloud passage and lower during the two following  
9 clouds. From the two plots, it can be seen that the difference between the ideal and non-ideal  
10 case is somewhat larger for the 70% case. On average, the pH values of the simulations  
11 considering [solution](#) non-ideality are -0.27 and -0.44 pH units lower under 90% r.h. and  
12 70% r.h. conditions, respectively. This, lower acidity in the non-ideal case is able to affect  
13 both aqueous phase chemical reactions (i.e., acid catalyzed reactions) and all dissociations.  
14 Further implications of this difference for the chemical processing are not discussed here, but  
15 outlined in a companion paper (Rusumdar et al., 2015).

16 Overall, the performed simulations demonstrated that the further developed SPACCIM model  
17 performs well and the simulation results emphasize the consideration of [solution](#) non-ideality  
18 in multiphase chemistry models especially for an adequate description of the chemical aerosol  
19 processing in deliquesced particles.

20

## 21 **4 Summary**

22 In the present work, a robust and comprehensive model framework is developed and  
23 implemented in order to treat the aqueous phase chemistry considering non-ideal solution  
24 effects in the context of the multiphase model SPACCIM. The implemented group-  
25 contribution concept enables the reliable estimation of activity coefficients for organic-  
26 inorganic mixtures composed of various ions and functional groups. Treatment of [solution](#)  
27 non-ideality for mixed-solvent systems requires a careful combination of standard-state  
28 properties with activity coefficient models. This was achieved in practice by ensuring the  
29 correct representation of Gibbs excess energy by three contributions to the excess Gibbs  
30 energy. Surface tension depreciation due to the organic compounds is effectively accounted  
31 and included in the model framework. Interaction parameters accounts for various

Gelöscht: 2

Gelöscht: including the considered non-ideality approach

1 contributions of interactions. Mixed organic-inorganic systems from the literature are  
2 critically assessed and a new database is created. For all tested types of systems and data, the  
3 designed model SpactMod has been shown to reproduce both the original model results and  
4 experimental results with good accuracy. Sensitivity studies have shown that the inclusion of  
5 middle-range interaction contributions [is](#) necessary. This inclusion enhances the robustness of  
6 the model. The current developed framework is open to extension to further organic  
7 functional groups, and ions, when thermodynamic data on such systems become available.  
8 Indeed, compound specific parameter, such as charge, organic functional groups and  
9 interaction parameters, required for the activity coefficient model as well as chemical reaction  
10 data are read from input files. The interaction parameters will be easily incorporate and the  
11 database can flexibly updated. Besides, the computer code will facilitate the changes and  
12 future inclusions. The implemented numerical schemes merely give good computational  
13 efficiency. Due to the limitations regarding the lack of experimental data, and the ability to  
14 treat the organic-electrolyte mixtures of atmospheric relevance at various complexities,  
15 predictions are improved considerably while using extended interaction parameters. In future,  
16 the database will be extended with new parameters of [recent studies](#) ((Zuend et al., 2011;  
17 Mohs and Gmehling, 2013; Ganbavale et al., 2015)\_within this activity coefficient module.  
18 First test simulations with the advanced SPACCIM model have demonstrated the applicability  
19 of SpactMod within the model framework. Furthermore, the simulations emphasize that the  
20 treatment of [solution](#) non-ideality is mandatory for modeling multiphase chemistry processes  
21 in deliquesced particles. For important ions, the model runs have shown activity coefficients  
22 <1 and a strong dependency on the charge state as well as on the microphysical conditions.  
23 Thus, the model results implicate that the chemical processing of ions in deliquesced particles  
24 is potentially lowered and different to a chemical regime present under ideal cloud conditions.  
25 For organic compounds, the modeled activity coefficients [the activity coefficients are both](#)  
26 [lower and higher than unity](#), suggesting that the chemical processing [of organics](#) can be either  
27 increased or decreased under deliquesced particle conditions depending on the particular  
28 species. The complexity of consideration of non-ideal solutions and its influence on  
29 multiphase chemistry is investigated in detail in a companion paper (Rusumdar et al., 2015).

30

Gelöscht: are

Gelöscht: (

Gelöscht: partly

Gelöscht: >1)

Gelöscht: organic

## 1 Appendix A: SPACCIM's activity coefficient module

### 2 A.1 Middle-range contribution-model extension

3 The activity coefficients responsible for the MR interaction forces are obtained by  
 4 differentiating the Eq. (30) with respect to the number of moles of solvent main groups,  
 5 cations, and anions respectively. Thus, expressions for a specific cation  $c^*$  on a mole fraction  
 6 basis can be written as:

Gelöscht: 1

$$\begin{aligned}
 \ln \gamma_c^{MR, (x), \infty} &= \frac{1}{M_{av}} \sum_k B_{k,c^*}(I) x'_k + \frac{z_{c^*}^2}{2M_{av}} \sum_k \sum_i B'_{k,i}(I) x'_k m_i + \sum_a B_{c^*,a}(I) m_a \\
 &+ \frac{z_{c^*}^2}{2} \sum_c \sum_a B'_{c,a}(I) m_c m_a + \sum_a C_{c^*,a}(I) m_a \sum_i m_i |z_i| \\
 &+ \sum_c \sum_a \left[ C_{c,a}(I) |z_{c^*}| + C'_{c,a}(I) \frac{z_{c^*}^2}{2} \sum_i m_i |z_i| \right] m_c m_a \\
 &+ \sum_c R_{c^*,c} m_c + \sum_c \sum_a Q_{c,c^*,a} m_c m_a
 \end{aligned} \tag{A1}$$

8 For a better understanding, Eq. (A1) can be divided into different terms:

$$\ln \gamma_i^{MR} = T_i^{solvent} + T_i^{ion-solvent} + T_i^{ion} + T_i^{ion-ion} + T_i^{ternary} \tag{A2}$$

10 with

$$T_i^{solvent} = \frac{1}{M_{av}} \sum_k B_{k,c^*}(I) x'_k, \tag{A3}$$

$$T_i^{ion-solvent} = \frac{1}{M_{av}} \sum_k B_{k,c^*}(I) x'_k, \tag{A4}$$

$$T_i^{ion} = \sum_a B_{c^*,a}(I) m_a + \sum_c R_{c^*,c} m_c + \sum_a C_{c^*,a}(I) m_a \sum_i m_i |z_i|, \tag{A5}$$

$$\begin{aligned}
 T_i^{ion-ion} &= \frac{z_{c^*}^2}{2} \sum_c \sum_a B'_{c,a}(I) m_c m_a \\
 &+ \sum_c \sum_a \left[ C_{c,a}(I) |z_{c^*}| + C'_{c,a}(I) \frac{z_{c^*}^2}{2} \sum_i m_i |z_i| \right] m_c m_a,
 \end{aligned} \tag{A6}$$

$$T_i^{ternary} = \sum_c \sum_a Q_{c,c^*,a} m_c m_a. \tag{A7}$$

1

2 The term  $T^{ternary}$  stands for the ternary terms in Eq. (30) which was incorporated by Zuend et  
3 al. (2008) to improve the treatment of systems at high ionic strength.

Gelöscht: 31

4

5 As mentioned in Sect. 3, the activity coefficient module SpactMod is substantially based on  
6 AIOMFAC (Zuend et al., 2008). But it has been extended by including the new interaction  
7 parameters for the species shown in Fig. 4, based on mod. LIFAC (Kiepe et al., 2006). A  
8 sufficient evaluation was performed using the actual experimental database, which has been  
9 significantly enlarged within the last years (see Raatikainen and Laaksonen (2005); Tong et  
10 al. (2008)).

Gelöscht: the

11

12 The general concentration dependence of the interaction parameters can be written as  
13 analogous to Eq. (31):

Gelöscht: 2

14

$$15 \quad B_{i,j} = b_{i,j} + c_{i,j} \exp(a_1 \sqrt{I}) \quad (A8)$$

16 where,  $b_{i,j}$ ,  $c_{i,j}$  and  $a_1$  are adjustable interaction parameters. However, according to  
17 mod. LIFAC (Kiepe et al., 2006), the second virial coefficient  $B_{i,j}$  is the interaction  
18 coefficient between the species  $i$  and  $j$ . The relations of the ion $\leftrightarrow$ ion interaction parameter  
19  $B_{c,a}$  and ion $\leftrightarrow$ solvent group interaction parameter  $B_{k,ion}$  to the ionic strength are described  
20 by Kiepe et al. (2006).

21

$$22 \quad B_{c,a} = b_{c,a} + c_{c,a} \exp(-\sqrt{I} + 0.125I), \quad (A9)$$

$$23 \quad B_{k,i} = b_{k,i} + c_{k,i} \exp(-1.2\sqrt{I} + 0.25I). \quad (A10)$$

24 The equation for interaction parameters shown in the two versions (Eqs. 31 – 32, A9 and  
25 A10) was compared and the final model equations are derived. As a result, Eq. (A9) can be  
26 written as similar to Eq. (32):

Gelöscht: 2

Gelöscht: 4

Gelöscht: 3

1  $B_{c,a}(I) = b_{c,a} + c_{c,a} \exp\left(-\left(1.0 - 0.125\sqrt{I}\right)\sqrt{I}\right)$  (A11)

2 Based on this, while using the similar model equations, the database was utilized with the ion  
3  $\leftrightarrow$ ion interaction parameters as:

4  $b_{c,a}^{(1)} = b_{c,a}, b_{c,a}^{(2)} = c_{c,a}, b_{c,a}^{(3)} = \left(1.0 - 0.125\sqrt{I}\right).$  (A12)

5 Since ion  $\leftrightarrow$  ion  $\leftrightarrow$  ion interaction parameters (ternary interactions) were not available with  
6 mod. LIFAC, the interaction parameters for  $c_{c,a}^{(1)}$  and  $c_{c,a}^{(2)}$  were assigned to zero. Similar to ion  
7  $\leftrightarrow$ ion interaction parameters, the model equations to compute the solvent  $\leftrightarrow$ ion interaction  
8 parameters were also modified. Compared to Eq. (31) and Eq. (A10), the parameters are  
9 assigned as:

10  $b_{k,i}^{(1)} = b_{k,i}, b_{k,i}^{(2)} = c_{k,i}, b_{k,i}^{(3)} = \left(1.2 - 0.125\sqrt{I}\right).$  (A13)

11 Afterwards without altering the model equations given in AIOMFAC, computation of activity  
12 coefficients for all species is performed. Even, the ternary and quaternary interactions were  
13 also assigned to zero during the computation of activity coefficients for solvent groups.  
14 Hence, the model equations reduced to original model equations as described in [Kiepe et al.](#)  
15 [\(2006\)](#) and [Yan et al. \(1999\)](#). Similarly, for the ions, the ternary interactions (Eq. (A6)) are  
16 not considered to compute the activity coefficients, which are not explicitly described in the  
17 original AIOMFAC. So this term is equal to zero, and hence the Eq. (3.19) and Eq. (3.20)  
18 given in [Zuend et al. \(2008\)](#) lead to the original model equations (see Eq. (12) in [Kiepe et al.](#)  
19 [\(2006\)](#)). The chemical species included in the multiphase mechanism are categorized by  
20 different classes in the input files. While using these input files, this algorithm performs a  
21 search, and gathers the information, whether the computation of interaction parameters needs  
22 to perform according to AIOMFAC or the modified equations specified according to [Kiepe et](#)  
23 [al. \(2006\)](#). Thus, the adjustable interaction parameters are used to compute and finally utilized  
24 by the activity coefficients responsible for MR interactions.

25

26

27

Gelöscht: leads

Gelöscht: s

1

Table A1: MR Parameters  $b_{k,i}^{(1)}$  and  $b_{k,i}^{(2)}$  between solvents and ions (AIOMFAC- Black/ mod. LIFAC- Red)

2

Ion	Group	$b_{k,i}^{(1)}$ (kg mol <sup>-1</sup> )	$b_{k,i}^{(2)}$ (kg mol <sup>-1</sup> )	Ion	Group	$b_{k,i}^{(1)}$ (kg mol <sup>-1</sup> )	$b_{k,i}^{(2)}$ (kg mol <sup>-1</sup> )
Na <sup>+</sup>	CH <sub>n</sub>	0.124972	- 0.031880	Na <sup>+</sup>	OH	0.080254	0.002201
K <sup>+</sup>	CH <sub>n</sub>	0.121449	0.015499	K <sup>+</sup>	OH	0.065219	-0.170779
NH <sub>4</sub> <sup>+</sup>	CH <sub>n</sub>	0.103096	-0.001083	NH <sub>4</sub> <sup>+</sup>	OH	0.039373	0.001083
Ca <sup>2+</sup>	CH <sub>n</sub>	0.000019	-0.060807	Ca <sup>2+</sup>	OH	0.839628	-0.765776
Mg <sup>2+</sup>	CH <sub>n</sub>	- 0.34610	-0.44995	Mg <sup>2+</sup>	OH	0.281980	0.07617
Zn <sup>2+</sup>	CH <sub>n</sub>	- 0.10163	- 0.06578	Zn <sup>2+</sup>	OH	0.036480	0.02249
Cl <sup>-</sup>	CH <sub>n</sub>	0.014974	0.142574	Cl <sup>-</sup>	OH	-0.042460	-0.128063
NO <sub>3</sub> <sup>-</sup>	CH <sub>n</sub>	0.018368	0.669086	NO <sub>3</sub> <sup>-</sup>	OH	-0.128216	-0.962408
SO <sub>4</sub> <sup>2-</sup>	CH <sub>n</sub>	0.101044	-0.070253	SO <sub>4</sub> <sup>2-</sup>	OH	-0.164709	0.574638

I <sup>-</sup>	CH <sub>n</sub>	0.01206	- 0.02777	I <sup>-</sup>	OH	-0.04479	0.04151
				F <sup>-</sup>	OH	0.15233	-0.04145
				CH <sub>3</sub> COO <sup>-</sup>	OH	0.02672	-0.02117
Na <sup>+</sup>	H <sub>2</sub> O	0.00331	-0.00143	Na <sup>+</sup>	CH <sub>3</sub> OH	0.16617	0.03928
K <sup>+</sup>	H <sub>2</sub> O	0.00258	- 0.00088	K <sup>+</sup>	CH <sub>3</sub> OH	0.10797	0.19164
NH <sub>4</sub> <sup>+</sup>	H <sub>2</sub> O	0.00088	0.00288	NH <sub>4</sub> <sup>+</sup>	CH <sub>3</sub> OH	0.20529	- 0.10550
Ca <sup>2+</sup>	H <sub>2</sub> O	0.01105	0.00641	Ca <sup>2+</sup>	CH <sub>3</sub> OH	0.37818	0.00247
Mg <sup>2+</sup>	H <sub>2</sub> O	0.00050	0.01163	Cu <sup>2+</sup>	CH <sub>3</sub> OH	0.00789	- 0.06944
Cu <sup>2+</sup>	H <sub>2</sub> O	- 0.00571	- 0.00760	Zn <sup>2+</sup>	CH <sub>3</sub> OH	0.16775	- 0.44229
Zn <sup>2+</sup>	H <sub>2</sub> O	- 0.01848	0.00001				
Cl <sup>-</sup>	H <sub>2</sub> O	-0.00128	- 0.00020	Cl <sup>-</sup>	CH <sub>3</sub> OH	- 0.03352	0.00242
NO <sub>3</sub> <sup>-</sup>	H <sub>2</sub> O	0.03228	- 0.00083	NO <sub>3</sub> <sup>-</sup>	CH <sub>3</sub> OH	- 0.07716	- 0.00669
SO <sub>4</sub> <sup>2-</sup>	H <sub>2</sub> O	0.02278	0.00271	Br <sup>-</sup>	CH <sub>3</sub> OH	- 0.00944	- 0.06080
Br <sup>-</sup>	H <sub>2</sub> O	- 0.00247	- 0.00008	I <sup>-</sup>	CH <sub>3</sub> OH	- 0.02090	- 0.14894

1

---

$\text{NO}_2^-$	$\text{H}_2\text{O}$	0.00549	- 0.00565	$\text{F}^-$	$\text{CH}_3\text{OH}$	0.07436	- 0.04388
$\text{I}^-$	$\text{H}_2\text{O}$	-0.00537	0.00018	$\text{CH}_3\text{COO}^-$	$\text{CH}_3\text{OH}$	0.00046	0.01249
$\text{F}^-$	$\text{H}_2\text{O}$	0.00652	0.00132				
$\text{CH}_3\text{COO}^-$	$\text{H}_2\text{O}$	0.01918	0.00230				
$\text{Na}^+$	$\text{CH}_2\text{CO}$	-0.21019	0.94813				
$\text{K}^+$	$\text{CH}_2\text{CO}$	-0.44195	1.10287				
$\text{Cl}^-$	$\text{CH}_2\text{CO}$	0.54064	-0.62981				
$\text{Br}^-$	$\text{CH}_2\text{CO}$	0.48898	-0.96778				
$\text{I}^-$	$\text{CH}_2\text{CO}$	0.08245	0.03292				
$\text{CH}_3\text{COO}^-$	$\text{CH}_2\text{CO}$	0.26560	-0.93032				

---

2

3

1

Table A2: Mod. LIFAC Binary cation-anion MR interaction parameters

2

Cation	Anion	$b_{c,a}^{(1)}$	$b_{c,a}^{(2)}$
Na <sup>+</sup>	F <sup>-</sup>	-0.00694	-0.08166
Na <sup>+</sup>	I <sup>-</sup>	0.27922	-0.13430
Na <sup>+</sup>	NO <sub>3</sub> <sup>-</sup>	0.04425	-0.41980
Na <sup>+</sup>	CH <sub>3</sub> COO <sup>-</sup>	0.25018	0.31363
K <sup>+</sup>	F <sup>-</sup>	0.18434	-0.28912
K <sup>+</sup>	I <sup>-</sup>	0.12860	0.02379
K <sup>+</sup>	NO <sub>3</sub> <sup>-</sup>	-0.06095	-0.67019
K <sup>+</sup>	CH <sub>3</sub> COO <sup>-</sup>	0.27327	0.45129
Mg <sup>+</sup>	Cl <sup>-</sup>	0.45150	1.19298
Mg <sup>+</sup>	Br <sup>-</sup>	0.59615	1.37619
Mg <sup>+</sup>	I <sup>-</sup>	0.76336	1.58654
Mg <sup>+</sup>	NO <sub>3</sub> <sup>-</sup>	0.28427	1.72405
Mg <sup>+</sup>	SO <sub>4</sub> <sup>2-</sup>	0.53597	1.03876
Ca <sup>+</sup>	Br <sup>-</sup>	0.60948	0.30140
Ca <sup>+</sup>	I <sup>-</sup>	0.59261	1.46632
Ca <sup>+</sup>	SO <sub>4</sub> <sup>2-</sup>	-15.8421	-0.00212
Cu <sup>2+</sup>	Cl <sup>-</sup>	0.21233	0.11695

---

$\text{Cu}^{2+}$	$\text{NO}_3^-$	0.45706	-0.41585
$\text{Cu}^{2+}$	$\text{SO}_4^{2-}$	1.24148	-5.86466
$\text{Zn}^{2+}$	$\text{Cl}^-$	0.04463	0.43088

---

1

2

3

1

Table A3: AIOMFAC Binary cation  $\leftrightarrow$  anion MR interaction parameters.

2

<b>Cation</b>	<b>Anion</b>	$b_{c,a}^{(1)}$ [kg mol <sup>-1</sup> ]	$b_{c,a}^{(2)}$ [kg mol <sup>-1</sup> ]	$b_{c,a}^{(3)}$ [kg <sup>1/2</sup> mol <sup>-1/2</sup> ]	$c_{c,a}^{(1)}$ [kg <sup>2</sup> mol <sup>-2</sup> ]	$c_{c,a}^{(2)}$ [kg <sup>1/2</sup> mol <sup>-1/2</sup> ]
H <sup>+</sup>	Cl <sup>-</sup>	0.182003	0.243340	0.8	0.033319	0.504672
H <sup>+</sup>	Br <sup>-</sup>	0.120325	0.444859	0.8	0.080767	0.596776
H <sup>+</sup>	NO <sub>3</sub> <sup>-</sup>	0.210638	0.122694	0.8	-0.101736	1.676420
H <sup>+</sup>	SO <sub>4</sub> <sup>2-</sup>	0.097108	-0.004307	1.0	0.140598	0.632246
H <sup>+</sup>	HSO <sub>4</sub> <sup>-</sup>	0.313812	-4.895466	1.0	-0.358419	0.807667
Li <sup>+</sup>	Cl <sup>-</sup>	0.106555	0.206370	0.8	0.053239	0.535548
Li <sup>+</sup>	Br <sup>-</sup>	0.106384	0.316480	0.8	0.057602	0.464658
Li <sup>+</sup>	NO <sub>3</sub> <sup>-</sup>	0.076313	0.300550	0.8	0.046701	0.664928
Li <sup>+</sup>	SO <sub>4</sub> <sup>2-</sup>	0.114470	0.035401	0.8	-0.263258	1.316967
Na <sup>+</sup>	Cl <sup>-</sup>	0.053741	0.079771	0.8	0.024553	0.562981
Na <sup>+</sup>	Br <sup>-</sup>	0.180807	0.273114	0.8	-0.506578	2.209050
Na <sup>+</sup>	NO <sub>3</sub> <sup>-</sup>	0.001164	-0.102546	0.410453	0.002535	0.512657
Na <sup>+</sup>	SO <sub>4</sub> <sup>2-</sup>	0.001891	-0.424184	0.8	-0.223851	1.053620
Na <sup>+</sup>	HSO <sub>4</sub> <sup>-</sup>	0.021990	0.001863	0.8	0.019921	0.619816

1

---

K <sup>+</sup>	Cl <sup>-</sup>	0.016561	-0.002752	0.8	0.020833	0.670530
K <sup>+</sup>	Br <sup>-</sup>	0.033688	0.060882	0.8	0.015293	0.565063
K <sup>+</sup>	NO <sub>3</sub> <sup>-</sup>	0.000025	-0.413172	0.357227	-0.000455	0.342244
K <sup>+</sup>	SO <sub>4</sub> <sup>2-</sup>	0.004079	-0.869936	0.8	-0.092240	0.918743
NH <sub>4</sub> <sup>+</sup>	Cl <sup>-</sup>	0.001520	0.049074	0.116801	0.011112	0.653256
NH <sub>4</sub> <sup>+</sup>	Br <sup>-</sup>	0.002498	0.081512	0.143621	0.013795	0.728984
NH <sub>4</sub> <sup>+</sup>	NO <sub>3</sub> <sup>-</sup>	-0.000057	-0.171746	0.260000	0.005510	0.529762
NH <sub>4</sub> <sup>+</sup>	SO <sub>4</sub> <sup>2-</sup>	0.000373	-0.906075	0.545109	-0.000379	0.354206
NH <sub>4</sub> <sup>+</sup>	HSO <sub>4</sub> <sup>-</sup>	0.009054	0.214405	0.228956	0.017298	0.820465
Mg <sup>2+</sup>	Cl <sup>-</sup>	0.195909	0.332387	0.8	0.072063	0.397920
Mg <sup>2+</sup>	NO <sub>3</sub> <sup>-</sup>	0.430671	0.767242	0.8	-0.511836	1.440940
Mg <sup>2+</sup>	SO <sub>4</sub> <sup>2-</sup>	0.122364	-3.425876	0.8	-0.738561	0.864380
Ca <sup>2+</sup>	Cl <sup>-</sup>	0.104920	0.866923	0.8	0.072063	0.365747
Ca <sup>2+</sup>	NO <sub>3</sub> <sup>-</sup>	0.163282	0.203681	0.8	-0.075452	1.210906

2

3

1

Table A4: UNIFAC interaction parameter (E-AIM). Values from Peng et al. (2001) are presented in red.

2

Organics	CH <sub>n</sub>	OH	CH <sub>3</sub> OH	H <sub>2</sub> O	CH <sub>2</sub> CO	CHO	CCOO	HCOO	CH <sub>2</sub> O	COOH
CH <sub>n</sub>	0.0	986.5	697.2	1318.0	476.4	677.0	232.1	507.00	251.5	663.5
OH	156.4	0.0	-137.1	276.4	84	-203.60	101.1	267.80	28.06	224.39
CH <sub>3</sub> OH	16.51	249.1	0.0	-181.0	23.39	306.4	-10.72	179.70	-128.60	-202
H <sub>2</sub> O	-89.71	-153.0	289.6	0.0	-195.4	-116.0	72.870	233.87	540.5	-69.29
CH <sub>2</sub> CO	26.76	164.5	108.7	472.5	0.0	-37.36	-213.7	-190.40	-103.60	669.4
CHO	505.7	529.00	-340.2	480.80	128.0	0.0	-110.3	766.00	304.1	497.5
CCOO	114.8	245.40	249.63	200.0	372.2	185.10	0.0	-241.80	-235.7	660.2
HCOO	329.30	139.40	227.80	124.63	385.40	-236.50	1167.0	0.0	-234.00	-268.1
CH <sub>2</sub> O	83.36	237.7	238.40	-314.7	191.10	-7.838	461.3	457.30	0.0	664.00
COOH	315.3	-103.03	339.80	-145.88	-297.8	-165.50	-256.3	193.90	-338.5	0.0

3

4

5

1

Table A5: UNIFAC Relative Vander Waals group volume ( $R_k$ ) and surface area ( $Q_k$ ) parameters for solvent groups.

2

No	Family Name	Main Group	Subgroup	$R_t$	$Q_t$
1	Alkane	$CH_n$ (n= 0,1,2,3)	CH3	0.9011	0.848
			CH2	0.6744	0.540
			CH	0.4469	0.228
			C	0.2195	0.00
2	Alcohol	OH	OH	1.0000	1.20
3	Water	$H_2O$	$H_2O$	0.9200	1.400
4	Methanol	$CH_3OH$	$CH_3OH$	1.4311	1.432
5	Carbonyl	$CH_2CO$	$CH_3CO$	1.6724	1.488
			$CH_2CO$	1.4457	1.180
6	Aldehyde	CHO	CHO	0.9980	0.948
7	Acetate	CCOO	$CH_3COO$	1.9031	1.728
			$CH_2COO$	1.6764	1.420
8	Formate	HCOO	HCOO	1.2420	1.188
9	Ether	$CH_2O$	$CH_3O$	1.1450	1.088
			$CH_2O$	0.9183	0.780
			CH-O	0.6908	0.468
10	Carboxylic acid	COOH	COOH	1.3013	1.224
			HCOOH	1.5280	1.532

3

4

1 Table A6: Relative van der Waals subgroup volume ( $R_t^H$ ) and surface area ( $Q_t^H$ ) parameters for cations and anions considering dynamic  
 2 hydration. Values from AIOMFAC and mod. LIFAC are presented in black and red, respectively.

3

Ion	ADHN <sup>a,b</sup>	$R_t$	$Q_t$	$R^H$ <sup>c</sup>	$Q^H$ <sup>c</sup>	Reference
H <sup>+</sup>	1.93	0.0	0.0	1.78	2.70	Zuend et al. (2008)
Na <sup>+</sup>	0.22	0.18	0.18	0.38	0.62	Zuend et al. (2008)
K <sup>+</sup>	0.00	0.44	0.58	0.440	0.58	Zuend et al. (2008)
NH <sub>4</sub> <sup>+</sup>	0.00	0.69	0.78	0.69	0.78	Zuend et al. (2008)
Mg <sup>2+</sup>	5.85	0.06	0.16	5.44	8.35	Zuend et al. (2008)
Ca <sup>2+</sup>	2.10	0.31	0.46	2.24	3.40	Zuend et al. (2008)
Fe <sup>2+</sup>	0.00	0.90	0.84	0.901	0.84	<sup>d</sup>
Cu <sup>2+</sup>	0.00	0.13	0.26	0.13	0.26	Kiepe et al. (2006)
Mn <sup>2+</sup>	0.00	0.90	0.84	0.901	0.84	<sup>d</sup>
Zn <sup>2+</sup>	2.18	0.12	0.24	2.12	3.29	Kiepe et al (2006)
Cl <sup>-</sup>	0.00	0.99	0.99	0.99	0.99	Zuend et al. (2008)
Br <sup>-</sup>	0.00	1.25	1.16	1.25	1.16	Zuend et al. (2008)
NO <sub>3</sub> <sup>-</sup>	0.00	0.95	0.97	0.95	0.97	Zuend et al. (2008)
HSO <sub>4</sub> <sup>-</sup>	0.00	1.65	1.40	1.65	1.40	Zuend et al. (2008)
SO <sub>4</sub> <sup>2-</sup>	1.83	1.66	1.40	3.34	3.96	Zuend et al. (2008)
OH <sup>-</sup>	2.80	1.16	1.27	3.74	5.196	Kiepe et al. (2006)

$\text{CO}_3^{2-}$	0.00	2.06	2.25	2.06	2.26	Kiepe et al. (2006)
$\text{NO}_2^-$	0.00	1.52	1.68	1.52	1.6	Kiepe et al. (2006)
$\text{I}^-$	0.00	1.55	1.34	1.55	1.34	Kiepe et al. (2006)
$\text{F}^-$	5.02	0.29	0.44	4.92	7.45	Kiepe et al. (2006)
$\text{HCOO}^-$	0.00	0.901	0.84	0.901	0.84	<sup>d</sup>
$\text{CH}_3\text{COO}^-$	0.00	1.74	1.04	1.74	1.0437	Kiepe et al. (2006)
$\text{HOOCCH}_2\text{COO}^-$	0.00	0.901	0.84	0.901	0.84	<sup>d</sup>
$\text{HOCC}_2\text{H}_4\text{COO}^-$	0.00	0.901	0.84	0.901	0.84	<sup>d</sup>
$\text{HCO}_3^-$	0.00	0.901	0.84	0.901	0.84	<sup>d</sup>
$\text{CHOCOO}^-$	0.00	0.901	0.84	0.901	0.84	<sup>d</sup>

<sup>1</sup> The apparent dynamic hydration numbers (ADHN) at 303.15 K and 0.1 M take from Kiriukhin and Collins (2002).

<sup>b</sup> Values of ADHN = 0 are assigned to the ions for which the data is unavailable.

<sup>c</sup> calculated using Eq. (34) and (35), respectively.

<sup>d</sup> ADHN data is not available

1

2

3

# 1 Appendix B: List of symbols, indices and acronyms

## 2 Table B1. List and description of symbols and indices.

Symbol/Index	Description
$a_i$	Activity of species $i$
$a_A$	Activity of compound A
$a_i^k$	Activity of species $i$ in the $k^{th}$ particle/cloud droplet class
$a_w$	Water activity
$a_w^k$	Water activity in the $k^{th}$ particle/cloud droplet class
$A_{(aq)}$	Compound A in the aqueous phase
$A_{(g)}$	Compound A in the gas phase
$A$	Debye-Hückel parameter
$b$	Debye-Hückel parameter
$B_{c,a}(I)$	Ionic strength dependent binary interaction coefficient between cations and anions
$b_{k,i}^{(1)}, b_{k,i}^{(2)}, b_{c,a}^{(1)}, b_{c,a}^{(2)}, c_{c,a}^{(1)}, c_{c,a}^{(2)}$	Fitted parameters (AIOMFAC)
$B_{k,i}(I)$	Ionic strength dependent binary interaction coefficient between solvent main groups and ions
$c^*$	Specific cation
$C_{c,a}(I)$	Interaction coefficient between cation $\leftrightarrow$ anion pairs with respect to the total charge concentration
$c^G$	Vector of the concentrations of the gas phase species
$c_i$	Mass concentration of an aqueous phase species $i$
$c_{i,k}^s$	Saturation vapor mole concentration
$c_i^G$	$i^{*th}$ gas phase chemical species
$\mathbf{c}^k$	Vector of all concentrations
$c_i^k$	$i^{th}$ aqueous phase chemical species in the $k^{th}$ particle/cloud droplet class
$c_{sol}$	Solute concentration
$c_{sol}^k$	Solute concentration in the $k^{th}$ particle class
$D_i^G$	Gas diffusion coefficient
$F(c_l^1, \dots, c_l^M)$	Mass transfer between different droplet classes by microphysical processes
$G_{LR}^{ex}$	Long-range (LR) electrostatic interactions contributing to excess Gibbs free energy
$G_{MR}^{ex}$	Middle-range (MR) electrostatic interactions contributing to excess Gibbs free energy
$G_{SR}^{ex}$	Short-range (SR) electrostatic interactions contributing to excess Gibbs free energy
$G^{ex}(p, T, n_j)$	Excess Gibbs energy

Symbol/Index	Description
$H_i$	Dimensionless Henry's law constant of species $i$
$i, i^*$	Species index
<b>I</b>	Identity matrix
$I$	Ionic strength
$j$	Species index
<b>J</b>	Approximation of the Jacobian
$k = 1, \dots, M$	Particle/cloud droplet class index
$k_i^{ki}$	Mass transfer coefficient of species $i$ into the $k^{th}$ particle/cloud droplet class
$K_{eq}$	Equilibrium constant
$K_i^H$	Henry's law constant of species $i$
$L$	Liquid water content
$L_k$	Liquid water content of the $k^{th}$ droplet class inside the box volume
$m_A$	Molality of compound A
$M_c$	Molar mass of carbon
$m_i$	Molality of an aqueous phase species $i$
$m_i^k$	Molality of dissolved gas phase species $i$ in particle class $k$
$m_j$	Molality of the $j^{th}$ species
$mol_{sol_i}^k$	Moles of soluble material of the $i^{th}$ species in the $k^{th}$ particle/droplet class
$M_{sol}$	Mean molar mass of solute
$M_s$	Molar mass of solvent $s$
$mol_w^k$	Molar water fraction
$N_A$	Number of aqueous phase species
$n_a$	Moles of anions
$N_t^{ADH}$	Dynamic hydration numbers
$n_c, n_c'$	Moles of cations
$n_{cb}$	Number of carbon atoms
$N_G$	Number of gas phase species
$n_j$	Number of moles of component $j$
$p$	Total pressure
$p_{i,k}^s$	Saturation vapor pressure of gas phase species $i$ over a particle in size bin $k$
$p_w$	Equilibrium partial pressure of water over the solution droplet
$p_w^o$	Equilibrium water vapor pressure over a flat surface of pure water
$Q_{c,c',a}(I)$	Ternary interaction coefficient involving two different cations
$q_i / r_i$	Surface area / volume of component $i$

Symbol/Index	Description
$r_A$	Reaction rate
$r_{drop} (m)$	Mean wet droplet radius
$r_k$	Droplet radius of the $k^{th}$ particle/cloud droplet class
$R$	Universal gas constant
$R_{c,c'}(I)$	Binary interaction coefficient involving two different cations
$RH$	Ambient relative humidity
$R_l^A$	Aqueous phase chemical reaction terms of species $l$ (chemical production and degradation fluxes)
$R_l^G$	Gas phase chemical reaction terms of species $l^*$ (chemical production and degradation fluxes)
$R_i / Q_i$	Relative van der Waals subgroup volume/surface area parameters
$R_i^H / Q_i^H$	Hydrated group volume and surface area parameters
$R_w / Q_w$	$R_i / Q_i$ values of the water molecule
$T (K)$	Temperature
$x_w$	Mole fraction of water
$x_i$	Mole fraction of component $i$
$z_i$	Number of elementary charges of ion $i$
$\{a_i\}$	Thermodynamic activity of species $i$
$\{A\}$ etc.	Individual thermodynamic activities
$\{A_{(aq)}\} = m_A \gamma_A$	Activity of an un-dissociated compound
$\{A_{(g)}\}$	Activity of a gas over a particle surface
$\{A_{(s)}\} = m_s$	Activity of a solid
$\{A^+\} = m_{A^+} \gamma_{A^+}$	Activity of an ion in solution
$[C^k]$	Concentration of WSOC (Water Soluble Organic Carbon) in particle class $k$
$\{H_2O_{(aq)}\} = a_w$	Activity of liquid water in a particle
$\alpha_i$	Mass accommodation coefficient of the $i^{th}$ species
$\beta$	Parameter of the integration method
$\gamma_A$	Activity coefficient of compound A
$\gamma_i$	Molality based activity coefficient of species $i$
$\gamma_w$	Molality based water activity coefficient
$\gamma_j^k$	Activity coefficient of the $j^{th}$ species in the $k^{th}$ particle/droplet class
$\gamma_{\pm}$	Mean activity coefficient
$\gamma_+ / \gamma_-$	Activity coefficients of a cation and anion
$\epsilon_w$	Static permittivity

Symbol/Index	Description
$\kappa_i$	Prefactor of the Henry term (solubility index)
$\lambda_i (= \pm 1)$	Factor +1 for products and -1 for reactants
$\mu$	Time dependent entrainment/detrainment rate
$\mu_i^{(m)}(p, T, n_j) / \mu_i^{(x)}(p, T, n_j)$	Chemical potentials
$v_i$	Molecular speed of gas phase species $i$
$v_w$	Partial molar volume of water
$\rho_w$	Density
$\sigma_w$	Surface tension of pure water
$\sigma_{w,s}$	Droplet solution surface tension
$\ln \gamma_j^{SR}$	Short-range activity coefficient $\gamma_j$ of a molecular component $j$ (can be solute or solvent)
$\ln \gamma_i^{SR,(x),\infty}$	Unsymmetrical normalized activity coefficient

1

2

3 Table B2. List and description of acronyms.

Acronym	Description
ADCHAM	Aerosol Dynamics, gas- and particle-phase chemistry model for laboratory CHAMber studies
ADDEM	Aerosol Diameter Dependent Equilibrium Model
AIM	Aerosol Inorganic Model
GFEMN	Gibbs free energy minimization model
AIOMFAC	Aerosol Inorganic-Organic Mixtures Functional groups Activity Coefficients
BDF	Backward differential formula
CAPRAM	Chemical Aqueous Phase RAdical Mechanism
CSB	Clegg-Seinfeld-Brimblecombe model
E-AIM	Extended Aerosol Inorganic Model
EQSAM3	3rd Equilibrium Simplified Aerosol Model (EQSAM3)
EQUISOLV II	EQUilibrium SOLVer version 2
ISORROPIA	Thermodynamic equilibrium aerosol model (= "equilibrium" in Greek)
ISORROPIA II	Thermodynamic equilibrium aerosol model version 2
LR	Long-range
MADM	Multicomponent Aerosol Dynamics Model
MARS-A	Model for an Aerosol Reacting System – version A

Acronym	Description
MESA	Multicomponent Equilibrium Solver for Aerosols
mod. LIFAC	Modified Liquid Functional Activity Coefficient Model
MOSAIC	MOdel for Simulating Aerosol Interactions and Chemistry
MR	Middle-range
ODE	Ordinary differential equation
SPACCIM	Spectral Aerosol Cloud Chemistry Interaction Model
SpactMod	SPACCIM activity coefficient module
SR	Short-range
TMIs	Transition Metal Ions
UHAERO	Inorganic atmospheric aerosol phase equilibrium model (UHAERO)
UNIFAC	UNIversal Functional-group Activity Coefficients
WSOC	Water Soluble Organic Carbon

1

2

3 |

1

## 2 **Acknowledgement**

3 The authors would like to thank Claudia Marcolli and Thomas Peter (ETH Zurich) for the  
4 performed water activity measurements of the aqueous test solutions. Furthermore, we would  
5 like to thank Andreas Zünd (Mc Gill University, Montreal) for providing a set of additional  
6 interaction parameters of AIOMFAC.

7

## 8 **References**

9

10 Achard, C., Dussap, C. G., and Gros, J. B.: Representation of vapour-liquid equilibria in  
11 water-alcohol-electrolyte mixtures with a modified UNIFAC-group-contribution method,  
12 *Fluid Phase Equilib.*, 98, 71-89, 1994.

13 Amundson, N. R., Caboussat, A., He, J. W., Martynenko, A. V., Savarin, V. B., Seinfeld, J.  
14 H., and Yoo, K. Y.: A new inorganic atmospheric aerosol phase equilibrium model  
15 (UHAERO), *Atmos. Chem. Phys.*, 6, 975-992, 2006.

16 Amundson, N. R., Caboussat, A., He, J. W., Martynenko, A. V., Landry, C., Tong, C., and  
17 Seinfeld, J. H.: A new atmospheric aerosol phase equilibrium model (UHAERO): organic  
18 systems, *Atmos. Chem. Phys.*, 7, 4675-4698, 10.5194/acp-7-4675-2007, 2007.

19 Ansari, A. S., and Pandis, S. N.: Prediction of multicomponent inorganic atmospheric aerosol  
20 behavior, *Atmos. Environ.*, 33, 745-757, 1999a.

21 Ansari, A. S., and Pandis, S. N.: An analysis of four models predicting the partitioning of  
22 semivolatile inorganic aerosol components, *Aerosol Sci Tech*, 31, 129-153, Doi  
23 10.1080/027868299304200, 1999b.

24 Antypov, D., and Holm, C.: Osmotic coefficient calculations for dilute solutions of short stiff-  
25 chain polyelectrolytes, *Macromolecules*, 40, 731-738, 2007.

26 Binkowski, F. S., and Roselle, S. J.: Models-3 Community Multiscale Air Quality (CMAQ)  
27 model aerosol component 1. Model description, *J. Geophys. Res. Atmos.*, 108, 2003.

28 Bräuer, P., Tilgner, A., Wolke, R., and Herrmann, H.: Mechanism development and  
29 modelling of tropospheric multiphase halogen chemistry: The CAPRAM Halogen Module 2.0  
30 (HM2), *J. Atmos. Chem.*, 70, 19-52, 10.1007/S10874-013-9249-6, 2013.

31 Chang, E. I., and Pankow, J. F.: Prediction of activity coefficients in liquid aerosol particles  
32 containing organic compounds, dissolved inorganic salts, and water - Part 2: Consideration of  
33 phase separation effects by an X-UNIFAC model, *Atmos. Environ.*, 40, 6422-6436, 2006.

34 Clegg, S. L., Brimblecombe, P., and Wexler, A. S.: A thermodynamic model of the system  $H^+$   
35  $- NH_4^+ - SO_4^{2-} - NO_3^- - H_2O$  at 298.15 K, *J. Phys. Chem. A*, 102, 2155-2171, 1998a.

36 Clegg, S. L., Brimblecombe, P., and Wexler, A. S.: Thermodynamic Model of the System  $H^+$   
37  $- NH_4^+ - SO_4^{2-} - NO_3^- - H_2O$  at Tropospheric Temperatures, *J. Phys. Chem. A*, 102, 2137-  
38 2154, 1998b.

- 1 Clegg, S. L., Seinfeld, J. H., and Brimblecombe, P.: Thermodynamic modelling of aqueous  
2 aerosols containing electrolytes and dissolved organic compounds, *J. Aerosol. Sci.*, 32, 713-  
3 738, 2001.
- 4 Clegg, S. L., Kleeman, M. J., Griffin, R. J., and Seinfeld, J. H.: Effects of uncertainties in the  
5 thermodynamic properties of aerosol components in an air quality model - Part 1: Treatment  
6 of inorganic electrolytes and organic compounds in the condensed phase, *Atmos. Chem.*  
7 *Phys.*, 8, 1057-1085, 2008.
- 8 Debye, P., and Hückel, E.: Zur Theorie der Elektrolyte, *Physikalische Zeitschrift*, 24, 185-  
9 206, 1923.
- 10 Deguillaume, L., Tilgner, A., Schrodner, R., Wolke, R., Chaumerliac, N., and Herrmann, H.:  
11 Towards an operational aqueous phase chemistry mechanism for regional chemistry-transport  
12 models: CAPRAM-RED and its application to the COSMO-MUSCAT model, *J. Atmos.*  
13 *Chem.*, 64, 1-35, 10.1007/S10874-010-9168-8, 2010.
- 14 Demaret, J. P., and Gueron, M.: Composite cylinder models of DNA - Application of the  
15 electrostatics of the B-Z transition, *Biophys. J.*, 65, 1700-1713, 1993.
- 16 Erdakos, G. B., Chang, E. I., Pankow, J. F., and Seinfeld, J. H.: Prediction of activity  
17 coefficients in liquid aerosol particles containing organic compounds, dissolved inorganic  
18 salts, and water-Part 3: Organic compounds, water, and ionic constituents by consideration of  
19 short-, mid-, and long-range effects using X-UNIFAC.3, *Atmos. Environ.*, 40, 6437-6452,  
20 2006.
- 21 Ervens, B., George, C., Williams, J. E., Buxton, G. V., Salmon, G. A., Bydder, M.,  
22 Wilkinson, F., Dentener, F., Mirabel, P., Wolke, R., and Herrmann, H.: CAPRAM 2.4  
23 (MODAC mechanism): An extended and condensed tropospheric aqueous phase mechanism  
24 and its application, *J. Geophys. Res. Atmos.*, 108, 10.1029/2002jd002202, 2003.
- 25 Ervens, B., Feingold, G., Clegg, S. L., and Kreidenweis, S. M.: A modeling study of aqueous  
26 production of dicarboxylic acids: 2. Implications for cloud microphysics, *J. Geophys. Res.*  
27 *Atmos.*, 109, 2004.
- 28 Ervens, B., Turpin, B. J., and Weber, R. J.: Secondary organic aerosol formation in cloud  
29 droplets and aqueous particles (aqSOA): a review of laboratory, field and model studies,  
30 *Atmos. Chem. Phys.*, 11, 11069-11102, 10.5194/Acp-11-11069-2011, 2011.
- 31 Facchini, M., Mircea, M., Fuzzi, S., and Charlson, R.: Cloud albedo enhancement by surface-  
32 active organic solutes in growing droplets, *Nature*, 401, 257-259, 1999.
- 33 Facchini, M. C., Decesari, S., Mircea, M., Fuzzi, S., and Loglio, G.: Surface tension of  
34 atmospheric wet aerosol and cloud/fog droplets in relation to their organic carbon content and  
35 chemical composition, *Atmos Environ*, 34, 4853-4857, Doi 10.1016/S1352-2310(00)00237-5,  
36 2000.
- 37 Fast, J. D., Gustafson, W. I., Easter, R. C., Zaveri, R. A., Barnard, J. C., Chapman, E. G.,  
38 Grell, G. A., and Peckham, S. E.: Evolution of ozone, particulates, and aerosol direct radiative  
39 forcing in the vicinity of Houston using a fully coupled meteorology-chemistry-aerosol  
40 model, *J. Geophys. Res. Atmos.*, 111, 2006.
- 41 Fountoukis, C., and Nenes, A.: ISORROPIA II: a computationally efficient thermodynamic  
42 equilibrium model for  $K^+$  -  $Ca^{2+}$  -  $Mg^{2+}$  -  $NH_4^+$  -  $Na^+$  -  $SO_4^{2-}$  -  $NO_3^-$  -  $Cl^-$  -  $H_2O$  aerosols,  
43 *Atmos. Chem. Phys.*, 7, 4639-4659, 2007.

1 Fredenslund, A., Jones, R. L., and Prausnitz, J. M.: Group-contribution estimation of activity  
2 coefficients in non-ideal liquid mixtures, *AIChE J.*, 21, 1086-1098, 1975.

3 Ganbavale, G., Zuend, A., Marcolli, C., and Peter, T.: Improved AIOMFAC model  
4 parameterisation of the temperature dependence of activity coefficients for aqueous organic  
5 mixtures, *Atmos Chem Phys*, 15, 447-493, 10.5194/acp-15-447-2015, 2015.

6 Gilardoni, S., Liu, S., Takahama, S., Russell, L. M., Allan, J. D., Steinbrecher, R., Jimenez, J.  
7 L., De Carlo, P. F., Dunlea, E. J., and Baumgardner, D.: Characterization of organic ambient  
8 aerosol during MIRAGE 2006 on three platforms, *Atmos. Chem. Phys.*, 9, 5417-5432, 2009.

9 Guo, J., Tilgner, A., Yeung, C., Wang, Z., Louie, P. K. K., Luk, C. W. Y., Xu, Z., Yuan, C.,  
10 Gao, Y., Poon, S., Herrmann, H., Lee, S., Lam, K. S., and Wang, T.: Atmospheric Peroxides  
11 in a Polluted Subtropical Environment: Seasonal Variation, Sources and Sinks, and  
12 Importance of Heterogeneous Processes, *Environ. Sci. & Technol.*, 48, 1443-1450,  
13 10.1021/Es403229x, 2014.

14 Hairer, E., Nørsett, S. P., and Wanner, G.: Solving Ordinary Differential Equations: Stiff and  
15 differential-algebraic problems, Springer, 1993.

16 Hallquist, M., Wenger, J. C., Baltensperger, U., Rudich, Y., Simpson, D., Claeys, M.,  
17 Dommen, J., Donahue, N. M., George, C., Goldstein, A. H., Hamilton, J. F., Herrmann, H.,  
18 Hoffmann, T., Iinuma, Y., Jang, M., Jenkin, M. E., Jimenez, J. L., Kiendler-Scharr, A.,  
19 Maenhaut, W., McFiggans, G., Mentel, T. F., Monod, A., Prevot, A. S. H., Seinfeld, J. H.,  
20 Surratt, J. D., Szmigielski, R., and Wildt, J.: The formation, properties and impact of  
21 secondary organic aerosol: Current and emerging issues, *Atmos. Chem. Phys.*, 9, 5155-5236,  
22 2009.

23 Hamer, W. J., and Wu, Y. C.: Osmotic Coefficients and Mean Activity Coefficients of Uni-  
24 Univalent Electrolytes in Water at 25 °C, *J. Phys. Chem. Ref. Data*, 1, 1047-1100, 1972.

25 Hansen, H. K., Rasmussen, P., Fredenslund, A., Schiller, M., and Gmehling, J.: Vapor-liquid  
26 equilibria by UNIFAC group contribution. 5. Revision and extension, *Ind. Eng. Chem. Res.*,  
27 30, 2352-2355, 1991.

28 Henning, S., Rosenorn, T., D'Anna, B., Gola, A. A., Svenningsson, B., and Bilde, M.: Cloud  
29 droplet activation and surface tension of mixtures of slightly soluble organics and inorganic  
30 salt, *Atmos Chem Phys*, 5, 575-582, 2005.

31 Herrmann, H.: Kinetics of aqueous phase reactions relevant for atmospheric chemistry, *Chem.*  
32 *Rev.*, 103, 4691-4716, 10.1021/Cr020658q, 2003.

33 Herrmann, H., Tilgner, A., Barzagli, P., Majdik, Z.-T., Gligorovski, S., Poulain, L., and  
34 Monod, A.: Towards a more detailed description of tropospheric aqueous phase organic  
35 chemistry: CAPRAM 3.0, *Atmos. Environ.*, 39, 4351-4363, 2005.

36 Herrmann, H., Schaefer, T., Tilgner, A., Styler, S. A., Weller, C., Teich, M., and Otto, T.:  
37 Tropospheric Aqueous-Phase Chemistry: Kinetics, Mechanisms, and Its Coupling to a  
38 Changing Gas Phase, *Chem Rev*, 115, 4259-4334, 10.1021/cr500447k, 2015.

39 Iliuta, M. C., Thomson, K., and Rasmussen, P.: Extended UNIQUAC model for correlation  
40 and prediction of vapour-liquid-solid equilibria in aqueous salt systems containing non-  
41 electrolytes. Part A. Methanol-water-salt systems, *Chem. Eng. Sci.*, 55, 2673-2686, 2000.

42 Jacobson, M. Z., Tabazadeh, A., and Turco, R. P.: Simulating equilibrium within aerosols and  
43 nonequilibrium between gases and aerosols, *J. Geophys. Res. Atmos.*, 101(D4), 9071-9091,  
44 1996.

1 Jacobson, M. Z.: Development and application of a new air pollution modeling system .Part  
2 II. Aerosol module structure and design, *Atmos. Environ.*, 31, 131-144, 1997.

3 Jungwirth, P., and Tobias, D. J.: Molecular Structure of Salt Solutions: A New View of the  
4 Interface with Implications for Heterogeneous Atmospheric Chemistry, *J. Phys. Chem. B*,  
5 105, 10468-10472, 2001.

6 Kiepe, J., Noll, O., and Gmehling, J.: Modified LIQUAC and Modified LIFACA Further  
7 Development of Electrolyte Models for the Reliable Prediction of Phase Equilibria with  
8 Strong Electrolytes, *Ind. Eng. Chem. Res.*, 45, 2361-2373, 2006.

9 Kiriukhin, M. Y., and Collins, K. D.: Dynamic hydration numbers for biologically important  
10 ions, *Biophys. Chem.*, 99, 155-168, 2002.

11 Knopf, D. A., Luo, B. P., Krieger, U. K., and Koop, T.: Thermodynamic dissociation constant  
12 of the bisulfate ion from Raman and ion interaction modeling studies of aqueous sulfuric acid  
13 at low temperatures, *J. Phys. Chem. A*, 107, 4322-4332, 2003.

14 Köhler, H.: The nucleus in and the growth of hygroscopic droplets, *Trans. Faraday Soc.*, 32,  
15 1152-1161, 1936.

16 Li, J. D., Polka, H. M., and Gmehling, J.: A GE model for single and mixed solvent  
17 electrolyte systems. 1. Model and results for strong electrolytes, *Fluid Phase Equilibr.*, 94, 89-  
18 114, 1994.

19 Liu, S., Takahama, S., Russell, L. M., Gilardoni, S., and Baumgardner, D.: Oxygenated  
20 organic functional groups and their sources in single and submicron organic particles in  
21 MILAGRO 2006 campaign, *Atmos. Chem. Phys.*, 9, 6849-6863, 2009.

22 Maffia, M. C., and Meirelles, A. J. A.: Water activity and pH in aqueous polycarboxylic acid  
23 systems, *J Chem Eng Data*, 46, 582-587, DOI 10.1021/je0002890, 2001.

24 Mao, J., Fan, S., Jacob, D. J., and Travis, K. R.: Radical loss in the atmosphere from Cu-Fe  
25 redox coupling in aerosols, *Atmos Chem Phys*, 13, 509-519, 10.5194/acp-13-509-2013, 2013.

26 Marcolli, C., and Peter, T.: Water activity in Polyol/water systems: new UNIFAC  
27 parametrization, *Atmos. Chem. Phys.*, 5, 1545-1555, 2005.

28 Metzger, S., Dentener, F., Pandis, S., and Lelieveld, J.: Gas/aerosol partitioning: 1. A  
29 computationally efficient model, *J Geophys Res-Atmos*, 107, Artn 4312  
30 10.1029/2001jd001102, 2002.

31 Metzger, S., Mihalopoulos, N., and Lelieveld, J.: Importance of mineral cations and organics  
32 in gas-aerosol partitioning of reactive nitrogen compounds: case study based on MINOS  
33 results, *Atmos. Chem. Phys.*, 6, 2549-2567, 2006.

34 Metzger, S., and Lelieveld, J.: Reformulating atmospheric aerosol thermodynamics and  
35 hygroscopic growth into fog, haze and clouds, *Atmos. Chem. Phys.*, 7, 3163-3193, 2007.

36 Ming, Y., and Russell, L. M.: Thermodynamic equilibrium of organic-electrolyte mixtures in  
37 aerosol particles, *AIChE Journal*, 48, 1331-1348, 2002.

38 Mircea, M., Facchini, M. C., Decesari, S., Fuzzi, S., and Charlson, R. J.: The influence of the  
39 organic aerosol component on CCN supersaturation spectra for different aerosol types, *Tellus*  
40 *B*, 54, 74-81, DOI 10.1034/j.1600-0889.2002.00256.x, 2002.

1 Mohs, A., and Gmehling, J.: A revised LIQUAC and LIFAC model (LIQUAC\*/LIFAC\*) for  
2 the prediction of properties of electrolyte containing solutions, *Fluid Phase Equilibr*, 337,  
3 311-322, 10.1016/j.fluid.2012.09.023, 2013.

4 Nenes, A., Pandis, S. N., and Pilinis, C.: ISORROPIA: A New Thermodynamic Equilibrium  
5 Model for Multiphase Multicomponent Inorganic Aerosols, *Aquat. Geochem.*, 4, 123-152,  
6 1998.

7 Nenes, A., Charlson, R. J., Facchini, M. C., Kulmala, M., Laaksonen, A., and Seinfeld, J. H.:  
8 Can chemical effects on cloud droplet number rival the first indirect effect?, *Geophys Res*  
9 *Lett*, 29, 10.1029/2002gl015295, 2002.

10 Peng, C., Chan, M. N., and Chan, C. K.: The hygroscopic properties of dicarboxylic and  
11 multifunctional acids: Measurements and UNIFAC predictions, *Environ Sci Technol*, 35,  
12 4495-4501, 10.1021/Es0107531, 2001.

13 Pilinis, C., Capaldo, K. P., Nenes, A., and Pandis, S. N.: MADM-A New Multicomponent  
14 Aerosol Dynamics Model, *Aerosol Sci. Technol.*, 32, 482-502, 2000.

15 Pitzer, K. S.: Activity coefficients in electrolyte solutions, CRC Press, 1991.

16 Prausnitz, J. M., Lichtenthaler, R. N., and De Azevedo, E. G.: Molecular Thermodynamics of  
17 Fluid-Phase Equilibria, Prentice-Hall Inc., Englewood Cliffs, New Jersey, USA, 2nd edn.,  
18 1986.

19 Prisle, N. L., Dal Maso, M., and Kokkola, H.: A simple representation of surface active  
20 organic aerosol in cloud droplet formation, *Atmos Chem Phys*, 11, 4073-4083, 10.5194/acp-  
21 11-4073-2011, 2011.

22 Prisle, N. L., Ottosson, N., Ohrwall, G., Soderstrom, J., Dal Maso, M., and Bjorneholm, O.:  
23 Surface/bulk partitioning and acid/base speciation of aqueous decanoate: direct observations  
24 and atmospheric implications, *Atmos Chem Phys*, 12, 12227-12242, 10.5194/acp-12-12227-  
25 2012, 2012.

26 Pruppacher, H. R., and Klett, J. D.: Microphysics of Clouds and Precipitation, Dordrecht, The  
27 Netherlands, Kluwer Academic Publishers, 1997.

28 Raatikainen, T., and Laaksonen, A.: Application of several activity coefficient models to  
29 water-organic-electrolyte aerosols of atmospheric interest, *Atmos. Chem. Phys.*, 5, 2475-  
30 2495, 10.5194/acp-5-2475-2005, 2005.

31 Raatikainen, T., and Laaksonen, A.: A simplified treatment of surfactant effects on cloud drop  
32 activation, *Geosci Model Dev*, 4, 107-116, 10.5194/gmd-4-107-2011, 2011.

33 Ravishankara, A. R.: Heterogeneous and Multiphase Chemistry in the Troposphere, *Science*,  
34 276, 1058-1065, 1997.

35 Roldin, P., Eriksson, A. C., Nordin, E. Z., Hermansson, E., Mogensen, D., Rusanen, A., Boy,  
36 M., Swietlicki, E., Svenningsson, B., Zelenyuk, A., and Pagels, J.: Modelling non-equilibrium  
37 secondary organic aerosol formation and evaporation with the aerosol dynamics, gas- and  
38 particle-phase chemistry kinetic multilayer model ADCHAM, *Atmos Chem Phys*, 14, 7953-  
39 7993, 10.5194/Acp-14-7953-2014, 2014.

40 Russell, L. M., Takahama, S., Liu, S., Hawkins, L. N., Covert, D. S., Quinn, P. K., and Bates,  
41 T. S.: Oxygenated fraction and mass of organic aerosol from direct emission and atmospheric  
42 processing measured on the R/V Ronald Brown during TEXAQS/GoMACCS 2006, *J.*  
43 *Geophys. Res.-Atmos.*, 114, 2009.

1 Rusumdar, A. J., Tilgner, A., Wolke, R., and Herrmann, H.: Treatment of non-ideality in the  
2 multiphase model SPACCIM- Part 2: Model studies on the multiphase chemical processing in  
3 deliquesced particles, in preparation for *Atmos. Chem. Phys.*, 2015.

4 Sander, R.: Compilation of Henry's law constants (version 4.0) for water as solvent, *Atmos*  
5 *Chem Phys*, 15, 4399-4981, 10.5194/acp-15-4399-2015, 2015.

6 Saxena, P., Hudischewskyj, A. B., Seigneur, C., and Seinfeld, J. H.: A comparative study of  
7 equilibrium approaches to the chemical characterization of secondary aerosols, *Atmos.*  
8 *Environ.*, 20, 1471-1483, 1986.

9 Schwartz, S. E.: Mass transport considerations pertinent to aqueous phase reactions of gases  
10 in liquid water clouds, In: *Chemistry of Multiphase Atmospheric Systems*, W. Jaeschke, ed.,  
11 Springer, Berlin, 415-471, 1986.

12 Sehili, A. M., Wolke, R., Knoth, O., Simmel, M., Tilgner, A., and Herrmann, H.: Comparison  
13 of different model approaches for the simulation of multiphase processes, *Atmos. Environ.*,  
14 39, 4403-4417, 2005.

15 Seinfeld, J. H., and Pandis, S. N.: *Atmospheric Chemistry and Physics- From Air Pollution to*  
16 *Climate Change*, 2. edition, John Wiley & Sons Inc., New York, USA, 2006.

17 Shrivastava, M., Fast, J., Easter, R., Gustafson, W. I., Zaveri, R. A., Jimenez, J. L., Saide, P.,  
18 and Hodzic, A.: Modeling organic aerosols in a megacity: comparison of simple and complex  
19 representations of the volatility basis set approach, *Atmos. Chem. Phys.*, 11, 6639-6662,  
20 10.5194/Acp-11-6639-2011, 2011.

21 Shulman, M. L., Jacobson, M. C., Carlson, R. J., Synovec, R. E., and Young, T. E.:  
22 Dissolution behavior and surface tension effects of organic compounds in nucleating cloud  
23 droplets, *Geophys Res Lett*, 23, 277-280, Doi 10.1029/95gl03810, 1996.

24 Simmel, M., and Wurzler, S.: Condensation and activation in sectional cloud microphysical  
25 models, *Atmos. Environ.*, 80, 218-236, 2006.

26 Sorjamaa, R., Svenningsson, B., Raatikainen, T., Henning, S., Bilde, M., and Laaksonen, A.:  
27 The role of surfactants in Kohler theory reconsidered, *Atmos Chem Phys*, 4, 2107-2117,  
28 2004.

29 Sorjamaa, R., and Laaksonen, A.: The influence of surfactant properties on critical  
30 supersaturations of cloud condensation nuclei, *J Aerosol Sci*, 37, 1730-1736,  
31 10.1016/j.jaerosci.2006.07.004, 2006.

32 Svenningsson, B., Rissler, J., Swietlicki, E., Mircea, M., Bilde, M., Facchini, M. C., Decesari,  
33 S., Fuzzi, S., Zhou, J., Monster, J., and Rosenorn, T.: Hygroscopic growth and critical  
34 supersaturations for mixed aerosol particles of inorganic and organic compounds of  
35 atmospheric relevance, *Atmos Chem Phys*, 6, 1937-1952, 2006.

36 Takahama, S., Schwartz, R. E., Russell, L. M., Macdonald, A. M., Sharma, S., and Leaitch,  
37 W. R.: Organic functional groups in aerosol particles from burning and non-burning forest  
38 emissions at a high-elevation mountain site, *Atmos. Chem. Phys.*, 11, 6367-6386, 2011.

39 Tilgner, A., and Herrmann, H.: Radical-driven carbonyl-to-acid conversion and acid  
40 degradation in tropospheric aqueous systems studied by CAPRAM, *Atmos. Environ.*, 44,  
41 5415-5422, 2010.

42 Tilgner, A., Bräuer, P., Wolke, R., and Herrmann, H.: Modelling multiphase chemistry in  
43 deliquescent aerosols and clouds using CAPRAM3. 0i, *J. Atmos. Chem.*, 70, 221-256, 2013.

1 Tong, C., Clegg, S. L., and Seinfeld, J. H.: Comparison of activity coefficient models for  
2 atmospheric aerosols containing mixtures of electrolytes, organics, and water, *Atmos.*  
3 *Environ.*, 42, 5459-5482, 2008.

4 Topping, D.: An analytical solution to calculate bulk mole fractions for any number of  
5 components in aerosol droplets after considering partitioning to a surface layer, *Geosci Model*  
6 *Dev.*, 3, 635-642, 10.5194/gmd-3-635-2010, 2010.

7 Topping, D., Connolly, P., and McFiggans, G.: Cloud droplet number enhanced by co-  
8 condensation of organic vapours, *Nat Geosci*, 6, 443-446, 10.1038/Ngeo1809, 2013.

9 Topping, D. O., McFiggans, G. B., and Coe, H.: A curved multi-component aerosol  
10 hygroscopicity model framework: Part 1 - Inorganic compounds, *Atmos. Chem. Phys.*, 5,  
11 1205-1222, 2005a.

12 Topping, D. O., McFiggans, G. B., and Coe, H.: A curved multi-component aerosol  
13 hygroscopicity model framework: Part 2 - Including organic compounds, *Atmos. Chem.*  
14 *Phys.*, 5, 1223-1242, 2005b.

15 Topping, D. O., McFiggans, G. B., Kiss, G., Varga, Z., Facchini, M. C., Decesari, S., and  
16 Mircea, M.: Surface tensions of multi-component mixed inorganic/organic aqueous systems  
17 of atmospheric significance: measurements, model predictions and importance for cloud  
18 activation predictions, *Atmos Chem Phys*, 7, 2371-2398, 2007.

19 Tuckermann, R., and Cammenga, H. K.: The surface tension of aqueous solutions of some  
20 atmospheric water-soluble organic compounds, *Atmos Environ*, 38, 6135-6138,  
21 10.1016/j.atmosenv.2004.08.005, 2004.

22 Wexler, A., Clegg, S., and L., S.: Atmospheric aerosol models for systems including the ions  
23 H<sup>+</sup>, NH<sub>4</sub><sup>+</sup>, Na<sup>+</sup>, SO<sub>4</sub><sup>2-</sup>, NO<sub>3</sub><sup>-</sup>, Cl<sup>-</sup>, Br<sup>-</sup>, and H<sub>2</sub>O, *J. Geophys. Res.-Atmos.*, 107, 2002.

24 Wexler, A. S., and Seinfeld, J. H.: The Distribution of Ammonium-Salts among a Size and  
25 Composition Dispersed Aerosol, *Atmos Environ a-Gen*, 24, 1231-1246, Doi 10.1016/0960-  
26 1686(90)90088-5, 1990.

27 Wolke, R., and Knoth, O.: Time-integration of multiphase chemistry in size-resolved cloud  
28 models, *Appl. Numer. Math.*, 42, 473-487, 2002.

29 Wolke, R., Sehili, A. M., Simmel, M., Knoth, O., Tilgner, A., and Herrmann, H.: SPACCIM:  
30 A parcel model with detailed microphysics and complex multiphase chemistry, *Atmos.*  
31 *Environ.*, 39, 4375-4388, 2005.

32 Yan, W., Topphoff, M., Rose, C., and Gmehling, J.: Prediction of vapor-liquid equilibria in  
33 mixed-solvent electrolyte systems using the group contribution concept, *Fluid Phase*  
34 *Equilibr.*, 162, 97-113, 1999.

35 Yu, S. C., Dennis, R., Roselle, S., Nenes, A., Walker, J., Eder, B., Schere, K., Swall, J., and  
36 Robarge, W.: An assessment of the ability of three-dimensional air quality models with  
37 current thermodynamic equilibrium models to predict aerosol NO<sub>3</sub><sup>-</sup>, *J Geophys Res-Atmos*,  
38 110, Artn D07s13  
39 10.1029/2004jd004718, 2005.

40 Zaveri, R. A., Easter, R. C., and Wexler, A. S.: A new method for multicomponent activity  
41 coefficients of electrolytes in aqueous atmospheric aerosols, *J Geophys Res-Atmos*, 110,  
42 10.1029/2004jd004681, 2005a.

- 1 Zaveri, R. A., Easter, R. C., and Peters, L. K.: A computationally efficient Multicomponent  
2 Equilibrium Solver for Aerosols (MESA), *J. Geophys. Res.-Atmos.*, 110, 2005b.
- 3 Zaveri, R. A., Easter, R. C., Fast, J. D., and Peters, L. K.: Model for Simulating Aerosol  
4 Interactions and Chemistry (MOSAIC), *J. Geophys. Res.-Atmos.*, 113, 2008.
- 5 Zhang, Y., Seigneur, C., Seinfeld, J. H., Jacobson, M., Clegg, S. L., and Binkowski, F. S.: A  
6 comparative review of inorganic aerosol thermodynamic equilibrium modules: similarities,  
7 differences, and their likely causes, *Atmos Environ*, 34, 117-137, Doi 10.1016/S1352-  
8 2310(99)00236-8, 2000.
- 9 Zhang, Y., Pun, B., Vijayaraghavan, K., Wu, S. Y., Seigneur, C., Pandis, S. N., Jacobson, M.  
10 Z., Nenes, A., and Seinfeld, J. H.: Development and application of the model of aerosol  
11 dynamics, reaction, ionization, and dissolution (MADRID), *J Geophys Res-Atmos*, 109, Artn  
12 D01202  
13 10.1029/2003jd003501, 2004.
- 14 Zuend, A., Marcolli, C., Luo, B. P., and Peter, T.: A thermodynamic model of mixed organic-  
15 inorganic aerosols to predict activity coefficients, *Atmos. Chem. Phys.*, 8, 2008.
- 16 Zuend, A., Marcolli, C., Booth, A. M., Lienhard, D. M., Soonsin, V., Krieger, U. K., Topping,  
17 D. O., McFiggans, G., Peter, T., and Seinfeld, J. H.: New and extended parameterization of  
18 the thermodynamic model AIOMFAC: calculation of activity coefficients for organic-  
19 inorganic mixtures containing carboxyl, hydroxyl, carbonyl, ether, ester, alkenyl, alkyl, and  
20 aromatic functional groups, *Atmos. Chem. Phys.*, 11, 9155-9206, 2011.

21  
22

1 **Tables:**

2 Table 1. Description of activities implemented in SPACCIM.

Activities	Description
Activity of a gas over a particle surface	$\{A_{(g)}\} = p_{A,s}$
Activity of an un-dissociated compound	$\{A_{(aq)}\} = m_A \gamma_A$
Activity of an ion in solution	$\{A^+\} = m_{A^+} \gamma_{A^+}$
Activity of liquid water in a particle	$\{H_2O_{(aq)}\} = a_w$
Activity of a solid	$\{A_{(s)}\} = m_s \text{ i. e. } \gamma_s = 1$

3

5

Gelöscht: Seitenumbruch  
ADHN<sup>a,b</sup> ... [1]

## Figures:

Fig. 1: Schematic of the model coupling strategy and its implementation considering the treatment of [solution](#) non-ideality and surface tension effects in SPACCIM.

Fig. 2: Scheme of activity coefficients and surface tension used in the microphysics and multiphase chemistry models.

Fig. 3: Sparse structure of Jacobian and two droplet classes [adapted from Wolke et al. (2005)].

Fig. 4: Scheme of the currently used interactions in the MR and SR part. Parameters for ion  $\leftrightarrow$  ion and ion  $\leftrightarrow$  organic main group interactions are all incorporated in the MR part and set to zero in the SR (UNIFAC) part.

Fig. 5: Comparison with measurements of aqueous electrolyte solutions (symbols) and corresponding calculations of the models [E-AIM/](#)AIM III (Clegg et al., 1998b), mod. LIFAC (Kiepe et al., 2006), Ming and Russell (Ming and Russell, 2002) and [SpactMod](#) at 298 K for the salt NaCl + NH<sub>4</sub>NO<sub>3</sub> at a molar salt mixing ratio of (3:1). [Note that SpactMod reproduces the results of AIOMFAC \(Zuend et al., 2008\) due to the same parameters applied.](#)

Fig. 6: Intercomparison between selected models for Ca(NO<sub>3</sub>)<sub>2</sub> salt: : Water activities (solid lines) and mean activity coefficients (dashed lines). [Again, SpactMod reproduces AIOMFAC.](#)

Fig. 7: Comparison between experimental and calculated water activities ( $a_w$ ) in aqueous citric acid solutions as a function of water fraction ( $x_w$ ) at 298.15K. Experimental data [are taken](#) from Maffia and Meirelles (2001).

Fig. 8: [Comparison between experimental \(symbols\) and calculated mean activity coefficients \(solid lines\) of binary salt mixtures as a function of molality \(mol kg<sup>-1</sup>\) at 298 K. Experimental data are taken from Hamer and Wu \(1972\).](#)

Fig. 9: [Comparison of modeled water activities for the aqueous solution composed of organic-electrolyte mixture: \(NH<sub>4</sub>\)<sub>2</sub>SO<sub>4</sub> + Glycerol + H<sub>2</sub>O \[\(2:1:1\) mole ratio\]. The SpactMod results are in agreement with AIOMFAC.](#)

Fig. 10: [Comparison between measured and modeled water activities for the aqueous solution composed of organic-electrolyte mixture: \(NH<sub>4</sub>\)<sub>2</sub>SO<sub>4</sub> + Ethanol + Acetic acid \[\(2:1:1\) mole ratio\].](#)

Fig. 11: Importance of different interactions in the aqueous solution composed of NaCl + (NH<sub>4</sub>)<sub>2</sub>SO<sub>4</sub> + Ethanol + Malonic acid [1:1:1:1 (mole ratio)].

Fig. 12: Modeled activity coefficients of main inorganic particle phase constituents (top) and important transition metal ions (TMIs, down) as the function of the simulation time for the two different relative humidity cases (left: 90% r.h., right: 70% r.h.). The blue bars mark the in-cloud time periods during the simulation time.

**Gelöscht:** AIOMFAC (Zuend et al., 2008)

**[2] verschoben (Einfügung)**

**[3] nach unten verschoben:** Comparison between measured and modeled water activities for the aqueous solution composed of organic-electrolyte mixture: (NH<sub>4</sub>)<sub>2</sub>SO<sub>4</sub> + Ethanol + Acetic acid [(2:1:1) mole ratio].

**Feldfunktion geändert**

**[3] verschoben (Einfügung)**

**Gelöscht:** Comparison between measured and modeled water activities for the aqueous solution composed of organic-electrolyte mixture: (NH<sub>4</sub>)<sub>2</sub>SO<sub>4</sub> + Ethanol + Acetic acid [(2:1:1) mole ratio].

**[2] nach oben verschoben:** Comparison between experimental (symbols) and calculated mean activity coefficients (solid lines) of binary salt mixtures as a function of molality (mol kg<sup>-1</sup>) at 298 K. Experimental data from Hammer and Wu (1972).

**Gelöscht:** Comparison of modeled water activities for the aqueous solution composed of organic-electrolyte mixture: (NH<sub>4</sub>)<sub>2</sub>SO<sub>4</sub> + Glycerol + H<sub>2</sub>O [(2:1:1) mole ratio].

**Gelöscht:** 9

**Gelöscht:** 0

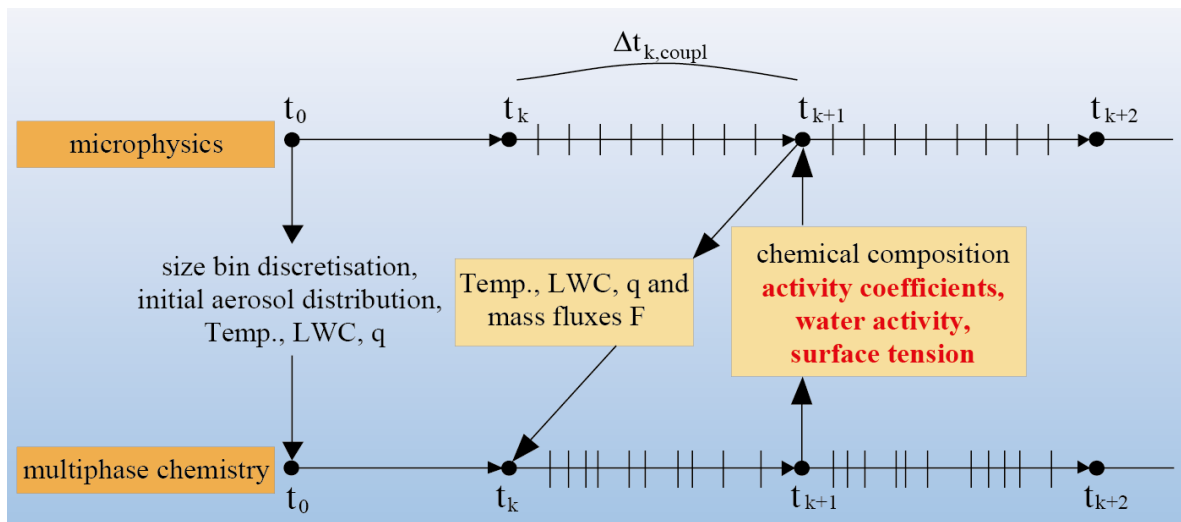
1 | Fig. 13: Modeled activity coefficients of organic carbonyl compounds (top) and organic  
2 | acids/anions (TMI, down) as the function of the simulation time for the two different relative  
3 | humidity cases (left: 90% r.h., right: 70% r.h.). The blue bars mark the in-cloud time periods  
4 | during the simulation time.

Gelöscht: 1

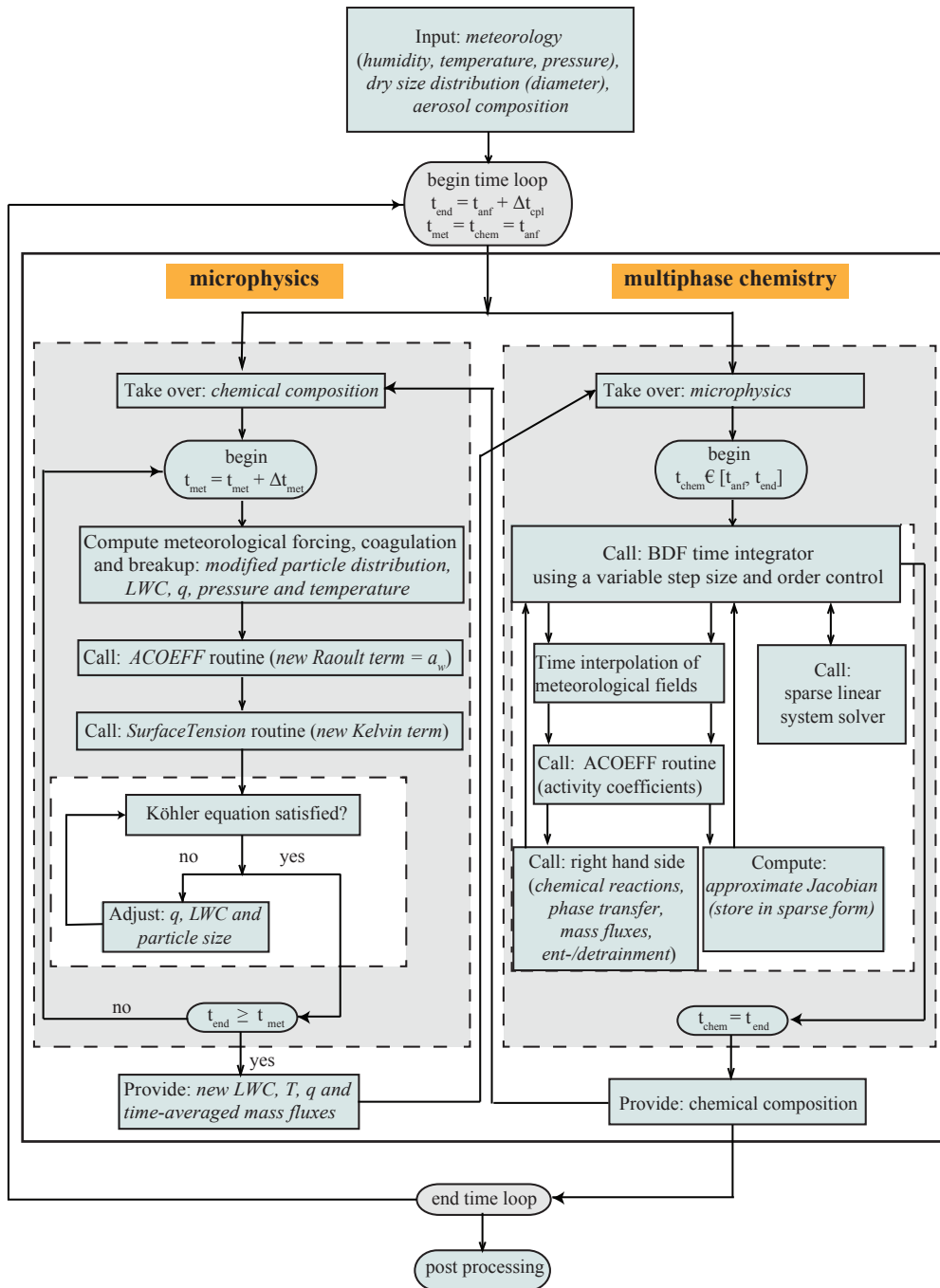
6 | Fig. 14: Modeled pH values as the function of the simulation time for the two different  
7 | relative humidity cases (left: 90% r.h., right: 70% r.h.) considering ideal (red line) and  
8 | non-ideal (blue line) solutions, respectively. The blue bars mark the in-cloud time periods  
9 | during the simulation time.

Gelöscht: 2

10

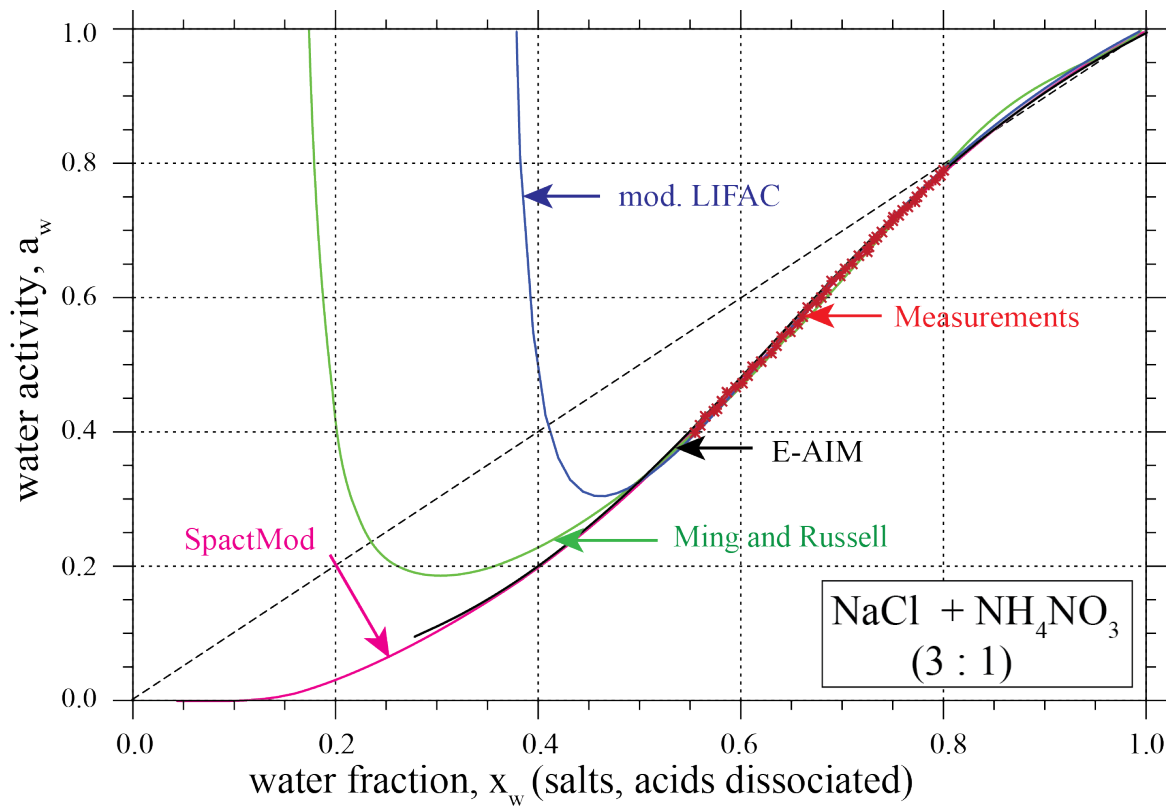


1  
2 Fig. 1  
3



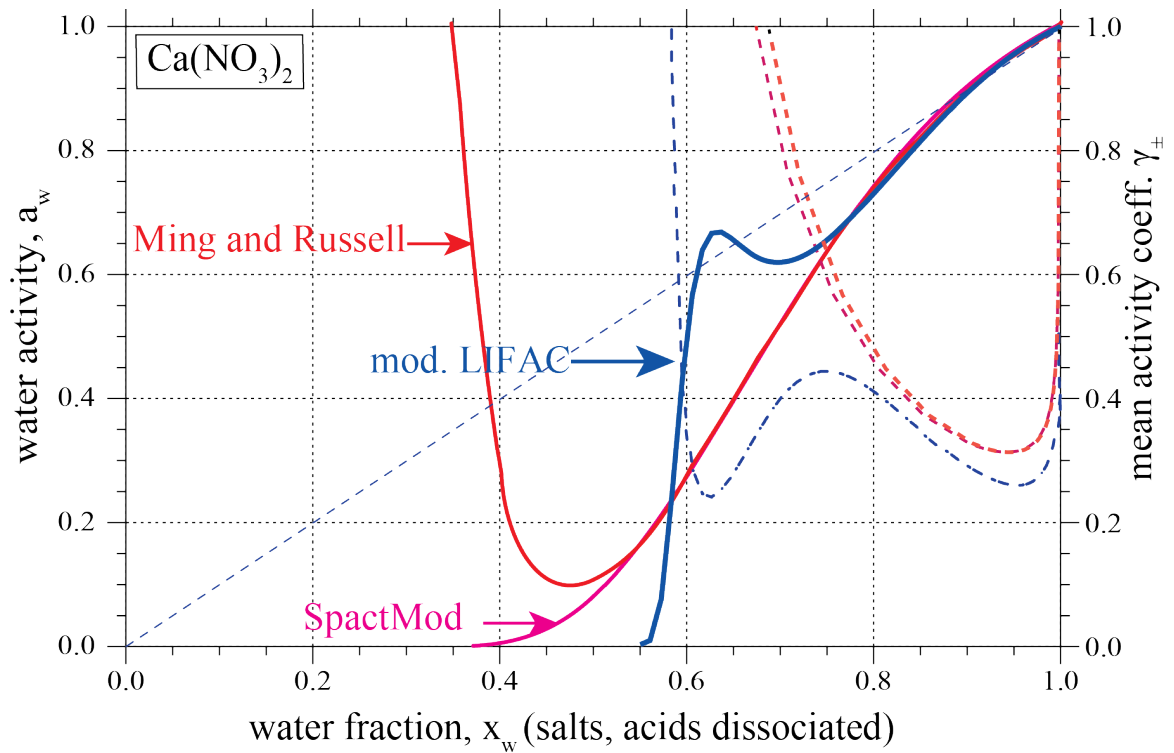
1  
2 Fig. 2





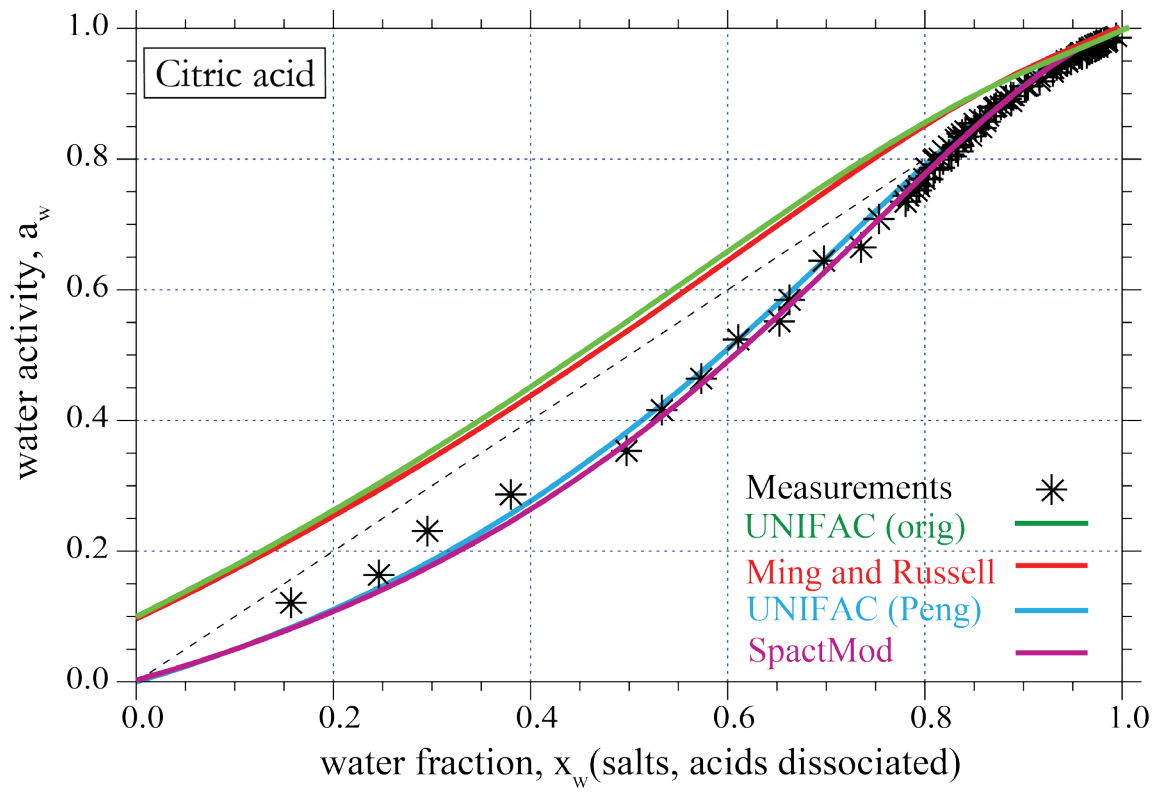
1  
2  
3

Fig. 5

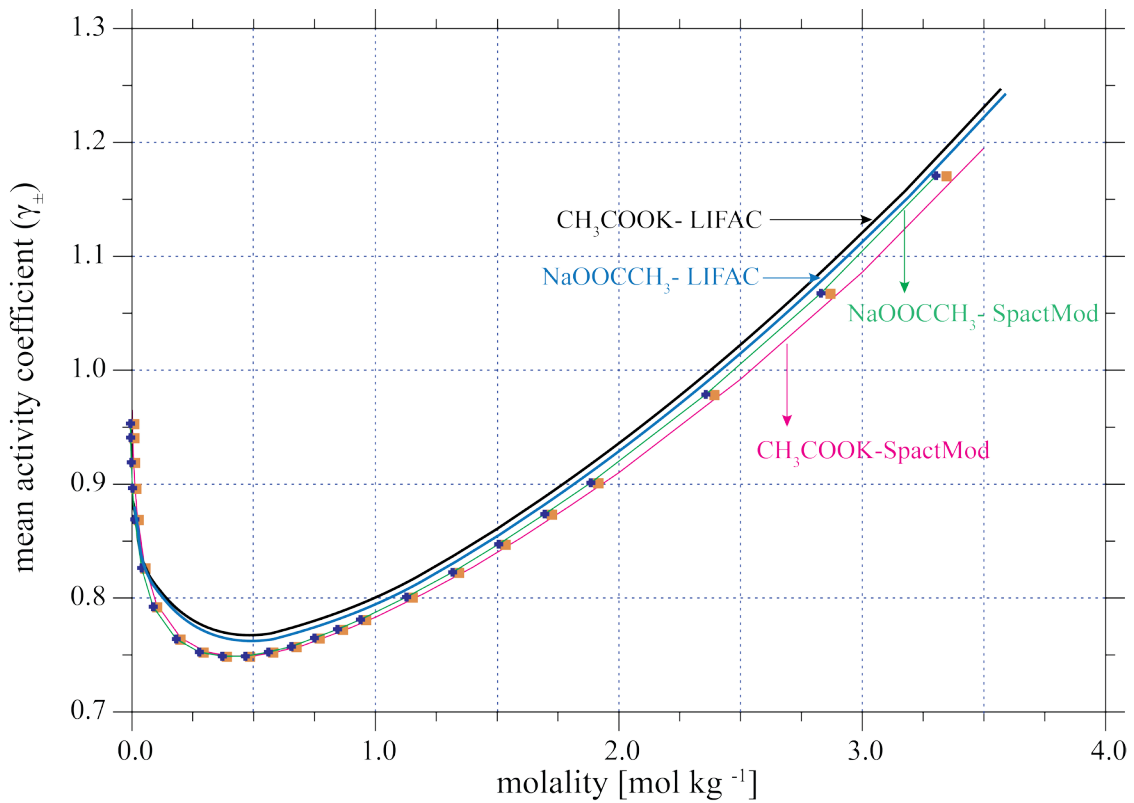


4  
5  
6

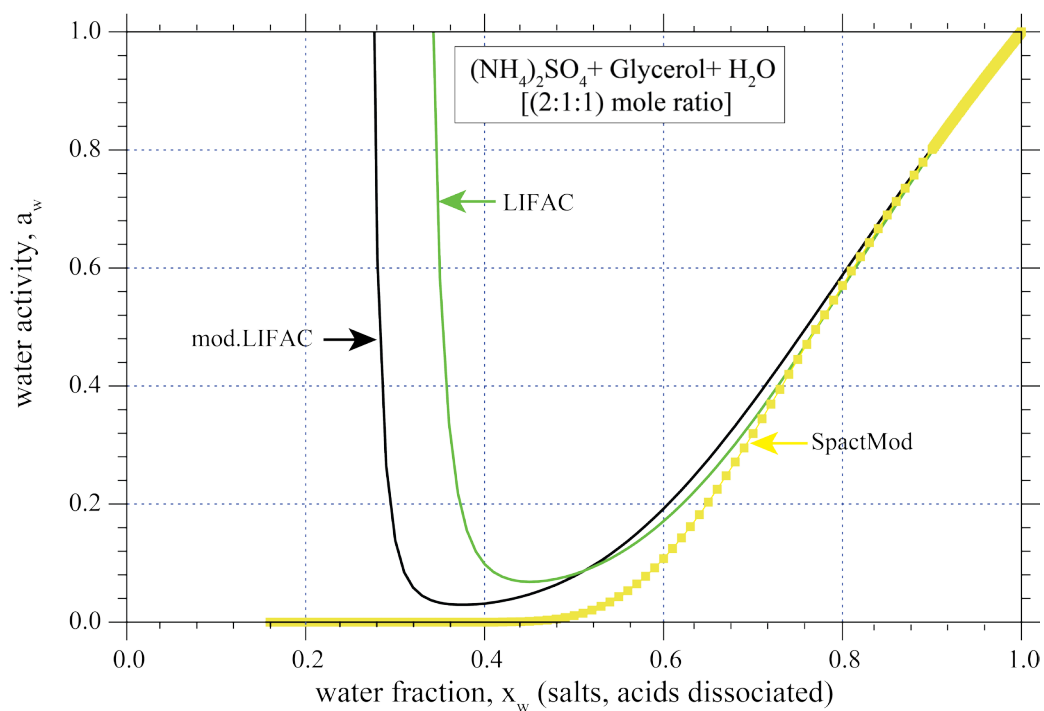
Fig. 6:



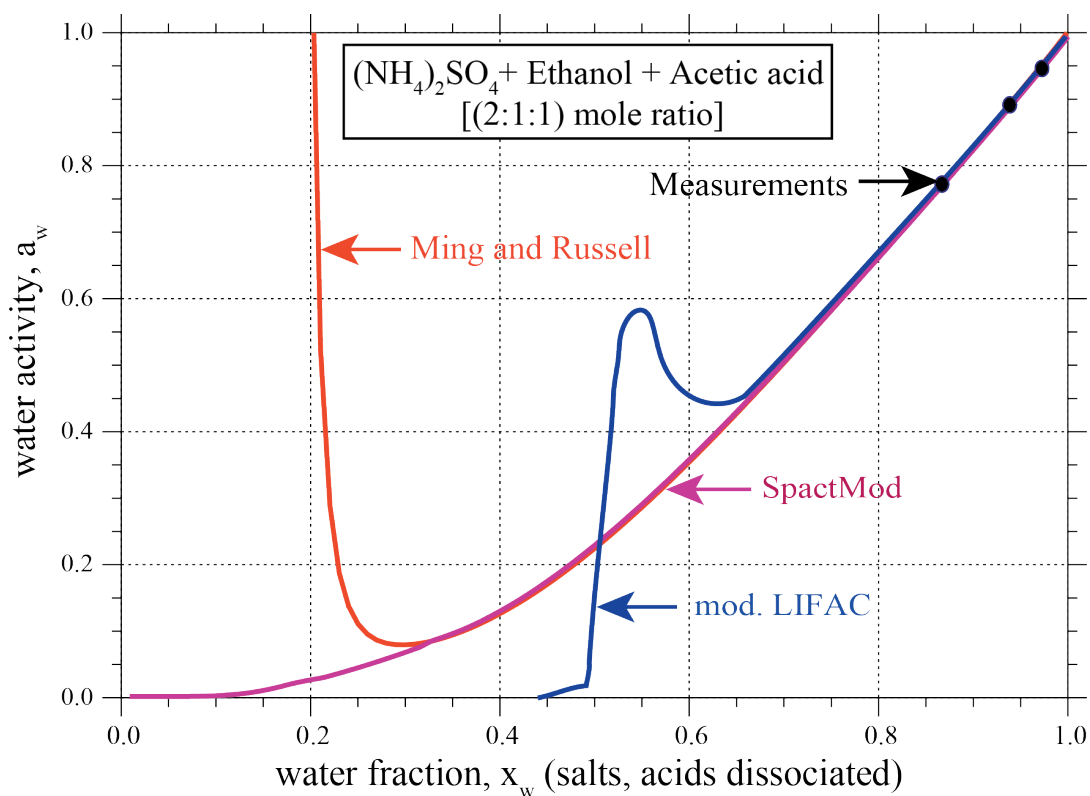
1  
2  
3  
4  
Fig. 7



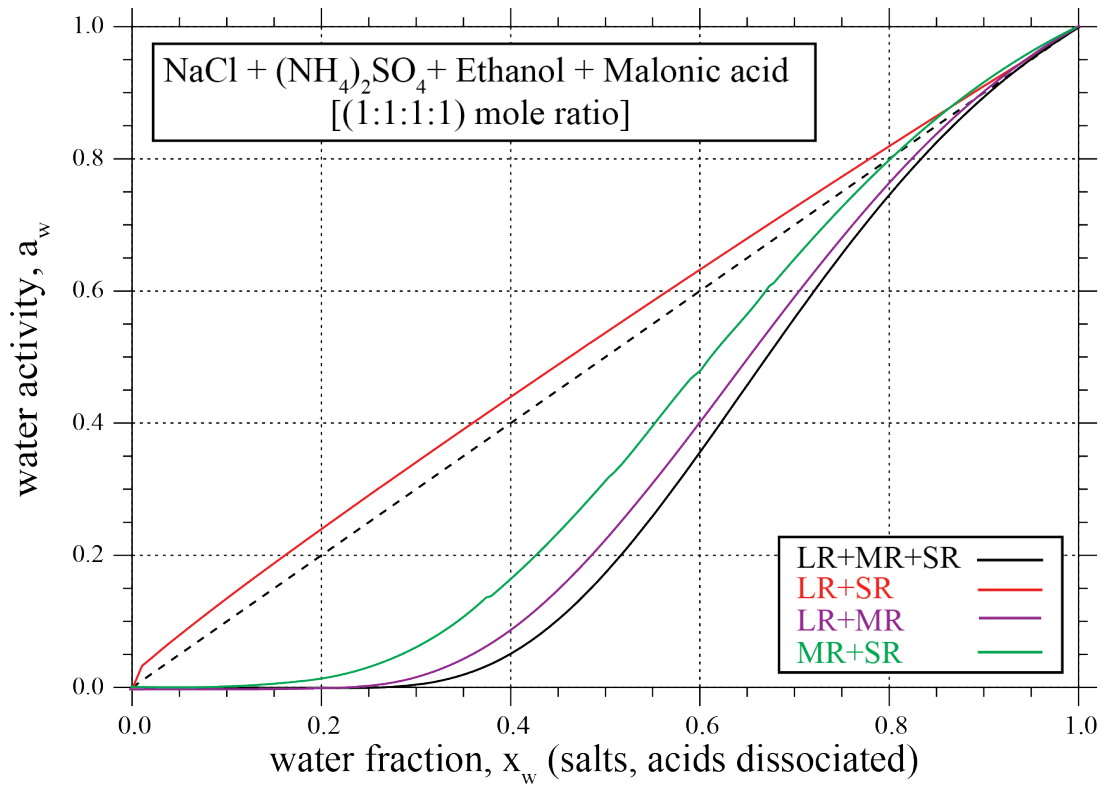
5  
6  
7  
8  
Fig. 8



1  
2 Fig. 9  
3  
4  
5

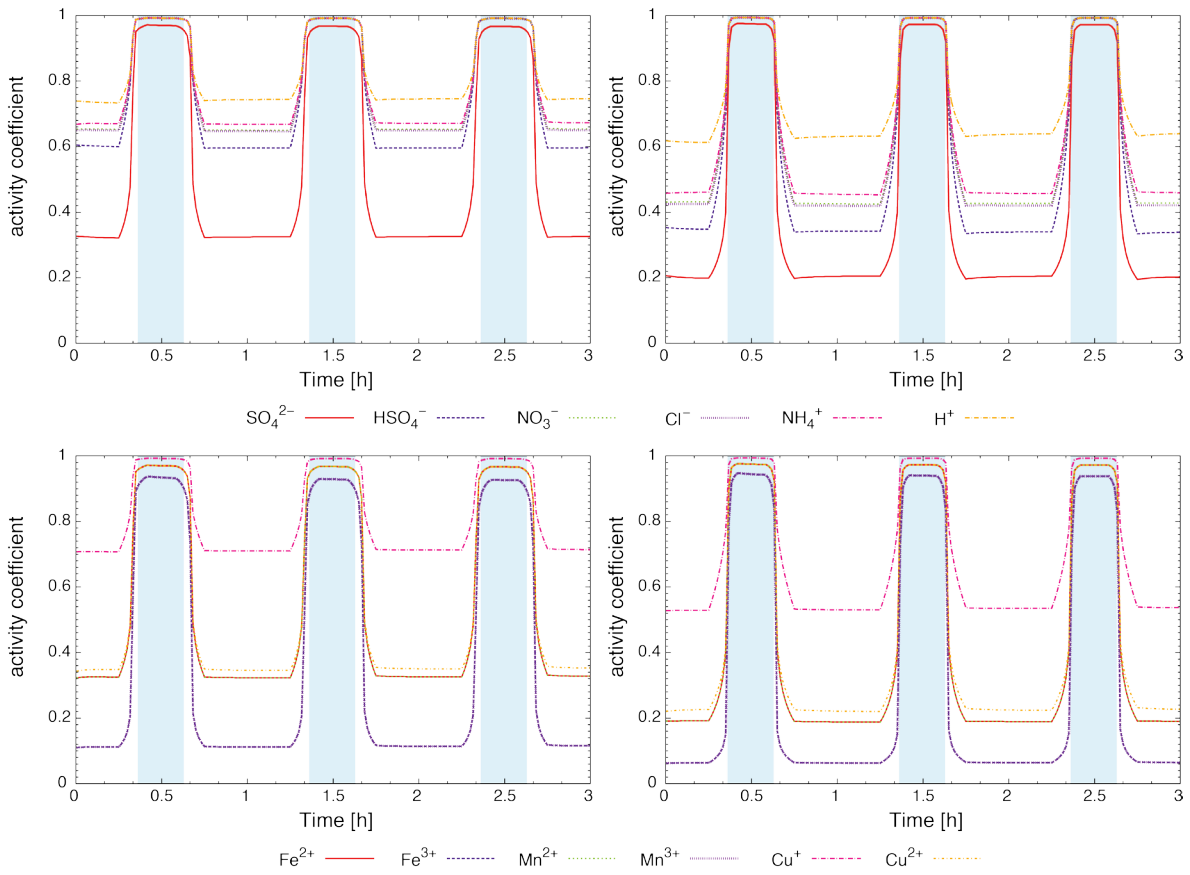


6  
7 Fig. 10  
8



1  
2  
3  
4

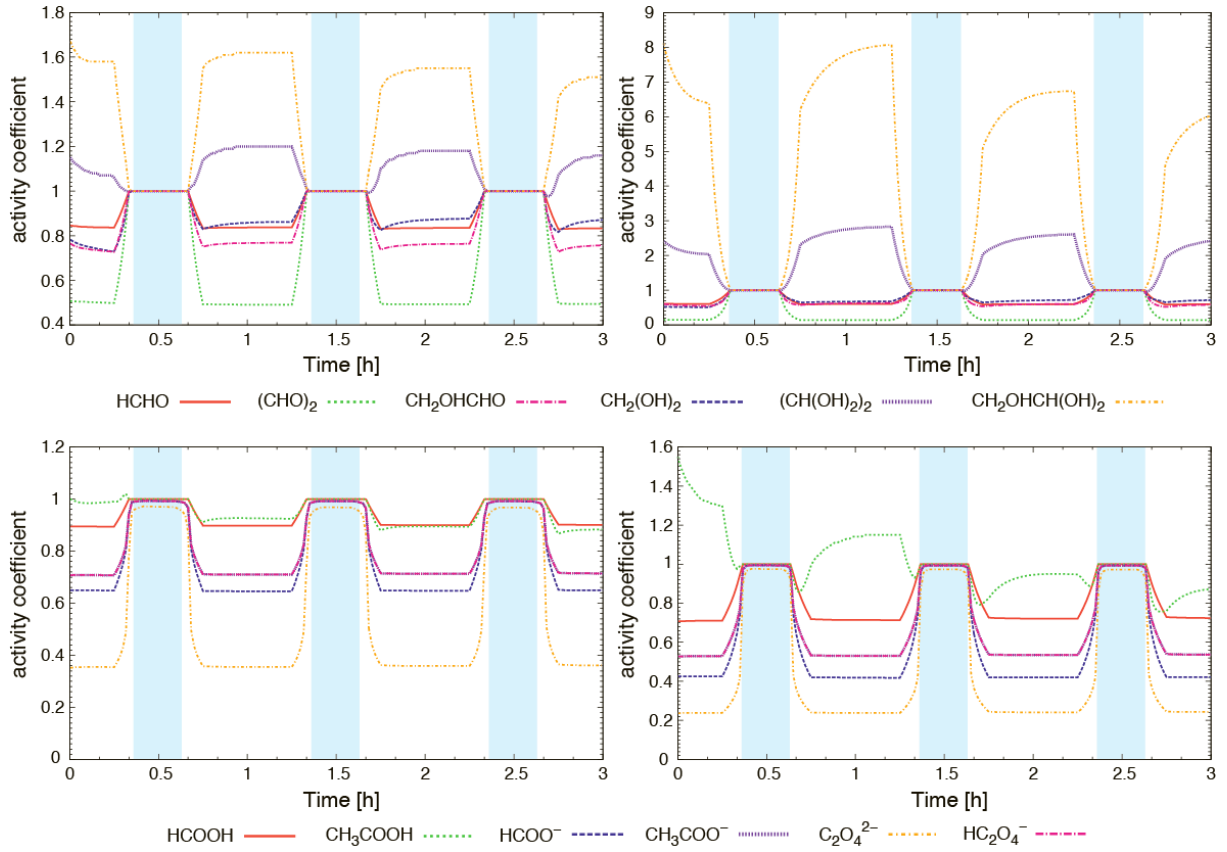
Fig. 11



5  
6

Fig. 12

1



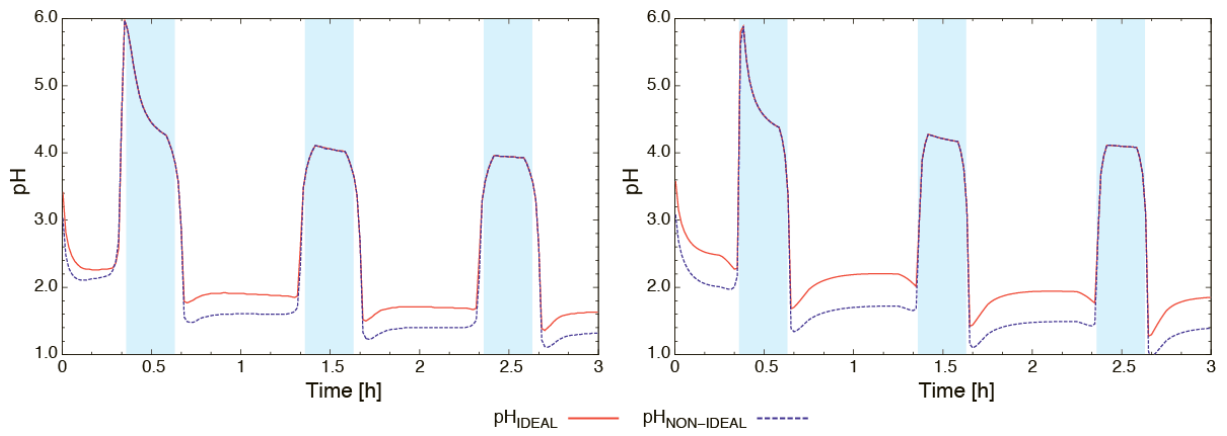
2

3

Fig. 13

4

5



6

7

Fig. 14

8